GLYCOMIMETIC FUNCTIONALIZED COLLAGEN HYDROGELS FOR PERIPHERAL NERVE REPAIR

By

SHIRLEY NARAIN MASAND

A dissertation submitted to the

Graduate School-New Brunswick

Rutgers, The State University of New Jersey

and

The Graduate School of Biomedical Sciences

University of Medicine and Dentistry of New Jersey

in partial fulfillment of the requirements

for the degree of

Doctor of Philosophy

Graduate Program in Biomedical Engineering

written under the direction of

David Ira Shreiber, PhD

and approved by

_____

_____

_____

_____

_____

New Brunswick, New Jersey

January 2013

ABSTRACT OF THE DISSERTATION

GLYCOMIMETIC FUNCTIONALIZED COLLAGEN HYDROGELS FOR PERIPHERAL NERVE REPAIR

By SHIRLEY NARAIN MASAND

Dissertation Director: David I. Shreiber

Despite the innate regenerative potential of the peripheral nervous system, functional recovery is often limited. The goal of this dissertation was to develop a clinically relevant biomaterial strategy to (1) encourage the regrowth of axons and (2) direct them down their appropriate motor tracts. To this end, we use peptide mimics of two glycans, polysialic acid (PSA) and an epitope first discovered on human natural killer cells (HNK-1), to functionalize type I collagen hydrogels. Previous studies have shown that these molecules, in their glycan and glycomimetic form, are associated with acceleration of neurite outgrowth, glial cell proliferation, and motoneuron targeting.

In vitro, we demonstrated the retained functionality of the peptide glycomimetics after conjugation to a type I collagen backbone. While HNK-functionalized collagen increased motor neurite outgrowth, PSA-functionalized collagen encouraged motor and sensory neurite outgrowth and Schwann cell extension and proliferation. When we introduce these glycomimetic-functionalized collagen hydrogels into a critical gap femoral nerve model, we show that both PSA and HNK-functionalized hydrogels yielded a significant increase in functional recovery when compared to saline, native and scramble-coupled hydrogels. However, there was an interesting divergence in the morphological results: PSA-functionalized hydrogels increased axon count and HNK-

functionalized hydrogels increased motoneuron targeting and myelination. We believed that these differences may be attributed to distinct mechanisms by which the glycomimetics impart their benefit. Interestingly, however, we found no synergistic gain in recovery with the use of our composite hydrogels which we speculated may be due to an inadequate dose of the individual glycomimetic. To address this possibility, we show that increasing the amount of functionalized peptide functionalized in our composite hydrogels led to increases in axon count and area of regeneration, but does not affect the degree of functional recovery. Finally, in order to assess potential mechanisms by which our glycomimetics impart benefit, we describe a novel platform for studying neural cell/biomaterial interaction through the use of two types of motoneuron cultures, dissociated spinal cord neurons and organotypic spinal cord slices. We show promising evidence that this strategy can be used to probe signaling pathways potentially involved in the action of these bioactives.

DEDICATION

To my parents— Each day you remind me that success isn't measured by what you have, but by what you give.

ACKNOWLEDGEMENTS

Reflecting back on my time in graduate school, I am humbled by the number of people that have supported me throughout this journey. First and foremost, my sincerest gratitude is given to Dr. David Shreiber. Dr. Shreiber, you have helped me discover my own potential. You gave me a chance and pushed me until I became the more capable, thoughtful, and confident scientist that I am today. There may have been times that I did not fully appreciate the journey, but you were a skilled guide. You are more than an advisor, and no words will ever adequately convey that. To my many other faculty mentors and dissertation committee members, thank you for always leaving your door open to me. To the BME staff, I think we have made the department a warmer place together.

To my fellow labmates in the Shreiber lab, and also in collaborating labs, over the years we have become a family, you have all been there with me to celebrate the highs and support me through tougher times. I look forward to hearing about each of your successes, and I am sure there will be many. To my students-- you have taught me more than you will ever know. Thank you for believing in me as much as I believe in each of you. Ian Gaudet and Aaron Carlson, you are both the brothers that I never had. I walk away with fond memories from our numerous tailgates, 'family' dinners, and daily powwows. While the circumstance of our relationship may change, the strength of our bond will certainly persevere.

Outside of Rutgers, I have been blessed with an amazing circle of friends that continually kept me connected to the 'real world'. I have been blessed with the opportunity to share in so many of the milestones in each of your lives and I am so glad that you were each able

to be a part of this. So many of you have asked about my work, read my papers, and been so enthusiastic about this process. Simply, thank you.

And finally to the people that were my life fuel throughout this process-- my family. To Shirin Raval, Sachin Raval, and Shweta Sachdev, thank you for always making me laugh when I didn't think it was possible. Thank you Mom, Dad, and Mama for being my pillar of strength. Your unwavering faith in me is the only reason I was able to get to where I am today. I had the perfect blend of parents, in my father I looked for patience and in my mother I found compassion. To Monish Dhansingani, thank you for so quickly falling into the role of brother!

I end my acknowledgements with the person who likely deserves her own degree for all that she has been though-- my sister and best friend. Dr. Anjali Masand, while you may be younger than me in age, you are an inspiration. Thank you for always answering my calls despite the time, giving sound advice despite the triviality of the circumstance, and reminding me that there was a light at the end of the tunnel no matter how dim. Several years ago, you gave me a journal inscribed with the following quotation from Rabbi Norman Lamm: "The achievement of excellence requires great effort, much planning, and even more time. But in the long run, mediocrity costs more, drains your energy, and wastes even more time than it takes to do things right." I can now say I more fully understand the depth of these words and will continue to live by them.

TABLE OF CONTENTS

TABLE OF FIGURES

TABLE OF TABLES

CHAPTER 1: INTRODUCTION

1.1 PERIPHERAL NERVOUS SYSTEM INJURY

The peripheral nervous system (PNS), with motor and sensory subdivisions, enables efferent and afferent communication of end targets with the brain and spinal cord. Peripheral nerves are arranged as parallel bundles of fibers without protection from bone or brain barrier making it particularly susceptible to damage. Trauma to the PNS results in halted communication between the nerve and its target which can lead to paralysis, anesthesia, and/or lack of autonomic control. If this damage results in neuronal death, these cells cannot be replaced as neurons are post-mitotic and fully differentiated. However, if the cell body remains viable, the PNS has the ability to regenerate.

When a nerve fiber is damaged but the cell soma remains intact, a finely regulated series of events begin to remove injured tissue to allow for regeneration [1]. More specifically, the axon and its synaptic endings distal to the point of injury disintegrate in a series of events termed Wallerian degeneration. Immediately following trauma, the axonal cytoskeletal proteins, including microtubules and neurofilaments, are broken down by calcium-dependent proteolysis. By 24 hours, the affected axons are completely fragmented into granular debris. Within 48 hours, the myelin sheath which surrounds the axon begins to form ovoids [2]. By day 3, Schwann cells, the myelinating component of the PNS, are activated and begin to phagocytose debris in the area before blood-circulating macrophages arrive [1, 3].

Following this degenerative process, Schwann cells begin to proliferate and release a variety of growth factors and adhesive molecules to encourage the sprouting of

neurites from the proximal stump. The Schwann cells arrange themselves into oriented columns and secrete extracellar matrix molecules termed bands of Bungner which create a physical guide for the neurite's growth cone towards its original distal target [1, 4]. The daughter sprouts from the damaged axon begin at the most distal intact node of Ranvier and grow on the basal lamina produced by the Schwann cells [5]. Despite a paucity of information explaining the mechanism of action between axon/Schwann cell appositions, it is well accepted that the Schwann cells create a highly supportive substrate for axon regrowth.

1.2 INCIDENCE, TREATMENT, AND CURRENT RESEARCH THRUSTS

In the United States, peripheral nerve damage accounts for 2.8% of traumatic injuries and results in over 50,000 surgical procedures each year [6, 7]. However, this number likely underestimates the actual number of PNS injuries as many are surgically irreparable [7]. These lesions are primarily the result of vehicular accidents and are also attributed to tumors, infections, or iatrogenic side effects of surgery [8].

Peripheral nerve injuries are most commonly classified using the Sunderland grading system, which divides PNS injury into 5 subtypes. Neuropraxia is the mildest injury type as it does not cause a loss of nerve continuity and generally results in full functional recovery. The second degree of injury is axonotmesis where there is an injury to the axon and its surrounding myelin, but the perineurium and epineurium are left intact. These injuries are generally correlated with an excellent prognosis since the endoneurial pathways for axon regeneration are preserved. The third degree injury classification involves axonotmesis coupled with endoneurial damage. Functional recovery in these cases will depend on the extent of endoneurial disruption. In a fourth-

degree injury only epineurial continuity is preserved and in a fifth-degree injury the nerve is completely severed. Fourth and fifth-degree injuries will not recover without surgical intervention [1].

Generally fourth and fifth degree injuries are associated with a loss of tissue resulting in a nerve gap. Clinical intervention strategies for peripheral nerve defects depend on the size of this gap. Direct neurosuture, which is the coaptation of two nerve ends, is used when the defect is 5 mm or less in size. This technique requires that the nerve ends are adjacent to one another and can be connected without inducing tension, which has been shown to be detrimental to regeneration [9]. For larger nerve gaps, the gold standard is the use of autografts, typically taken from the sensory sural nerve, superficial cutaneous nerve, or lateral medial antebrachii cutaneous nerves [10]. However, autografts are associated with a number of limitations like the need for secondary surgery, loss of function at the donor site, and size/modality mismatch. Additionally, complications have also been noted at the donor site like hyperesthesia and formation of neuromas. Most importantly, despite significant advances in microsurgical techniques, autografts generally do not result in complete functional recovery [11, 12]. While the size of the smallest suture material has dropped to 50 - 75 microns and surgeons have developed methods for increased precision, these improvements are still beyond the size scale of axons [13]. These collective drawbacks clearly motivate the need for an alternative construct to address peripheral nerve injury.

Previous research has attempted to use allografts and xenografts as it allows for the preservation of basal lamina and extracellular matrix, which can potentially contribute to the biological support and physical guidance of regenerating neurites [14]. This

approach, however, has been met with varying degrees of success and its use is further complicated by the required immunosuppression.

Artificial nerve conduits have also been explored as a potential therapeutic strategy for PNS injury. One main advantage of this approach is that their physical and chemical properties can be specifically tailored to maximize regeneration. These entubulations limit the infiltration of fibroblasts while directing regenerating axons from the proximal to distal nerve stump. Additionally, soluble growth factors and matrix elements which are released from resident Schwann cells accumulate within the tubes and may further enhance regeneration [15]. Williams et al. elucidated the importance of these events by conducting a temporal analysis of nerve regeneration through an artificial nerve conduit following a rat sciatic nerve transection. Within the first 24 hours of entubulation placement, the cavity is filled with neurotrophic factors. At approximately one week, the inter-stump distance is connected with an acellular matrix consisting mostly of fibrin [16]. If this matrix dose not form, regeneration fails to proceed [17]. At two weeks, Schwann cells begin to infiltrate this matrix and are soon followed by emerging axonal sprouts. In this model, it was demonstrated that the axonal extension rate within a hollow entubulation is approximately 1mm/day [16], similar results were later found in a non-human primate model [18].

The first artificial nerve conduits in clinical use were non-degradable silicone tubes. Unfortunately, their utility was limited by the frequent incidence of nerve compression which often required a secondary surgery for removal. Several hollow nerve guide implants have since received FDA approval**.** Both biological (collagen-based) and polymeric materials are available. Of these, four are degradable (Neurotube, Neurolac,

NeuraGen, and NeuroMatrix, Neuroflex) and one is non-degradable (SaluBridge). Clinical studies have shown the efficacy of these materials often approaching similar outcomes to autografts [19]; however they have not been approved or efficacious for longer deficits as they frequently fail due to collapse, fibrous tissue infiltration, or early degradation [20]. These critical gap sizes, where the likelihood of axon elongation through the length of the gap drops to 50% or less, may require advanced strategies for repair [21].

Current research has focused on the development of biomimetic entubulation strategies termed nerve guidance channels (NGCs). While early attempts at improving nerve regeneration focused on optimization of the outer conduit, recent evidence suggests that the inner lumen also plays an important role. These next generation NGCs are more comprehensive in their approach at encouraging regeneration. Some recently explored methods to optimize regeneration by modifying the inner lumen have included the use growth factors or supportive cells [22, 23].

Various neurotrophic factors, including nerve growth factor (NGF), neurotrophin-3 (NT-3), glial cell-line derived neurotrophic factor (GDNF), and fibroblast growth factor (FGF), are understood to play an integral role in neural cell behaviors including survival, migration, and proliferation [24]. These factors are dynamically regulated as a function of tissue state (i.e. development, injury, regeneration). For example, Bedi et al. demonstrated that adult dorsal root ganglia will extend neurites on lesioned nerves but fail to grow on normal mature nerves, pointing to the importance of these dynamic changes in regulating the growth of axons [25]. Although shown to be beneficial to PNS regeneration, the use of growth factors is complicated by their short half lives and

complex dosing requirements. The inclusion of these cues will likely require the design of adequate delivery mechanisms.

The potential for the use of supportive cells within an NGC has also received considerable attention. Schwann cells are the most attractive candidate for this function as their endogenous source has been shown to be critical for nerve repair via the release of growth factors and release of extracellular matrix components. While numerous studies have been published using Schwann cells within peripheral nerve gap injuries [26, 27], their use is met with several disadvantages including issues with engraftment, survival, immunogenicity, and sourcing. Alternative cell sources have also been explored, including human embryonic kidney cells [28], neural stem cells [29], and bone marrow stromal cells [30]. However, the efficacy and translation potential of these cell types remains to be seen.

1.3 BIOMATERIALS AND PERIPHERAL NERVE REPAIR

When the gap between two nerve stumps is large, the fibrin cable which supports neural cell infiltration fails to form [7]. To this end, an intraluminal biomaterial therapy has been explored as a potential therapeutic strategy for critical gap repair. Matsumoto et al. first demonstrated the utility of an intraluminal filler by successfully bridging a 8cm gap in a canine peroneal nerve with the use of laminin-coated collagen fibers [31]. It is generally accepted that an ideal filler for an NGC should offer a highly controlled environment for nerve cells to grow by providing both mechanical and biological support for emerging neurites. Further, within scaffold design parameters, the intraluminal architecture should include a surface with high density of interconnected pores which are uniformly distributed [32].

The cellular microenvironment following PNS injury contains many complex constituents including extracellular matrix molecules, growth factors, biochemical cues, and ligands. Intricate spatiotemporal regulation of these physical and chemical cues is required to coordinate cellular activities necessary for successful regeneration. Biomaterials can be designed to elicit these particular responses by incorporation of biomolecules [33]. These engineered materials can potentially recapitulate much of the dynamic signaling that occurs in vivo. In doing so, biomaterials provide a tool to gain mechanistic understanding of cell-cell and cell-substrate response. Understanding these responses, and more importantly developing the ability to control them, provides a therapeutic avenue for clinical translation of these scaffolds.

Table 1.1 Potential Roles of Biomimetic Materials (adapted from [34])

Provide a physical form and space for cells to form tissue
Provide a background upon which to present cell adhesion ligands
Store, maintain the activity of, and control the release of soluble components
Act to deliver and spatially organize cells and inductive signals
Morphologically guide tissue growth
Allow transport of oxygen, nutrients, and waste between cells and surrounding tissue
Act as surrogate micro-environments to direct cell behavior

In the context of biomaterials as intraluminal fillers for NGCs, both natural and synthetic options have been explored. These different material choices offer unique properties including mechanical strength, degradation, amenable chemistries for modification, and biocompatibility [35]. One of the more studied options is the use of hydrogels, which is water-saturated polymeric network. The use of a keratin hydrogel within an NGC in a 4 mm sciatic nerve model yielded axon densities that outperformed autograft controls [36], and these results were recently corroborated in a rabbit tibial nerve injury model [37]. Fibrin hydrogels have also demonstrated in vivo efficacy, with

myelinated axon areas that compard that of isograft controls [38]. Poly(ethylene glycol) hydrogels have also been shown to promote PNS regeneration, although issues with swelling have also been reported [39]. The use of Type I collagen has also been shown to positively effect regeneration when used as a biomaterial strategy for repair following injury to the PNS [40]. As mentioned earlier, two FDA-approved conduits are made from Type I collagen (NeuraGen, NeuraMatrix), making it an attractive candidate for use. Higher order modifications have also been introduced into the scaffold design of these intraluminal fillers including attachment of peptides, structural alignment, and chemical anisotropy [35].

1.4 PREFERENTIAL MOTOR REINNERVATION

Despite significant progress in encouraging the regrowth of axons across large gap sizes using various engineered strategies, functional recovery is still limited. This may be due in part to the malrouted reinnervation of emerging neurites where regenerating motoneurons often regrow towards the sensory targets and sensory axons regrow towards muscle. These incorrect neural circuits can lead to muscle weakness, lifelong pain, and inappropriate reflex arcs [41]. Sir Sydney Sunderland, a leader in the field of peripheral nerve injury, once said "The core of the problem is not promoting axon regeneration, but getting them back to where they belong." [42]

After injury, the specificity of regeneration seems to be influenced by both physical (entry into a correct endoneurial tube) and biological (neurotropic and neurotrophic) factors. One phenomenon known as preferential motor reinnervation (PMR) provides an innate mechanism to increase the efficiency of synaptic reconnection.

The phenomenon was first observed by Brushart et al. in the rodent femoral nerve, which provides ideal neuroanatomy for studying the fate of regenerating axons when given equal access to both motor and sensory targets. The femoral nerve begins as a mixed nerve with sensory and motor axons, which eventually branches off into the sensory cutaneous branch and the muscle branch to the quadriceps. If the femoral nerve is damaged proximal to the point to this branch point, the bifurcation serves as an anatomical decision point for regenerating axons. Since in the normal femoral nerve no motor axons are found in the cutaneous pathway, reinnervation of motor axons into this pathway following injury represents a failure of target specificity.

In the context of the femoral nerve, neurites from the proximal nerve ends grow randomly towards the distal end to connect with both motor and sensory targets after injury. However, as reinnervation continues the number of correctly projecting motor axons increases. This tendency for increasing accuracy is the basis for PMR. Unfortunately, as the distance between the proximal and distal end grows the likelihood of PMR decreases, as is the case with clinically relevant gap sizes [43-46].

The mechanisms which govern PMR are not clearly understood, but there are two schools of thought - 1) Schwann cell endoneurial tubes maintain a phenotypic identity which can then be recognized by regenerating motoneurons and/or 2) regenerating motoneurons assess the level of local trophic support in each pathway and remain in the one that provides more, termed trophomorphism.

Ramon y Cajal first suggested the potential for intrinsic differences between motor and sensory pathways in his hallmark studies with muscle spindle reinnervation.

More specifically, he showed that motor axons will escape the incorrect cutaneous pathway to approach their appropriate target, which he attributed to 'neurotrophic influences'. The first molecular difference found between motor and sensory pathways was the discovery of an epitope first found on human natural killer cells (HNK-1) found predominantly in the motor branch of the femoral nerve [47, 48]. Since then, other studies have also demonstrated differences between phenotypic motor and sensory pathways. For example, Nichols et al. showed that a motor or mixed nerve autograft outperforms a sensory nerve autograft when used to bridge a tibial nerve defect. These results suggest intrinsic phenotypic differences available to regenerating neurites in motor and sensory nerve pathways [49]. Hoke et al. demonstrated that Schwann cells express motor and sensory subtypes as elucidated by their unique growth factor release and that this distinct molecular identity is retained after injury [50]. These findings were later corroborated by gene expression studies done on RNA extracts from the cutaneous and quadriceps branch of the femoral nerve [51].

Recent evidence has also suggested that regenerating motor neurons may communicate with Schwann cells via the release of the neurotransmitter acetylcholine (ACh). In vitro and in vivo findings have shown that Schwann cells respond to application of ACh by hyperpolarizing [52] or releasing intracellular calcium [53]. These responses have been shown to be mediated by specific ACh receptors located on the cellular membrane [54]. Vrbova et al. show that selective blocking of Ach receptors reduced motoneuron regeneration and HNK-1 expression, which suggests a pivotal role for Schwann cell/axon communication in the regenerative process [55].

Madison et al. have argued that there is a hierarchy of importance of trophic cues in determining the degree of PMR. The most important determinant seems to be age. Robust PMR is observed in neonatal rats in the absence of distal end-organ targets, which suggests that the young nerve pathway is sufficient for PMR [45]. However, Robinson et al. show that PMR does not occur in adult animals when under similar conditions [56], suggesting a necessity for end-organ reinnervation to encourage PMR. To support this hypothesis, they show that the PMR response is most robust when cutaneous reinnervation is prevented, followed by when equal access is given to both pathways [57]. Follow-up studies from the Robinson/Madison group have also investigated the importance of Schwann cell number or density [58] and terminal branch size in determining pathway choices [59].

1.5 PSA AND HNK-1 IN PNI REPAIR

Polysialic acid (PSA) and HNK-1 have both been implicated in PMR and acceleration of regrowth following nerve damage. Franz et al. demonstrated that while PSA expression is minimal on healthy motor neurons, the level of expression dramatically increases following nerve injury. Importantly, when this upregulation is enzymatically interrupted following injury, PMR is significantly inhibited. HNK-1 is of particular significance in fine-tuning cellular interaction following injury in the nervous system [60, 61]. Notably, in the peripheral nervous system, HNK-1 is primarily expressed on Schwann cells that are associated with motor axons, implicating its role in modality specific action. Martini et al. demonstrated that the presence of HNK-1 increases motor neuron outgrowth, but does not affect sensory neuron outgrowth in vitro. Further, following injury, only Schwann cells that had been previously associated with

motor axon will re-express HNK-1. Sensory-associated Schwann cells do not produce the glycan even with prolonged exposure to motor axons. Collectively, this demonstrates the glia's ability to retain an intrinsic molecular memory following injury, which is important for axon regrowth and targeting [62, 63].

PSA and HNK-1 glycomimetics, identified through phage display and validated in vitro, have been used successfully in small gap repair of peripheral nerve injury when presented in soluble form [64, 65]. However, when a similar methodology was used to treat a larger 'critical' gap size, these cues failed to impart any functional benefit. We hypothesize that clinical translation of these bioactive cues may require increasing the lifetime of their presentation through conjugation to a biomaterial backbone with the additional advantage of providing mechanical support. Additionally, covalent conjugation of these bioactives allows for anisotropic patterning of these bioactives to gain mechanistic understanding and potentially increase regenerative potential following injury.

1.6 THESIS SUMMARY

The broad, long term objective of this research is the development of an implantable construct for peripheral nerve regeneration which both accelerates and directs axonal regrowth. Functional recovery following peripheral nerve injury is often hampered by the inability of emerging neurites to make appropriate connections with their distal targets. We aim to address this limitation by preparing axons for specific interactions with phenotypically specific tracts. Two naturally occurring carbohydrates, polysialic acid (PSA) and an epitope first discovered on human natural killer cells (HNK-

1), have been shown to be integrally involved in axonal regeneration and targeting. Peptide mimics of these carbohydrates, which are more stable and easily produced than their glycan counterparts, have been developed using phage display screening. Previous studies have confirmed the bioactivity of these glycomimetics in solution both *in vitro* and *in vivo*. However, a more stable method for drug delivery is required for clinical translation of these bioactive molecules.

In Chapter 2, we functionalize type I collagen with PSA and HNK-1 peptide mimics. We show that these molecules retain their bioactivity following functionalization to the collagen backbone. Grafted HNK-1 encouraged motor neuron outgrowth, while grafted PSA encouraged sensory and motor neuron outgrowth and enhanced Schwann cell proliferation and process extension.

Given the promising in vitro results, in Chapter 3 we evaluate the use of glycomimetic functionalized collagen hydrogels in a mouse femoral nerve injury model. Functional recovery was assessed using gait and hind limb extension, and was significantly better in all glycomimetic peptide-coupled collagen conditions versus non-functional scrambled peptide-coupled collagen, native collagen, and saline controls. Analysis of cross-sections of the regenerated nerve demonstrated that hydrogels coupled with the PSA glycomimetic, but not HNK, had significant increases in the number of myelinated axons over controls. Conversely, hydrogels coupled with HNK, but not PSA, showed improvement in myelination. Additionally, significantly more correctly projecting motoneurons were observed in groups containing coupled HNK-1 mimicking peptide, but not PSA mimicking peptide. Given the distinct morphological outcomes between the two glycomimetics, our study indicates that the enhancement of recovery

following peripheral nerve injury induced by PSA- and HNK-functionalized collagen hydrogels likely occurs through distinct mechanisms.

In Chapter 4 we evaluate two potential improvements to the use of glycomimetic functionalized collagen by 1) interfacing the hydrogel with a degradable NGC and 2) increasing the concentration of coupled peptide. In the work discussed in Chapter 3, we use a non-degradable polyethylene tube as the outer conduit which is likely not ideal for clinical translation as it may lead to nerve compression, swelling, and pain. We show that that coupled collagen hydrogels can be used as an intraluminal filling for a degradable NGC without reduction in functional or morphological recovery. In our previous in vivo work we did not notice any functional or morphological benefit in our composite hydrogels. We speculated that this may be due to an inadequate amount of each peptide. We show promising evidence that increasing concentrations of the individual glycomimetics within our composite hydrogels results in an improvement in morphological outcome.

In Chapter 5, we attempt to develop an in vitro platform to assess the mechanisms by which glycomimetic-functionalized collagen impart their benefit. We use two sources of motoneurons, dissociated embryonic spinal cord neurons and postnatal spinal cord explants, are used to quantify phenotypic outcomes on our materials. The use of kinase inhibitors is explored as a potential method to disrupt signaling pathways that may be involved.

1.7 REFERENCES

1. Burnett MG, Zager EL. Pathophysiology of peripheral nerve injury: a brief review. Neurosurg Focus. 2004;16(5):E1. Epub 2004/06/04.
2. Seckel BR. Enhancement of peripheral nerve regeneration. Muscle Nerve. 1990;13(9):785-800. Epub 1990/09/01.
3. Levy MN, Berne RM, Koeppen BM, Stanton BA. Berne & Levy principles of physiology. 4th ed. St. Louis, Mo.: Elsevier Mosby; 2006. xvi, 818 p. p.
4. Evans GR. Challenges to nerve regeneration. Semin Surg Oncol. 2000;19(3):312-8. Epub 2001/01/03.
5. Ide C, Tohyama K, Yokota R, Nitatori T, Onodera S. Schwann cell basal lamina and nerve regeneration. Brain Res. 1983;288(1-2):61-75. Epub 1983/12/12.
6. Diseases NCfHSboCo. 9th Revision, Clinical Modification for the following categories: ICD-9 CM Code: 04.3, 04.5, 04.6, 04.7.
7. Bellamkonda RV. Peripheral nerve regeneration: an opinion on channels, scaffolds and anisotropy. Biomaterials. 2006;27(19):3515-8. Epub 2006/03/15.
8. Schlosshauer B, Dreesmann L, Schaller HE, Sinis N. Synthetic nerve guide implants in humans: a comprehensive survey. Neurosurgery. 2006;59(4):740-7; discussion 7-8. Epub 2006/10/14.
9. Miyamoto Y. Experimental study of results of nerve suture under tension vs. nerve grafting. Plast Reconstr Surg. 1979;64(4):540-9. Epub 1979/10/01.
10. Johnson EO, Soucacos PN. Nerve repair: experimental and clinical evaluation of biodegradable artificial nerve guides. Injury. 2008;39 Suppl 3:S30-6. Epub 2008/08/30.
11. Meyer RS, Abrams RA, Botte MJ, Davey JP, Bodine-Fowler SC. Functional recovery following neurorrhaphy of the rat sciatic nerve by epineurial repair compared with tubulization. J Orthop Res. 1997;15(5):664-9. Epub 1998/01/08.
12. Zhao Q, Dahlin LB, Kanje M, Lundborg G. Specificity of muscle reinnervation following repair of the transected sciatic nerve. A comparative study of different repair techniques in the rat. J Hand Surg Br. 1992;17(3):257-61. Epub 1992/06/01.
13. Madison RD, Robinson GA, Chadaram SR. The specificity of motor neurone regeneration (preferential reinnervation). Acta Physiol (Oxf). 2007;189(2):201-6. Epub 2007/01/26.
14. Nectow AR, Marra KG, Kaplan DL. Biomaterials for the development of peripheral nerve guidance conduits. Tissue Eng Part B Rev.18(1):40-50. Epub 2011/08/05.
15. Belkas JS, Shoichet MS, Midha R. Peripheral nerve regeneration through guidance tubes. Neurol Res. 2004;26(2):151-60. Epub 2004/04/10.
16. Williams LR, Longo FM, Powell HC, Lundborg G, Varon S. Spatial-temporal progress of peripheral nerve regeneration within a silicone chamber: parameters for a bioassay. J Comp Neurol. 1983;218(4):460-70. Epub 1983/08/20.
17. Zhao Q, Dahlin LB, Kanje M, Lundborg G. Repair of the transected rat sciatic nerve: matrix formation within implanted silicone tubes. Restor Neurol Neurosci. 1993;5(3):197-204. Epub 1993/01/01.
18. Archibald SJ, Shefner J, Krarup C, Madison RD. Monkey median nerve repaired by nerve graft or collagen nerve guide tube. J Neurosci. 1995;15(5 Pt 2):4109-23. Epub 1995/05/01.
19. Archibald SJ, Krarup C, Shefner J, Li ST, Madison RD. A collagen-based nerve guide conduit for peripheral nerve repair: an electrophysiological study of nerve regeneration in rodents and nonhuman primates. J Comp Neurol. 1991;306(4):685-96. Epub 1991/04/22.

20. Doolabh VB, Hertl MC, Mackinnon SE. The role of conduits in nerve repair: a review. Rev Neurosci. 1996;7(1):47-84. Epub 1996/01/01.
21. Yannas IV, Hill BJ. Selection of biomaterials for peripheral nerve regeneration using data from the nerve chamber model. Biomaterials. 2004;25(9):1593-600.
22. Huang YC, Huang YY. Biomaterials and strategies for nerve regeneration. Artif Organs. 2006;30(7):514-22. Epub 2006/07/14.
23. Hudson TW, Evans GR, Schmidt CE. Engineering strategies for peripheral nerve repair. Clin Plast Surg. 1999;26(4):617-28, ix. Epub 1999/11/30.
24. Jiang X, Lim SH, Mao HQ, Chew SY. Current applications and future perspectives of artificial nerve conduits. Exp Neurol.223(1):86-101. Epub 2009/09/23.
25. Bedi KS, Winter J, Berry M, Cohen J. Adult Rat Dorsal Root Ganglion Neurons Extend Neurites on Predegenerated But Not on Normal Peripheral Nerves In Vitro. The European journal of neuroscience. 1992;4(3):193-200. Epub 1992/01/01.
26. Levi ADO, Guenard LV, Aebischer P, Bunge RP. The Functional-Characteristics of Schwann-Cells Cultured from Human Peripheral-Nerve after Transplantation into a Gap within the Rat Sciatic-Nerve. Journal of Neuroscience. 1994;14(3):1309-19.
27. Guenard V, Kleitman N, Morrissey TK, Bunge RP, Aebischer P. Syngeneic Schwann-Cells Derived from Adult Nerves Seeded in Semipermeable Guidance Channels Enhance Peripheral-Nerve Regeneration. Journal of Neuroscience. 1992;12(9):3310-20.
28. McConnell MP, Dhar S, Naran S, Nguyen T, Bradshaw RA, Evans GRD. In vivo induction and delivery of nerve growth factor, using HEK-293 cells. Tissue Eng. 2004;10(9-10):1492-501.
29. Heine W, Conant K, Griffin JW, Hoke A. Transplanted neural stem cells promote axonal regeneration through chronically denervated peripheral nerves. Exp Neurol. 2004;189(2):231-40. Epub 2004/09/24.
30. Choi BH, Zhu SJ, Kim BY, Huh JY, Lee SH, Jung JH. Transplantation of cultured bone marrow stromal cells to improve peripheral nerve regeneration. International journal of oral and maxillofacial surgery. 2005;34(5):537-42. Epub 2005/08/02.
31. Matsumoto K, Ohnishi K, Kiyotani T, Sekine T, Ueda H, Nakamura T, et al. Peripheral nerve regeneration across an 80-mm gap bridged by a polyglycolic acid (PGA)-collagen tube filled with laminin-coated collagen fibers: a histological and electrophysiological evaluation of regenerated nerves. Brain Research. 2000;868(2):315-28.
32. Kannan RY, Salacinski HJ, Butler PE, Seifalian AM. Artificial nerve conduits in peripheral-nerve repair. Biotechnol Appl Biochem. 2005;41(Pt 3):193-200. Epub 2005/05/18.
33. Zhang N, Yan H, Wen X. Tissue-engineering approaches for axonal guidance. Brain Res Brain Res Rev. 2005;49(1):48-64. Epub 2005/06/18.
34. Santin M. Strategies in regenerative medicine : integrating biology with materials design. New York: Springer; 2009. xviii, 506 p. p.
35. Nectow AR, Marra KG, Kaplan DL. Biomaterials for the development of peripheral nerve guidance conduits. Tissue Eng Part B Rev. 2012;18(1):40-50. Epub 2011/08/05.
36. Sierpinski P, Garrett J, Ma J, Apel P, Klorig D, Smith T, et al. The use of keratin biomaterials derived from human hair for the promotion of rapid regeneration of peripheral nerves. Biomaterials. 2008;29(1):118-28. Epub 2007/10/09.
37. Hill PS, Apel PJ, Barnwell J, Smith T, Koman LA, Atala A, et al. Repair of peripheral nerve defects in rabbits using keratin hydrogel scaffolds. Tissue engineering Part A. 2011;17(11-12):1499-505. Epub 2011/02/01.
38. Nakayama K, Takakuda K, Koyama Y, Itoh S, Wang W, Mukai T, et al. Enhancement of peripheral nerve regeneration using bioabsorbable polymer tubes packed with fibrin gel. Artif Organs. 2007;31(7):500-8.

39. Mahoney MJ, Anseth KS. Three-dimensional growth and function of neural tissue in degradable polyethylene glycol hydrogels. Biomaterials. 2006;27(10):2265-74.
40. Yoshii S, Oka M, Ikeda N, Akagi M, Matsusue Y, Nakamura T. Bridging a peripheral nerve defect using collagen filaments. J Hand Surg-Am. 2001;26A(1):52-9.
41. Sunderland S. Nerves and nerve injuries. 2d ed. Edinburgh ; New York, New York: Churchill Livingstone; distributed by Longman; 1978. xii, 1046 p. p.

42. Sunderland S. Nerve injuries and their repair : a critical appraisal. Edinburgh ; New York: Churchill Livingstone; 1991. x, 538 p. p.
43. Brushart TM, Seiler WAt. Selective reinnervation of distal motor stumps by peripheral motor axons. Exp Neurol. 1987;97(2):289-300. Epub 1987/08/01.
44. Brushart TM. Preferential reinnervation of motor nerves by regenerating motor axons. J Neurosci. 1988;8(3):1026-31. Epub 1988/03/01.
45. Brushart TM. Motor axons preferentially reinnervate motor pathways. J Neurosci. 1993;13(6):2730-8. Epub 1993/06/01.
46. Madison RD, Archibald SJ, Brushart TM. Reinnervation accuracy of the rat femoral nerve by motor and sensory neurons. J Neurosci. 1996;16(18):5698-703. Epub 1996/09/15.
47. Martini R, Bollensen E, Schachner M. Immunocytological localization of the major peripheral nervous system glycoprotein P0 and the L2/HNK-1 and L3 carbohydrate structures in developing and adult mouse sciatic nerve. Developmental biology. 1988;129(2):330-8. Epub 1988/10/01.
48. Martini R, Xin Y, Schmitz B, Schachner M. The L2/Hnk-1 Carbohydrate Epitope Is Involved in the Preferential Outgrowth of Motor Neurons on Ventral Roots and Motor Nerves. European Journal of Neuroscience. 1992;4(7):628-39.
49. Nichols CM, Brenner MJ, Fox IK, Tung TH, Hunter DA, Rickman SR, et al. Effect of motor versus sensory nerve grafts on peripheral nerve regeneration. Experimental Neurology. 2004;190(2):347-55.
50. Hoke A, Redett R, Hameed H, Jari R, Zhou C, Li ZB, et al. Schwann cells express motor and sensory phenotypes that regulate axon regeneration. J Neurosci. 2006;26(38):9646-55. Epub 2006/09/22.
51. Jesuraj NJ, Nguyen PK, Wood MD, Moore AM, Borschel GH, Mackinnon SE, et al. Differential gene expression in motor and sensory Schwann cells in the rat femoral nerve. Journal of neuroscience research. 2012;90(1):96-104. Epub 2011/09/21.
52. Villegas J. Characterization of acetylcholine receptors in the Schwann cell membrane of the squid nerve fibre. The Journal of physiology. 1975;249(3):679-89. Epub 1975/08/01.
53. Stevens B, Fields RD. Response of Schwann cells to action potentials in development. Science. 2000;287(5461):2267-71. Epub 2000/03/24.
54. Rawlins FA, Villegas J. Autoradiographic localization of acetylcholine receptors in the Schwann cell membrane of the squid nerve fiber. The Journal of cell biology. 1978;77(2):371-6. Epub 1978/05/01.
55. Vrbova G, Mehra N, Shanmuganathan H, Tyreman N, Schachner M, Gordon T. Chemical communication between regenerating motor axons and Schwann cells in the growth pathway. The European journal of neuroscience. 2009;30(3):366-75. Epub 2009/08/07.
56. Robinson GA, Madison RD. Developmentally regulated changes in femoral nerve regeneration in the mouse and rat. Exp Neurol. 2006;197(2):341-6. Epub 2005/11/23.
57. Uschold T, Robinson GA, Madison RD. Motor neuron regeneration accuracy: balancing trophic influences between pathways and end-organs. Exp Neurol. 2007;205(1):250-6. Epub 2007/03/21.

58. Madison RD, Sofroniew MV, Robinson GA. Schwann cell influence on motor neuron regeneration accuracy. Neuroscience. 2009;163(1):213-21. Epub 2009/06/10.
59. Robinson GA, Madison RD. Influence of terminal nerve branch size on motor neuron regeneration accuracy. Exp Neurol. 2009;215(2):228-35. Epub 2008/11/15.
60. Franz CK, Rutishauser U, Rafuse VF. Polysialylated neural cell adhesion molecule is necessary for selective targeting of regenerating motor neurons. J Neurosci. 2005;25(8):2081-91. Epub 2005/02/25.
61. Franz CK, Rutishauser U, Rafuse VF. Intrinsic neuronal properties control selective targeting of regenerating motoneurons. Brain. 2008;131(Pt 6):1492-505. Epub 2008/03/13.
62. Martini R, Schachner M, Brushart TM. The L2/HNK-1 carbohydrate is preferentially expressed by previously motor axon-associated Schwann cells in reinnervated peripheral nerves. J Neurosci. 1994;14(11 Pt 2):7180-91. Epub 1994/11/01.
63. Martini R, Xin Y, Schmitz B, Schachner M. The L2/HNK-1 Carbohydrate Epitope is Involved in the Preferential Outgrowth of Motor Neurons on Ventral Roots and Motor Nerves. Eur J Neurosci. 1992;4(7):628-39. Epub 1992/01/01.
64. Mehanna A, Jakovcevski I, Acar A, Xiao M, Loers G, Rougon G, et al. Polysialic acid glycomimetic promotes functional recovery and plasticity after spinal cord injury in mice. Mol Ther.18(1):34-43. Epub 2009/10/15.
65. Simova O, Irintchev A, Mehanna A, Liu J, Dihne M, Bachle D, et al. Carbohydrate mimics promote functional recovery after peripheral nerve repair. Ann Neurol. 2006;60(4):430-7. Epub 2006/09/08.

CHAPTER 2. NEURAL CELL TYPE-SPECIFIC RESPONSES TO GLYCOMIMETIC FUNCTIONALIZED COLLAGEN

Note: This chapter is reproduced from the following publication:

Masand SN, Perron IJ, Schachner M, Shreiber DI. Neural cell type-specific responses to glycomimetic functionalized collagen. Biomaterials; 33(3):790-797.

2.1 INTRODUCTION

Glycans are important regulators of cell and tissue fate in the nervous system [1]. Through their interactions with various neural recognition molecules, such as neural cell adhesion molecule (NCAM) and L1, glycans have been implicated in a diverse range of neurophysiologic processes including myelinogenesis, neurite outgrowth, and synaptogenesis. These molecules aid in the highly regulated spatiotemporal control of cell-cell and cell-substrate interactions during neural development, plasticity, and repair following injury [2].

Two naturally occurring glycans, an epitope first discovered on human natural killer cells (HNK-1) and polysialic acid (PSA), have been shown to be involved in axonal targeting, neuronal regeneration, and glial cell proliferation and migration [3, 4]. Interestingly, HNK-1 has been selectively associated with motoneurons in the peripheral nervous system (PNS), which suggests an explicit role as part of the trophic system which regulates modality specific regeneration [5]. Both of these molecules are upregulated following neural injury, and these lesion-induced changes are understood to be prerequisites for successful regeneration [6]. Importantly, when the expression of

PSA and HNK-1 is experimentally interrupted following PNS injury, regeneration and axonal targeting is significantly inhibited [3, 7, 8].

Despite their noted functional roles, carbohydrates in general have had limited use as therapeutics because of difficulties in their synthesis and their limited stability in vivo. For example, colominic acid – a carbohydrate derivative of PSA – has been used to functionalize electrospun scaffolds and silanized glass for studies of peripheral nerve regeneration, but the results have been mostly disappointing [9, 10]. Additionally, the heterogeneity of length, high metabolic clearance, and potential for immunogenicity of colominic acid remain to be resolved [11]. Alternative strategies have been studied to upregulate glycans following injury, including electrical stimulation of damaged tissue and the implantation of exogenous, genetically modified cells [3, 8, 12, 13]. For example, El Maarouf showed that implantation of astrocytes transfected with a viral vector that aids in the upregulation of PSA leads to increased corticospinal tract axon regeneration following spinal cord injury (SCI) [13]. Further, Eberhardt et al. show that electrical stimulation of damaged femoral nerves in the PNS increases HNK-1 expression, and thereby leads to an increase in muscle reinnervation [8]. While these approaches have produced favorable results in animal models, the likelihood of their clinical translation is limited.

Recent advances in the understanding of carbohydrate-protein interactions and the accessibility of various screening techniques have allowed for the discovery of glycomimetic peptides. These molecular mimics generally retain the functionality of their glycan counterparts, with the added potential benefits of ease of production, increased stability, and reduced cost [14, 15]. Peptide mimics of HNK-1 and PSA have

been developed using phage display screening [16, 17]. Previous studies have confirmed the bioactivity of these glycomimetics in soluble form both in vitro and in vivo [11, 18-21]. In a recent study using the PSA glycomimetic for repair following dorsal hemisection of the T9 mouse spinal cord, Marino et al. show that the peptide is only detectable for 48 hours after single-dose delivery in solution [11]. Mehanna et al. saw improved functional recovery following spinal cord compression in the mouse when the PSA and HNK-1 glycomimetics were delivered locally for two weeks using an osmotic pump [18] . Thus, a more stable, controllable method for presentation of these cues may be required for eliciting optimal biological effects, particularly for clinical applications that require extended exposure to the molecules.

Incorporating these molecules into a biomaterial strategy may allow for the necessary improvements in stability and presentation for clinical translation to regenerative therapies, if the molecules retain their bioactivity. Many other bioactive functionalized biomaterials have been developed, including those with laminin or immobilized growth factors, but these ligands generally have broad effects on neural cell behavior. Conversely, PSA and HNK-1 have unique and phenotypically specific responses that provide interesting opportunities for its in vivo use. Instead of simply accelerating or encouraging regeneration, biomaterials for nervous system injury may be improved by including cues that increase the efficiency of synaptic reconnection.

To this end, we have functionalized type I collagen scaffolds with the PSA and HNK-1 peptide mimics. Type I collagen is non-cytotoxic, has suitable chemical groups for modification, and has been shown to promote nervous system regeneration [22, 23]. Suspensions of the functionalized oligomeric type I collagen form stable hydrogels at

physiologic temperature and pH. Thus, the material retains all the functional benefits of a hydrogel including high surface area to volume ratio, pore interconnectivity, complete void filling, and suitable mechanical strength for neural tissue engineering applications. Additionally, since the carbohydrates are found tethered to the extracellular matrix or presented on the cell surface [2], grafting the glycomimetics to a scaffold may provide for more physiologically relevant presentation.

In this study, we assess the bioactivity of the glycomimetics after covalent conjugation to a collagen hydrogel. We assay the response of several neural cell types that have been previously shown to be differentially affected by the presence of the glycans and/or glycomimetics in solution. Collectively, these studies provide insight into the potential use of glycomimetic functionalized biomaterials as a novel approach for neural tissue engineering.

2.2 METHODS

2.2.1 Peptide Mimics

From sequences identified previously as functional glycomimetics [16, 17], one linear glycomimetic peptide was selected for HNK-1 (FLHTRLFV, MW: 1032.24) and for PSA (SSVTAWTTG, MW: 908.97). Additionally, a cyclic version of the PSA mimetic (cyc PSA: CSSVTAWTTGC) was tested; the peptide was made cyclical by bridging two flanking cysteine residues with a disulfide bridge. A scrambled version of the HNK-1 peptide (TVFHFRLL) and a reverse version of the PSA peptide (rev PSA: GTTWATVSS) served as controls. All peptides were acquired from a commercial vendor (Genscript, Piscataway, NJ). The scrambled and reverse sequences were queried

in PepBank, an online database of peptides, to ensure their lack of known biological activity.

2.2.2. Functionalization of Collagen

Peptide sequences were covalently conjugated onto oligomeric type I collagen using the heterobifunctional crosslinker 1-Ethyl-3-(3-dimethylaminopropyl) carbodiimide (EDC) as previously described [24]. Briefly, fetal calf type I collagen (EPC, Owensville, MO) was reconstituted to 3 mg/mL in 0.02N acetic acid to make an oligomeric collagen solution. To activate carboxyl groups, 2 mg of peptide were dissolved in 2 mL of MES buffer (Fluka) containing 1mM EDC (Pierce) and reacted for 15 minutes at 37 °C. Following this incubation, the activated peptide was added to 5 mL oligomeric collagen solution and rotated overnight at 4°C. The peptide/collagen solution was dialyzed overnight to remove unattached peptide with two dialysate changes. Finally, the purified solution was lyophilized and reconstituted to 3 mg/mL in 0.02N acetic acid. In a previous study using this conjugation technique, we confirmed that the resulting grafting efficiency is between 50-60%. Additionally, the grafting process does not significantly change mechanical properties, fiber diameter, or fiber density of the hydrogel [24].

2.2.3. Preparation of Hydrogels

Collagen hydrogels at 2.0mg/mL were prepared as previously described [25]. Briefly, native or functionalized oligomeric collagen solutions at 3 mg/mL were neutralized using solutions in the following ratios: 2% 1M Hepes (Fluka), 14% 0.1N NaOH, 10% 10X Minimum Essential Medium (Sigma), 5.2% M199 (Sigma), 0.1% Penicillin/Streptomycin (P/S; Sigma), 1% L-glutamine (L-glut; Sigma), 67.7% native or peptide-functionalized collagen. For simplicity, hydrogels grafted with the HNK-1

glycomimetic are referred to as HNK-grafted hydrogels. For composite hydrogels containing both of the grafted glycomimetics, 33.85% of each of the HNK- and PSA-functionalized collagen solutions were neutralized using the formulation above, and these composite hydrogels are abbreviated as PSA/HNK-grafted. The hydrogel solution was plated into a microtiter plate and incubated at 37°C to enable self-assembly.

2.2.4. Collagenase Assay

A collagenase assay was used to test the enzymatic stability of the modified hydrogel. Native or peptide grafted oligomeric collagen solutions were spiked with 10% FITC-collagen solution (EPC). The fluorescently tagged collagen fibrils have an equivalent periodic pattern to native collagen when assessed using electron microscopy. Additionally, radioactively labeled collagen and fluorescently labeled collagen do not differ significantly in their degradation [26]. Thus, the activity of collagenase is not affected by the addition of the fluorophore. Lyophilized collagenase was dissolved in PBS at a concentration of 15 Units/mL. The spiked oligomeric collagen was neutralized using appropriate buffers, and then 400 μL of the 2.0 mg/mL spiked solution was added to individual wells of a 12-well microtiter plate and placed in the incubator at 37°C. The collagenase solution was added after self-assembly and incubated at 37°C with the hydrogel. A 50 μL sample of the supernatant was collected at various time points and added to a 96 well microtiter plate, and the fluorescence intensity was measured on a fluorescence spectrometer (Tecan Instruments). An increase in fluorescence correlated to the amount of collagen liberated from the hydrogel.

2.2.5. Cell Culture

2.2.5.1. Dorsal root ganglia

Dorsal root ganglia (DRGs) were isolated from specific pathogen-free chick eggs at embryonic day 8 (Charles River Laboratories). For dissociated cultures, ganglia were added to 0.25% trypsin for 20 minutes. Cells were then pelleted, washed in media, mechanically dissociated and counted using trypan blue exclusion. Whole and dissociated cells were cultured in Dulbeco's Modified Eagle's Medium (DMEM) containing 10% fetal bovine serum (FBS), 1% L-glut, and 1% P/S, supplemented with 100ng/ml nerve growth factor (NGF; R&D Systems, Minneapolis, MN).

2.2.5.2. NSC-34

NSC-34 is hybrid cell line that was produced via the fusion of motor neuron enriched embryonic mouse spinal cord cells with mouse neuroblastoma cells [27]. Notably, consistent with a motoneuron phenotype, these cells extend neurites, generate action potentials, and express neurofilament and choline acetyltransferase. Generally, cultures will contain two populations—small, undifferentiated cells and larger, non-dividing cells with processes. To maintain their active proliferation, NSC-34 cells were incubated in high-glucose DMEM supplemented with 10% FBS, 0.5% P/S, and 0.5% L-glut. Cells were passaged every 2 - 3 days. To induce differentiation towards the motoneuron-like phenotype, media was changed to 1:1 DMEM plus Ham's F12, 1% FBS, 1% P/S, and 1% modified Eagle's medium with non-essential amino acids for 5 – 7 days prior to plating on hydrogels [28].

2.2.5.3. Spinal Cord Neurons

Dissociated spinal cord neurons (SCNs) were isolated from E15 Sprague Dawley rats as previously described [29]. Spinal cords were excised and meninges removed.

Cords were transferred to a 15 mL centrifuge containing 0.05% trypsin in HBSS and incubated at 37°C for 20 minutes. Following this incubation, the sample was centrifuged and supernatant removed and replaced with a 10% serum-containing media. The tissue pieces were mechanically dissociated via trituration and large pieces of debris were allowed to settle. The supernatant, which contained the single cell suspension, was transferred to a 50 mL centrifuge tube and placed in a 37°C humidified incubator. The remaining tissue pieces were subjected to a second dissociation and were then pooled with dissociated cells from the first. The combined supernatants were filtered through a 40-µm pore-sized nylon mesh. Cells were centrifuged for 5 minutes at 1000 rpm at 4°C, resuspended in 10% serum containing media, and triturated with a fire-polished Pasteur pipette. The cell suspension was transferred to a T-75 tissue culture flask and incubated for 30 minutes at 37 °C to enhance the purity of the culture via differential adhesion of the contaminating glia and fibroblasts vs. neurons. The neuron-enriched supernatant was removed with a serological pipette and transferred to a centrifuge tube. Following centrifugation, the cells were resuspended in neurobasal media supplemented with B-27, penicillin/streptomyocin, L-glutamine, and beta-mercapoethanol prior to plating.

2.2.5.4. RSC-96

RSC-96, a spontaneously transformed rat Schwann cell line, were grown in DMEM containing 10% FBS, 1% L-glut, and 1% P/S. Cells were passaged using standard cell culture techniques at 80% confluency.

2.2.6. Cellular Assays

2.2.6.1. Dorsal Root Ganglia Explant Outgrowth

Explant outgrowth has been shown to have high variability from egg to egg. Accordingly, native and either PSA- or reverse PSA-grafted conditions were included as baseline conditions for all experimental days. DRG explants were plated individually in a 24 well microtiter plate on native or functionalized collagen hydrogels and incubated for seven days in the presence of NGF. For studies investigating the bioactivity of the soluble peptide, the media was supplemented with 100μM of the glycomimetic once at the beginning of the culture period. Following this incubation period, ganglia were fixed and stained with mouse anti-neurofilament 200 (Sigma) followed by goat-anti-mouse AlexaFluor488 secondary antibody (Invitrogen). Epifluorescent images were taken on an Olympus IX81 using a 10X objective and analyzed using ImageJ (NIH). Explant outgrowth was measured by taking the length of individual neurites extending from the perimeter of the ganglion to growth cone end.

2.2.6.2. Dissociated Dorsal Root Ganglion Neuron Extension

Dissociated cell cultures were plated on collagen hydrogels in a 24 well microtiter plate at a seeding density of 25,000 cells/well. Cells were grown for 3 days in the presence of NGF and stained with mouse anti-NF200, followed by goat-anti-mouse AlexaFluor 488. Approximately 10 images were taken per well using a 10X objective. Images were analyzed using ImageJ, and neurite extension was considered to be the length of the presumptive axon, or the longest neurite. Measurements were only included if the recorded length was longer than the cell body diameter [16].

2.2.6.3. NSC-34 Extension

Differentiated cells were plated on native or functionalized hydrogels at a density of 10,000 cells/well in a 24 well microtiter plate. Cells were incubated for 7 days with one complete media change on day 3 or 4. Cultures were then fixed, and stained immunohistochemically with mouse anti-neurofilament 200, followed by goat anti-mouse AlexaFluor488 secondary antibody, TRITC-conjugated phalloidin (Sigma), and DAPI (Invitrogen). Approximately ten images per well were taken using a 10X objective and analyzed using ImageJ. As this culture contained both mature, non-proliferating motoneuron like cells and proliferating cells, only neurons with a large soma and neurites at least the length of their soma were measured [30].

2.2.6.4. Spinal Cord Neuron Extension

Dissociated spinal cord neurons were immediately plated on native or functionalized collagen hydrogels at 75,000 cells per/well in a 24 well microtiter plate. Following a 4-day incubation period, cells were fixed and stained using rabbit anti-MAP-2 (Millipore) followed by goat anti-rabbit AlexaFluor 488. Cultures were co-stained with TRITC-conjugated phalloidin and DAPI to identify contaminating cells and qualitatively assess the purity of the cell population. Approximately fifteen images per well were taken using a 20X objective and analyzed using ImageJ. Neurite extension was considered to be the length of the presumptive axon, or the longest neurite. Measurements were only included if the recorded length was longer than the cell body diameter [16].

2.2.6.5. RSC-96 Proliferation

RSC-96 cells were grown in low (0.5%) serum containing media for 48 hours to synchronize the cell cycle prior to plating for proliferation studies. Cells were then resuspended in 10% serum containing media and plated on collagen hydrogels at a seeding density of 10,000 cells/well in a 24 well microtiter plate**.** After 23 hrs, 10 µM bromodeoxyuridine (BrdU) was added to the cells for one hour. Cells were then fixed and stained with an anti-BrdU goat anti-mouse AlexaFluor568 and counterstained with DAPI. Five images per well were captured using a 10X objective. ImageJ was used to quantify the number of $BrdU^+$ and $DAPI^+$ cells.

2.2.6.7. RSC-96 Process Extension

In an effort to slow proliferation prior to plating, cell cultures were grown in low serum containing media for 24 hours. Cells were seeded on collagen hydrogels at 5,000 cells/well in a 48 well microtiter plate and maintained in low serum media for 4 days. For histological staining, cells were fixed followed by incubation with TRITC-conjugated phalloidin for 1 hour at room temperature. Only cells with limited contact with neighboring cells and extensions at the length of the longest axis of the cell body were measured. Extension measurements were normalized to the average extension length on native collagen.

2.2.7. Statistical Analysis

The number of samples per experimental condition is summarized in **Table 2.1**. Variance analysis using a two-way ANOVA (length of processes/percent proliferation and type of hydrogel) was used followed by posthoc pairwise comparisons with Tukey's test. Differences were considered significant at $p < 0.05$.

	Sensory		**Motor**		**Glial**	
Condition (Sequence)	Explant Extension	Dissociated Extension	NSC-34 Extension	SCN Extension	RSC-96 Proliferation	RSC-96 Extension
Native	n = 12	n = 6	n = 3	n = 4	n = 4	n = 3
Scramble (TVFHFRLL)	n = 3	n = 3	n = 3	n = 3	n = 4	n = 3
PSA (SSVTAWTTG)	n = 9	n = 6	n = 3	n = 4	n = 4	n = 3
cyc PSA (CSSVTAWTTGC* G)	n = 3	N/A	N/A	N/A	N/A	N/A
rev PSA (GTTWATVSS)	n = 7	N/A	N/A	N/A	N/A	N/A
HNK (FLHTRLFV)	n = 3	n = 6	n = 3	n = 4	n = 4	n = 3
PSA/HNK	N/A	n = 6	n = 3	n = 4	n = 3	n = 3
Soluble PSA (SSVTAWTTG)	n = 3	N/A	N/A	N/A	N/A	N/A
Soluble rev PSA (GTTWATVSS)	n = 3	N/A	N/A	N/A	N/A	N/A

Table 2.1 Summary of experimental conditions. 'n' represents the number of independent experiments per hydrogel condition. * Denotes a disulfide linkage between cysteine residues.

2.3 RESULTS and DISCUSSION:

2.3.1. Hydrogel Degradation

Type I collagen has been used in a number of regenerative strategies for nervous system repair. It is biocompatible, provides a biologically active scaffold, and can be formed into a hydrogel, sponge, or powder. In a previous study using a similar functionalization scheme, we showed that the grafting process does not significantly affect fiber diameter, porosity, or mechanical strength of the scaffold [24]. However, as the long-term use of this scaffold is as a biomaterial therapy, the rate of proteolytic degradation of the material should also be preserved by functionalization.

The enzymatic degradation of the functionalized collagen was compared to native collagen with a collagenase assay, where the intensity of liberated fluorescently labeled collagen was sampled over time. The results in **Figure 2.1** show the increase in fluorescence intensity over time following collagenase treatment for both samples. There were no significant differences between the measured fluorescence in the native and glycomimetic grafted conditions during the 48 hours of collagenase exposure. Therefore, the proteolytic stability and degradation rate of the collagen hydrogel is not affected by the grafting process.

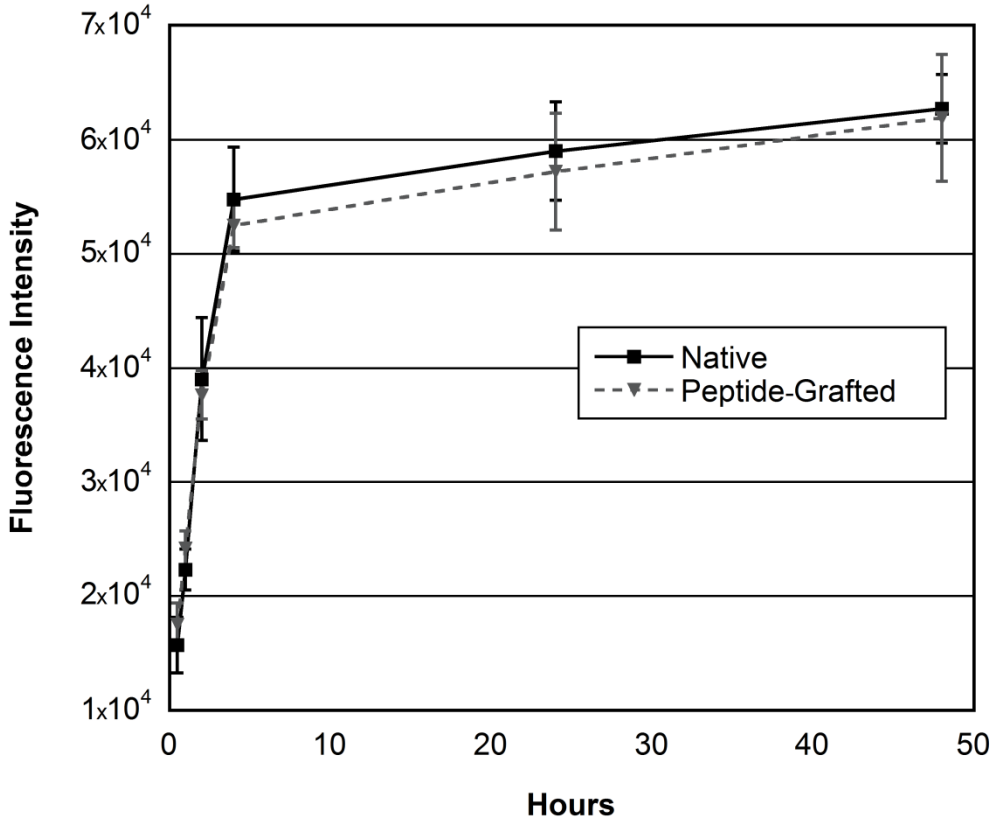

Figure 2.1 Proteolytic stability of glycomimetic peptide-grafted hydrogels. FITC-tagged collagen was used to fluorescently spike native and peptide-grafted hydrogels. After collagenase exposure, the supernatant from the hydrogels was collected and the fluorescence intensity measured, which correlated with the amount of liberated collagen. The intensity of liberated collagen did not differ between the native and peptide-grafted hydrogels.

2.3.2. Sensory Neurons

2.3.2.1. Whole explant DRGs

Whole explant studies were performed to assess the bioactivity of the peptides in grafted form and reduce the number of conditions in subsequent studies with other cultures (**Figure 2.2A**). Similar to previous studies [31], native and peptide-grafted collagen hydrogels supported the adhesion, extension, and migration of cells from chick DRG explants which contained neurons, Schwann cells, and fibroblasts. Thus, the native collagen substrate is suitable for neural culture and our modification of the matrix does not affect this biocompatibility.

DRG neurite extension was not significantly different on HNK-grafted hydrogels when compared to native or scramble-grafted conditions, whereas the grafted linear PSA was significantly different from native, scramble-, and HNK- grafted conditions ($p = 0.0002$, $p = 0.0039$, and $p = 0.0123$, respectively). These results are in agreement with previously reported studies that demonstrate that HNK-1, whether in the carbohydrate or the glycomimetic form, do not affect outgrowth of sensory neurons [16].

In the initial studies by Torregrossa et al., which discovered and assessed the bioactivity of the PSA mimotope, DRGs were incubated with media supplemented with the cyclic, linear, or reverse version of the peptide sequence. Only the cyclic version of the peptide significantly increased neurite outgrowth. The response of the glycomimetics when grafted to collagen was substantially different than when in solution. Neurite extension on hydrogels grafted with cyclic PSA (cycPSA) was not significantly different than on the native or other peptide-grafted hydrogels. However, the linear PSA-grafted

glycomimetic significantly increased neurite extension compared to native and scramble-grafted conditions. Interestingly, the grafted linear reverse PSA (revPSA) sequence also significantly increased extension compared to native hydrogels ($p = 0.0323$), though not when compared to other peptide-grafted hydrogels. The conjugation of a scrambled peptide to the collagen backbone did not significantly improve or inhibit neurite extension compared to native collagen. Thus, the effects of peptide-grafted collagen on neuronal extension are sequence specific, and the grafting process itself does not significantly affect outgrowth.

Tethering the linear and reverse sequences to collagen limits the conformational changes available to the peptides when compared to the soluble form, perhaps similar to the constraints imparted by cyclizing the peptide. We suspect that the stable conformations of the soluble, linear peptides mask the active binding sites, but that these conformations are unavailable in the grafted or cyclized peptides. While it was unexpected that the linear reverse sequence of PSA would impart any effect, previous studies have reported the bioactivity of the reverse sequence of peptides. In a study by Ratcliffe et al. that evaluated the guiding behavior of laminin, YIGSR, a bioactive motif on laminin, and its reverse sequence RSGIY significantly affected the guidance behavior of sensory axons. Notably, in a manner similar to our results, the reverse sequence was not as effective [32]. The linear and linear reverse sequences were also tested in soluble form with DRGs on native collagen hydrogels. Neurite extension was not significantly different between cultures incubated with and without the soluble peptide (**Figure 2.3**). Thus, the linear and linear reverse sequences appear to only affect neurite extension when immobilized, such as through conjugation to collagen..

There is also evidence to suggest that immobilized cyclic peptides may require a spacer arm to achieve optimal biological effects. Kantlehner et al. showed that an adequate spacer arm was required for osteoblast adhesion and proliferation on poly(methyl methacrylate) surfaces functionalized with cyclic RGD [33]. Without this spacer, the grafted molecule may not be effectively available for interaction with ligands on the cell surface [34]. Generally, however, the necessity for a spacer in a functionalization scheme must be examined case-by-case [35]. There is also the potential for limited grafting efficiency with the cyclic version of the peptide due to the disulfide bridge creating steric hinderance on the carboxyl end of the peptide. Thus, the cyclized peptide may not be readily activated by EDC or may not have sufficient access to free primary amines on the collagen backbone. However, the EDC can readily activate the carboxyl end of linear and linear reverse nonamer sequence and this peptide likely has more access to the lysine and arginine residues on collagen. Unfortunately, the difficulty in synthesizing a FITC-tagged cyclic PSA molecule precluded any quantitative comparisons. The influence of peptide sequence, structure, conformation, and mode of presentation may merit future investigation to render scaffolds with optimal bioactivity. However, given our objective to develop a biomaterial that elicited specific behaviors from different neural cells, the remainder of the PSA studies were performed with only the linear form of the peptide mimic.

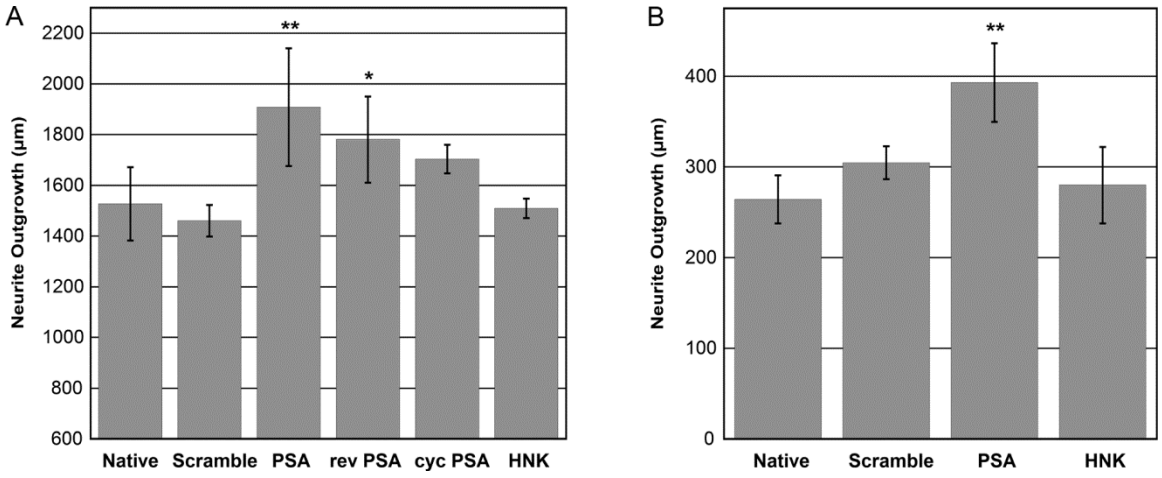

Figure 2.2 Neurite outgrowth from sensory neurons on glycomimetic peptide-grafted hydrogels. Sensory neurite extension from (A) dorsal root ganglia explants and (B) dissociated dorsal root ganglia neurons on native and peptide-grafted collagen hydrogels. Neurons respond best to the hydrogels grafted with the linear form of the PSA-, and did not respond to the scramble-, cyc PSA-, or HNK- grafted hydrogels. While rev PSA-grafted hydrogels yielded significantly longer neurites from explants than native, they were not statistically different from other conditions. Mean values +/- SD are shown. *Denotes statistically significant difference ($p < 0.05$) from native condition. **Denotes statistically significant difference ($p < 0.05$) from native, scramble grafted, and HNK-grafted hydrogels.

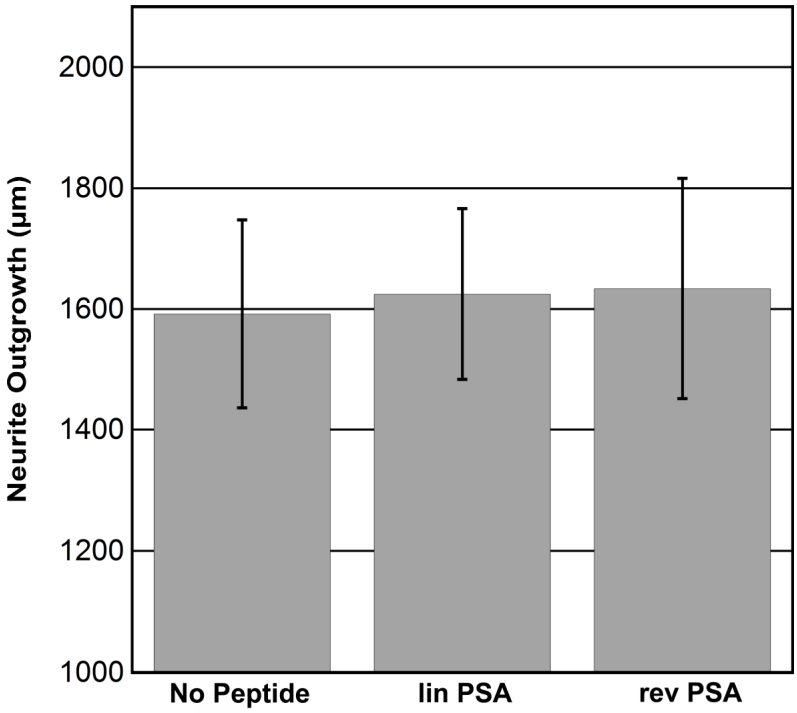

Figure 2.3 Neurite outgrowth from sensory neurons on native collagen hydrogels supplemented with soluble peptide. Sensory neurite extension from dorsal root ganglia explants cultured on native collagen hydrogels, supplemented with soluble linear (linPSA) or soluble reverse PSA (revPSA) peptide mimics. No statistical differences in explants outgrowth were noted between conditions.

2.3.2.2. Dissociated DRG Cultures

With dissociated DRG cultures, we can visualize the neuron in its entirety and have less experimental variability between cultures (**Figure 2.2B**). More so than whole explants, these cultures have been noted to be particularly sensitive to the presentation of neurotrophic factors, and the cultures can be purified to limit the influence of Schwann cells and fibroblasts on neurite extension [36]. As shown in **Figure 2.2B**, neurite extension on native and scramble grafted hydrogels was not significantly different from one another. However, neurite extension was significantly increased on PSA-functionalized hydrogels compared to native, scrambled-, and HNK- grafted conditions ($p < 0.0001$, $p = 0.0148$, and $p = 0.0003$, respectively). Similar to the whole explant cultures, HNK-grafted conditions were not significantly different than scramble grafted or native conditions. Interestingly, in dissociated cultures the percent difference in neurite extension between native and PSA-grafted hydrogels was approximately 2 times more than in the whole explant cultures (48.7% and 24.9% respectively), which may be a function of the level of interaction between the sensory neuron and the substrate. In dissociated cultures, the neuron grows directly on the functionalized surfaces, whereas neurites in explant cultures are more likely to interact with migrating Schwann cells and fibroblasts.

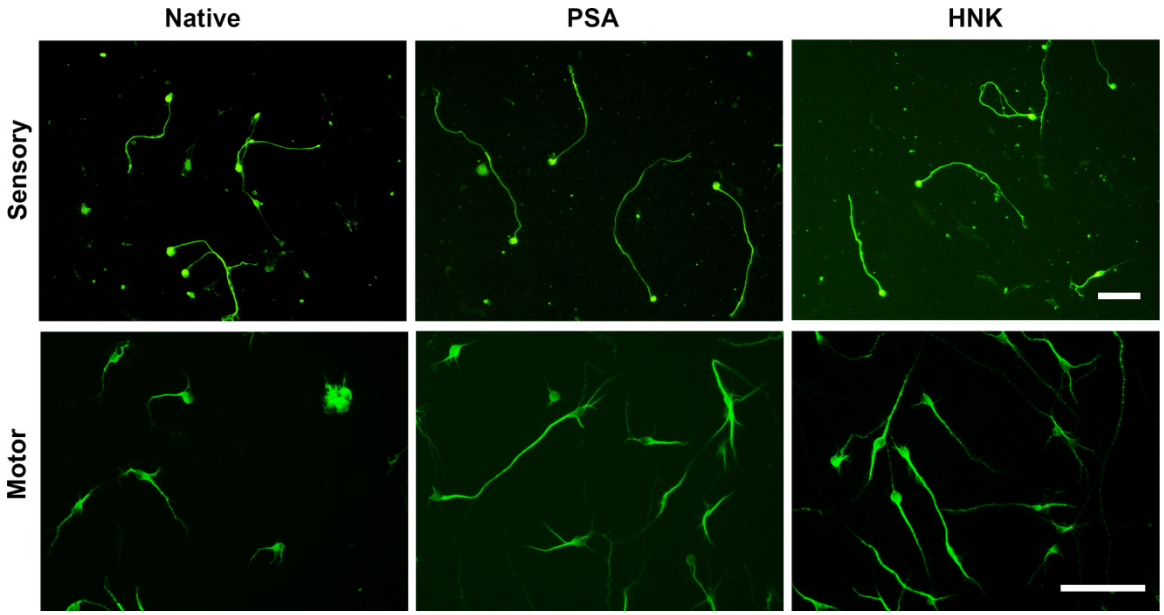

Figure 2.4 Neuronal phenotypic specificity of glycomimetic peptide-grafted hydrogels. Representative images of NF-200 immunolableled dissociated DRG neurons (top panel), which extended significantly longer neurites on hydrogels grafted with PSA compared to native and HNK-grafted conditions. Representative images of MAP-2 immunostained dissociated spinal cord neurons (bottom panel), which extended significantly longer neurites on both PSA- and HNK-grafted hydrogels compared to native collagen. Scale bar represents 100 µm.

2.3.3. Motor Neurons

2.3.3.1. NSC-34

As with sensory neurons, the linear grafted PSA glycomimetic significantly increased neurite extension when compared to native and scramble-grafted hydrogels ($p < 0.0001$ and $p = 0.0002$). HNK-functionalized hydrogels also increased motor neuron extension compared to native and scramble-grafted hydrogels ($p = 0.0001$ and $p = 0.0048$). However, neurite extension was not significantly different between the PSA- and HNK- functionalized conditions. No statistical differences were noted in neurite outgrowth from NSC-34 cells between native and scramble-grafted collagen hydrogels (**Figure 2.5A**).

When considering the results of both neuronal populations, HNK-functionalized hydrogels encouraged motor neuron outgrowth, but not sensory. Previously reported studies have demonstrated the glycan HNK-1 is expressed selectively on Schwann cells associated with motor axons [5]. In addition, when presented in solution, both the carbohydrate and the glycomimetic were shown to enhance neurite outgrowth from motoneurons, however outgrowth from sensory neurons was unaffected [5, 16]. Thus, conjugation to collagen does not appear to affect the modality specific responses to the HNK-1 mimotope.

As these molecules in their carbohydrate form interact with distinct ligands, including NCAM, L1, P0, and myelin associated glycoprotein (MAG) [2], we also applied a combination of the peptides to perhaps induce a synergistic increase in motoneuron outgrowth. The amount of each of the glycomimetics in the composite

hydrogel was 50% of that of the full strength grafted glycomimetics. Although the combined peptides significantly increased neurite extension compared to native and scramble-grafted conditions ($p < 0.0001$ and $p = 0.0019$), there was no statistical difference between the composite substrate and those grafted with either of the glycomimetics alone.

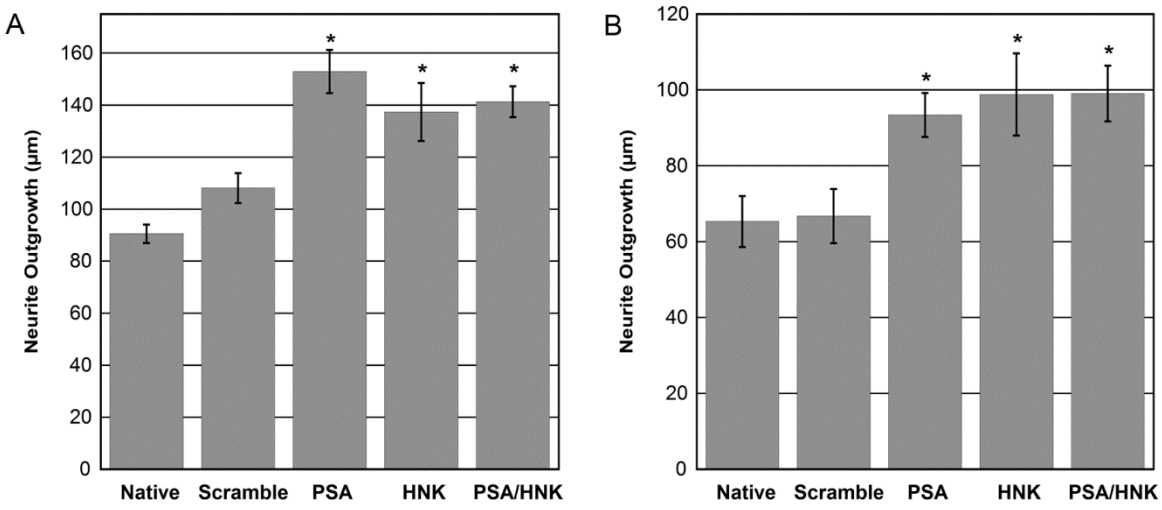

Figure 2.5 Neurite outgrowth from motor neurons on glycomimetic peptide-grafted hydrogels. (A) NSC-34 neurite outgrowth and (B) dissociated spinal cord neuron outgrowth on native and peptide-grafted hydrogels. PSA- and HNK- grafted hydrogels induced significantly longer neurite extension compared to native and scramble- grafted conditions. Additionally, a PSA/HNK composite hydrogel, made from a 50/50 mix of the individual glycomimetic collagen solutions, yielded significantly longer neurites than native and scramble-grafted hydrogels. However, none of the glycomimetic peptide-grafted conditions were different from one another. Mean values +/- SD are shown. * Denotes statistically significant difference ($p < 0.05$) from native and scramble-grafted hydrogels.

2.3.3.2. Primary Rat SCNs

We also investigated the functional response in primary spinal cord neuron-enriched cell cultures (**Figure 2.4 & 2.5B**). The grafted scrambled peptide did not significantly improve or inhibit neurite extension from primary SCNs compared to native hydrogels. Similar to NSC-34 cultures, we observed that the neurites on the PSA-functionalized hydrogels were significantly longer than native and scramble-grafted collagen hydrogels ($p = 0.0013$ and $p = 0.004$). HNK-grafted hydrogels yielded significantly longer neurites compared to native and scramble-grafted hydrogels as well ($p = 0.0002$ and $p = 0.0008$). Additionally, while the PSA/HNK composite hydrogel significantly increased neurite extension compared to native and scramble-grafted hydrogels ($p = 0.0002$ and $p = 0.0007$), there were no significant differences between the composite hydrogel and the individual glycomimetic peptide-grafted hydrogels. It is possible that our composite hydrogels did not further improve neurite extension in either of our motoneuron cultures because there was an inadequate amount of each glycomimetic. Future studies will investigate various ratios of the PSA/HNK composite hydrogels to find the critical amount of each required.

2.3.4. Schwann Cells

PSA, HNK-1, and their glycomimetics have been shown to affect glial cell behaviors. As neuron/glial apposition is crucial to nervous system regeneration, the ability to manipulate this interaction may be of importance. Thus, we assayed how our grafted biomaterials affect the proliferation (**Figure 2.6A, B**) and process extension (**Figure 2.6C, D**) of Schwann cell populations. There were no significant differences in

the percentage of proliferating Schwann cells between native and scramble grafted hydrogels. Additionally, HNK-grafted glycomimetics did not significantly affect RSC-96 proliferation rate. Interestingly however, only hydrogels functionalized with PSA significantly increased RSC-96 proliferation compared to native (PSA $p = 0.0005$; PSA/HNK $p = 0.0035$), scramble grafted, and HNK- grafted conditions. There were no significant differences in process extension among native, scramble-grafted, and HNK-grafted hydrogels. The only significant differences in extension were in PSA-containing hydrogels (PSA; PSA/HNK), compared to native (PSA $p = 0.0017$; PSA/HNK $p = 0.0001$), scramble-grafted (PSA $p < 0.0001$; PSA/HNK $p < 0.0001$), and HNK- grafted (PSA $p = 0.0145$; PSA/HNK $p = 0.0011$) conditions. Both experiments are in agreement with a previous study that demonstrates the ability for the PSA glycomimetic in solution to increase Schwann cell proliferation rates and process extension length [19].

Schwann cells have been categorized into motor or sensory phenotypes as dictated by the type of axons with which they interact [37]. As the glycan HNK-1 is reported to be expressed on Schwann cells associated with motor axons only [5], there may be phenotypic-specific effects of the glycomimetic counterparts on Schwann cells. It is possible that the cell line that we have chosen in our study does not adequately represent the motor Schwann cell phenotype, which would explain the lack of activity of HNK-grafted hydrogels. Unfortunately, isolating and maintaining a motor Schwann cell population is not trivial. Evidence suggests that many of the phenotypic specific markers, like the glycan HNK-1, are lost upon removal from in situ conditions. For example, a recent study by Bock et al. showed that the glycan HNK-1 is expressed in situ on adult

canine Schwann cells but are immunonegative for the glycan upon in vitro culture [38]. Future studies will evaluate the glial response of HNK-grafted scaffolds in vivo.

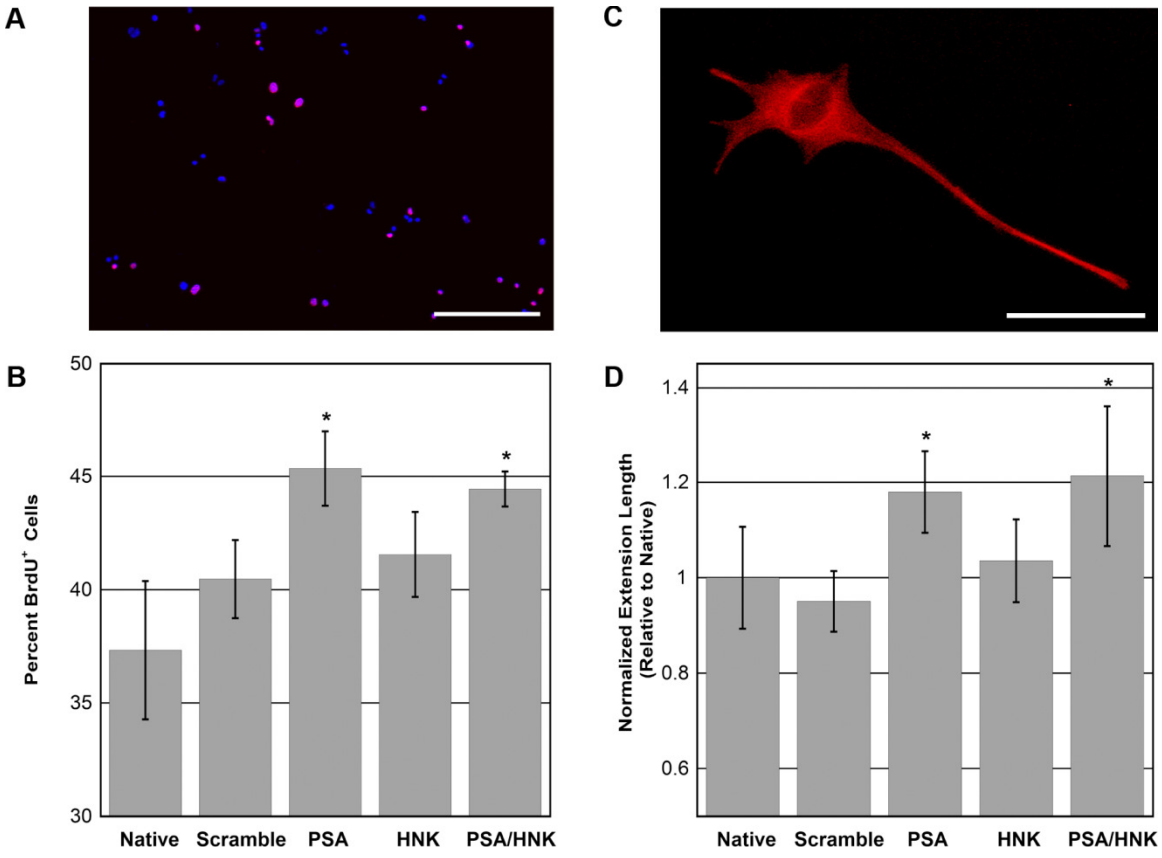

Figure 2.6 Schwann cell response on peptide modified hydrogels. (A) Representative image of DAPI (blue) and $BrdU^+$ (red) stained Schwann cells on hydrogels. Scale bar = 200 µm (B) Percentage of proliferating Schwann cells on native and peptide-grafted hydrogels. (C) Representative image of phalloidin stained Schwann cell cultured on a hydrogel. Scale bar = 50 µm (D) Process extension length of Schwann cells on native and peptide grafted hydrogels normalized to the average response on native collagen. Schwann cell proliferation and process extension was significantly affected by grafted gels that included PSA peptides. Mean values +/- SD are shown. * Denotes statistically significant difference ($p < 0.05$) from native, scramble-grafted, and HNK-grafted conditions.

2.3.5. Applications of Glycomimetic Functionalized Collagen

The phenotypic specificity of glycomimetic functionalized biomaterials may be of particular importance in the PNS. Despite significant progress in encouraging axonal growth following PNS injury, functional recovery is still incomplete which may be due in part to the malrouted reinnervation of emerging neurites. PSA, HNK-1, and their glycomimetics have been implicated in promoting preferential motor reinnervation, a phenomenon by which motor axons reconnect with their appropriate motor targets thereby increasing the accuracy of regeneration [39]. While the glycomimetic in solution has been shown to encourage motor axon targeting following PNI [20], this strategy may not suffice for more challenging injury models. Thus, inclusion of these cues in a biomaterial therapy that localizes and sustains their presentation may have important implications for large, clinically relevant gap sizes.

Recent work has shown that growth cones are responsive to gradients of conjugated cues including laminin and NGF, and that these anisotropic cues can often accelerate the rate of regeneration in vitro and in vivo [40-42]. When presented in solution, the ability to control the presentation of the glycomimetics is not trivial. However, once conjugated to collagen we may be able to pattern the glycomimetics and thereby motivate directional preference in outgrowth. For example, we have previously shown the ability to generate linear gradients of IKVAV and YIGSR grafted collagen scaffolds within microfluidic devices which results in a significant growth bias over isotropic presentation [31].

We note that while other materials, synthetic or natural in origin, can be functionalized with this peptide, the use of collagen provides some notable benefits. The native collagen hydrogel in our study supported the adhesion, extension, and proliferation of all neural populations that were interrogated. This innate bioactivity is likely attributed to the available ligands on collagen, including RGD and GFOGER. The potential does exist that these ligands work in combination with the grafted glycomimetic peptides to elicit or magnify the observed behaviors. Further, the use of collagen allows for the manipulation of the mechanical and structural properties of the scaffold. While we used collagen as a hydrogel in this study, the oligomeric collagen can easily be formed into a sponge or a longitudinally aligned fiber to provide an additional guidance field [22]. Additionally, the hydrogel can self-assemble in situ allowing for complete void filling of an injury-induced gap or use as an intraluminal filling within a nerve guidance conduit.

2.4 CONCLUSION

Despite their role as important regulators of cell and tissue fate in the nervous system, particularly following injury, the therapeutic potential of glycans has been largely unrealized due to difficulties in synthesizing and purifying carbohydrates and their quick degradation in vivo. However, the recent discovery of glycomimetics has provided opportunity to utilize this class of molecules for neural repair. While peptide mimetics of two glycans, PSA and HNK-1, have been used in models of peripheral and spinal cord injury, presentation in solution results in relatively short residence times and limited functional recovery. In this study, we have functionalized oligomeric type I collagen with PSA and HNK-1 peptide mimics. We show that HNK-grafted collagen hydrogels

encourages motor neuron outgrowth, while grafted PSA encourages sensory and motor neuron outgrowth and enhances Schwann cell proliferation and extension. The phenotypic specificity of these molecules may be of particular importance in encouraging preferential motor reinnervation in the PNS and targeting regeneration in the CNS. To the best of our knowledge, this work provides the first successful use of a glycomimetic functionalized biomaterial, and creates a novel, promising approach for nervous system repair.

2.5 ACKNOWLEDGEMENTS

Funding for these studies was provided by the National Institutes of Health (NIH 1R21EB009245-01A1) and US Army contract #W81XWH-04-2-0031, and fellowships from the Rutgers-UMDNJ Biotechnology Training Program (NIH Grant Number 5T32GM008339-20), the National Science Foundation (NSF DGE 0801620, IGERT on the Integrated Science and Engineering of Stem Cells), and the Aresty Research Center for Undergraduates. We confirm that all studies involving experimental animals were conducted under the ethical approval of all relevant bodies.

2.6 REFERENCES

1. Kleene R, Schachner M. Glycans and neural cell interactions. Nat Rev Neurosci. 2004;5(3):195-208. Epub 2004/02/21.
2. Loers G, Schachner M. Recognition molecules and neural repair. J Neurochem. 2007;101(4):865-82. Epub 2007/01/27.
3. Franz CK, Rutishauser U, Rafuse VF. Intrinsic neuronal properties control selective targeting of regenerating motoneurons. Brain. 2008;131(Pt 6):1492-505. Epub 2008/03/13.
4. Abo T, Balch CM. A differentiation antigen of human NK and K cells identified by a monoclonal antibody (HNK-1). J Immunol. 1981;127(3):1024-9. Epub 1981/09/01.
5. Martini R, Schachner M, Brushart TM. The L2/HNK-1 carbohydrate is preferentially expressed by previously motor axon-associated Schwann cells in reinnervated peripheral nerves. J Neurosci. 1994;14(11 Pt 2):7180-91. Epub 1994/11/01.

6. Martini R. Expression and functional roles of neural cell surface molecules and extracellular matrix components during development and regeneration of peripheral nerves. J Neurocytol. 1994;23(1):1-28. Epub 1994/01/01.
7. Franz CK, Rutishauser U, Rafuse VF. Polysialylated neural cell adhesion molecule is necessary for selective targeting of regenerating motor neurons. J Neurosci. 2005;25(8):2081-91. Epub 2005/02/25.
8. Eberhardt KA, Irintchev A, Al-Majed AA, Simova O, Brushart TM, Gordon T, et al. BDNF/TrkB signaling regulates HNK-1 carbohydrate expression in regenerating motor nerves and promotes functional recovery after peripheral nerve repair. Exp Neurol. 2006;198(2):500-10. Epub 2006/02/08.
9. Assmann U, Szentivanyi A, Stark Y, Scheper T, Berski S, Drager G, et al. Fiber scaffolds of polysialic acid via electrospinning for peripheral nerve regeneration. J Mater Sci Mater Med. 2010;21(7):2115-24. Epub 2010/06/10.
10. Steinhaus S, Stark Y, Bruns S, Haile Y, Scheper T, Grothe C, et al. Polysialic acid immobilized on silanized glass surfaces: a test case for its use as a biomaterial for nerve regeneration. J Mater Sci Mater Med. 2010;21(4):1371-8. Epub 2010/02/02.
11. Marino P, Norreel JC, Schachner M, Rougon G, Amoureux MC. A polysialic acid mimetic peptide promotes functional recovery in a mouse model of spinal cord injury. Exp Neurol. 2009;219(1):163-74. Epub 2009/05/19.
12. Luo J, Bo X, Wu D, Yeh J, Richardson PM, Zhang Y. Promoting survival, migration, and integration of transplanted Schwann cells by over-expressing polysialic acid. Glia. 2010. Epub 2010/12/31.
13. El Maarouf A, Petridis AK, Rutishauser U. Use of polysialic acid in repair of the central nervous system. Proc Natl Acad Sci U S A. 2006;103(45):16989-94. Epub 2006/11/01.
14. Magnani JL, Ernst B. Glycomimetic drugs - a new source of therapeutic opportunities. Discov Med. 2009;8(43):247-52. Epub 2009/12/31.
15. Ernst B, Magnani JL. From carbohydrate leads to glycomimetic drugs. Nat Rev Drug Discov. 2009;8(8):661-77. Epub 2009/07/25.
16. Simon-Haldi M, Mantei N, Franke J, Voshol H, Schachner M. Identification of a peptide mimic of the L2/HNK-1 carbohydrate epitope. J Neurochem. 2002;83(6):1380-8. Epub 2002/12/11.
17. Torregrossa P, Buhl L, Bancila M, Durbec P, Schafer C, Schachner M, et al. Selection of poly-alpha 2,8-sialic acid mimotopes from a random phage peptide library and analysis of their bioactivity. J Biol Chem. 2004;279(29):30707-14. Epub 2004/05/08.
18. Mehanna A, Jakovcevski I, Acar A, Xiao M, Loers G, Rougon G, et al. Polysialic acid glycomimetic promotes functional recovery and plasticity after spinal cord injury in mice. Mol Ther. 2010;18(1):34-43. Epub 2009/10/15.
19. Mehanna A, Mishra B, Kurschat N, Schulze C, Bian S, Loers G, et al. Polysialic acid glycomimetics promote myelination and functional recovery after peripheral nerve injury in mice. Brain. 2009;132(Pt 6):1449-62. Epub 2009/05/21.
20. Simova O, Irintchev A, Mehanna A, Liu J, Dihne M, Bachle D, et al. Carbohydrate mimics promote functional recovery after peripheral nerve repair. Ann Neurol. 2006;60(4):430-7. Epub 2006/09/08.
21. Florian C, Foltz J, Norreel JC, Rougon G, Roullet P. Post-training intrahippocampal injection of synthetic poly-alpha-2,8-sialic acid-neural cell adhesion molecule mimetic peptide improves spatial long-term performance in mice. Learn Mem. 2006;13(3):335-41. Epub 2006/05/18.

22. Ceballos D, Navarro X, Dubey N, Wendelschafer-Crabb G, Kennedy WR, Tranquillo RT. Magnetically aligned collagen gel filling a collagen nerve guide improves peripheral nerve regeneration. Exp Neurol. 1999;158(2):290-300. Epub 1999/07/23.
23. Joosten EA, Bar PR, Gispen WH. Collagen implants and cortico-spinal axonal growth after mid-thoracic spinal cord lesion in the adult rat. J Neurosci Res. 1995;41(4):481-90. Epub 1995/07/01.
24. Monteiro GA, Fernandes AV, Sundararaghavan HG, Shreiber DI. Positively and Negatively Modulating Cell Adhesion to Type I Collagen Via Peptide Grafting. Tissue Eng Part A. 2009. Epub 2009/02/07.
25. Shreiber DI, Barocas VH, Tranquillo RT. Temporal variations in cell migration and traction during fibroblast-mediated gel compaction. Biophys J. 2003;84(6):4102-14. Epub 2003/05/29.
26. Baici A, Cohen G, Fehr K, Boni A. A handy assay for collagenase using reconstituted fluorescein-labeled collagen fibrils. Anal Biochem. 1980;108(2):230-2. Epub 1980/11/01.
27. Cashman NR, Durham HD, Blusztajn JK, Oda K, Tabira T, Shaw IT, et al. Neuroblastoma x spinal cord (NSC) hybrid cell lines resemble developing motor neurons. Dev Dyn. 1992;194(3):209-21. Epub 1992/07/01.
28. Eggett CJ, Crosier S, Manning P, Cookson MR, Menzies FM, McNeil CJ, et al. Development and characterisation of a glutamate-sensitive motor neurone cell line. J Neurochem. 2000;74(5):1895-902. Epub 2000/05/09.
29. Jiang XY, Fu SL, Nie BM, Li Y, Lin L, Yin L, et al. Methods for isolating highly-enriched embryonic spinal cord neurons: a comparison between enzymatic and mechanical dissociations. J Neurosci Methods. 2006;158(1):13-8. Epub 2006/06/22.
30. Kupershmidt L, Weinreb O, Amit T, Mandel S, Carri MT, Youdim MB. Neuroprotective and neuritogenic activities of novel multimodal iron-chelating drugs in motor-neuron-like NSC-34 cells and transgenic mouse model of amyotrophic lateral sclerosis. FASEB J. 2009;23(11):3766-79. Epub 2009/07/30.
31. Sundararaghavan HG, Masand SN, Shreiber DI. Microfluidic generation of haptotactic gradients through 3D collagen gels for enhanced neurite growth. J Neurotrauma. 2011. Epub 2011/04/09.
32. Ratcliffe EM, D'Autreaux F, Gershon MD. Laminin terminates the Netrin/DCC mediated attraction of vagal sensory axons. Dev Neurobiol. 2008;68(7):960-71. Epub 2008/04/18.
33. Kantlehner M, Schaffner P, Finsinger D, Meyer J, Jonczyk A, Diefenbach B, et al. Surface coating with cyclic RGD peptides stimulates osteoblast adhesion and proliferation as well as bone formation. Chembiochem. 2000;1(2):107-14. Epub 2002/02/06.
34. Beer JH, Springer KT, Coller BS. Immobilized Arg-Gly-Asp (Rgd) Peptides of Varying Lengths as Structural Probes of the Platelet Glycoprotein-Iib/Iiia Receptor. Blood. 1992;79(1):117-28.
35. Hersel U, Dahmen C, Kessler H. RGD modified polymers: biomaterials for stimulated cell adhesion and beyond. Biomaterials. 2003;24(24):4385-415. Epub 2003/08/19.
36. Banker G, Goslin K. Culturing nerve cells. 2nd ed. Cambridge, Mass.: MIT Press; 1998. xii, 666 p., 11 p. of plates p.
37. Hoke A, Redett R, Hameed H, Jari R, Zhou C, Li ZB, et al. Schwann cells express motor and sensory phenotypes that regulate axon regeneration. J Neurosci. 2006;26(38):9646-55. Epub 2006/09/22.
38. Bock P, Beineke A, Techangamsuwan S, Baumgartner W, Wewetzer K. Differential expression of HNK-1 and p75(NTR) in adult canine Schwann cells and olfactory ensheathing cells in situ but not in vitro. J Comp Neurol. 2007;505(5):572-85. Epub 2007/10/11.

39. Brushart TM. Motor axons preferentially reinnervate motor pathways. J Neurosci. 1993;13(6):2730-8. Epub 1993/06/01.
40. Dodla MC, Bellamkonda RV. Differences between the effect of anisotropic and isotropic laminin and nerve growth factor presenting scaffolds on nerve regeneration across long peripheral nerve gaps. Biomaterials. 2008;29(1):33-46. Epub 2007/10/13.
41. Cao X, Shoichet MS. Defining the concentration gradient of nerve growth factor for guided neurite outgrowth. Neuroscience. 2001;103(3):831-40. Epub 2001/03/29.
42. Moore K, MacSween M, Shoichet M. Immobilized concentration gradients of neurotrophic factors guide neurite outgrowth of primary neurons in macroporous scaffolds. Tissue Eng. 2006;12(2):267-78. Epub 2006/03/22.

CHAPTER 3: THE EFFECT OF GLYCOMIMETIC FUNCTIONALIZED COLLAGEN ON PERIPHERAL NERVE REPAIR

Note: This chapter is reproduced from the following publication:

Masand SN, Chen J, Perron IJ, Hammerling BC, Loers G, Schachner M, et al. The effect of glycomimetic functionalized collagen on peripheral nerve repair. Biomaterials 2012.

3.1 INTRODUCTION

Despite significant progress in encouraging the regrowth of peripheral nervous system (PNS) axons across large gap sizes, functional outcomes remain substantially sub-optimal. Research and development of regenerative strategies have primarily addressed means of preventing unwanted ingrowth of fibrous scar tissue, providing mechanical and trophic support for neural components, and presenting structural cues for longitudinally oriented neurite outgrowth [1, 2]. Each of these approaches attempts to overcome obstacles in the injury microenvironment that are largely viewed as the primary sources of functional failure. There is now increasing evidence to suggest that the malrouted reinnervation of neurites towards inappropriate targets also contributes to poor functional outcome [3] as well as muscle weakness, lifelong pain, and inappropriate reflex arcs [4]. Although many of the incorrect neural circuits are pruned during the regeneration process, their growth is effectively wasted. Despite the potential benefits of improving the quality of end target reinnervation following PNS injury, regenerative strategies that specifically address axon targeting are rare.

Growth cones respond to many local cues that regulate axonal guidance and targeting during development. Though not as well studied, the post-PNS injury

microenvironment can also direct regenerating axons. One particularly interesting example is a phenomenon known as preferential motor reinnervation (PMR), which has been shown to increase the efficiency of synaptic reconnection of motor axons. Immediately following injury, proximal neurites grow randomly towards the distal end connecting with both motor and sensory targets. However, as reinnervation continues, the number of motor axons connecting with their appropriate motor targets increases [5-8]. Although the mechanisms that govern PMR are not clearly understood, it is generally accepted that trophic factors, including recognition molecules, that can be expressed locally in the spinal cord and very distally from the injury site are largely involved.

Two glycans, polysialic acid (PSA) and an epitope first discovered on human natural killer cells (HNK-1), have been implicated in acceleration of regrowth and PMR following nerve damage. Franz et al. demonstrated that the level of expression of PSA dramatically increases in motoneurons following nerve injury compared to that from uninjured-motoneurons. When this upregulation is enzymatically interrupted following injury, PMR is significantly inhibited [9]. Among myelinating Schwann cells, HNK-1 is predominantly expressed on those that are associated with motor axons, implicating the modality specific role of this glycan in the PNS [10, 11]. Martini et al. demonstrated that the presence of HNK-1 increases motoneuron outgrowth, but does not affect sensory neuron outgrowth in vitro [12]. Further, following injury, only myelinating Schwann cells that had been previously associated with motor axons re-express HNK-1. Sensory-associated Schwann cells do not produce the glycan even after prolonged exposure to motor axons [11]. Eberhardt et al. showed that electrical stimulation of damaged femoral

nerves in the PNS increased HNK-1 expression, which correlated to an increase in muscle reinnervation and functional recovery [13].

Despite their functional roles, difficulties in synthesis and/or poor stability in vivo have limited the therapeutic use of glycans. Alternative strategies to upregulate these molecules following injury, such as electrical stimulation of nerve stumps and implantation of genetically modified cells, have yielded promising results [13-16]. However, the likelihood of their clinical translation is limited. Recent advances in analytic techniques have allowed the discovery of glycomimetic peptides which provides new opportunities to exploit this class of therapeutic targets. These molecular mimics generally retain the functionality of their carbohydrate counterparts, with the added potential benefits of ease of production, increased stability, and reduced cost [17, 18].

Recently, peptide mimics of PSA and HNK-1 have been isolated using phage display screening [19, 20]. These glycomimetics have been used successfully in small gap repair of peripheral nerve injury when presented in soluble form in both mouse [21, 22] and non-human primate models [23], but their use in more challenging injury models requires increasing the lifetime of their presentation. To this end, we have coupled the glycomimetics to a type I collagen backbone, thereby providing well-controlled, sustained presentation of these cues. Collagen hydrogels provide a useful intraluminal filling as collagen is easily modified, resorbable, and porous. Further, cells can stably bind to collagen via integrins, which leads to regeneration-conducive rearrangements of cellular activities via signal transduction and cytoskeletal functions. Collagen alone has previously been shown to be efficacious in improving regeneration following peripheral nerve injury [24, 25]. In its hydrogel form, collagen provides a highly controlled

environment for nerve cells to grow by providing both mechanical and biological support for neuritogenesis [26]. In a previous study, we confirmed the in vitro bioactivity of type I collagen hydrogels that were functionalized with PSA and HNK-1 glycomimetics and showed that the molecules retain their modality specific responses towards neural cells after conjugation [27].

Herein, we evaluate the utility of the glycomimetic peptide-coupled collagen for critical gap peripheral nerve injuries. We use the femoral nerve injury model (FNI) with a critical gap size of 5 mm, which exceeds the previously used gap size of 2 mm. The FNI model, first introduced by Brushart to understand the mechanism of PMR [5-7], is a particularly well-suited experimental paradigm to study morphological and functional measures of recovery. The femoral nerve begins as a mixed nerve containing sensory and motor axons, and then bifurcates into the sensory saphenous branch and the motor/sensory quadriceps branch. This modality-exclusive branching allows for evaluation of the targeting efficiency, as the bifurcation provides an anatomical decision point for regenerating motor axons; correctly targeting motor axons must choose the quadriceps branch. Thus, in addition to standard scores of morphological and functional recovery, we can evaluate PMR using retrograde labeling techniques (**Figure 3.1**).

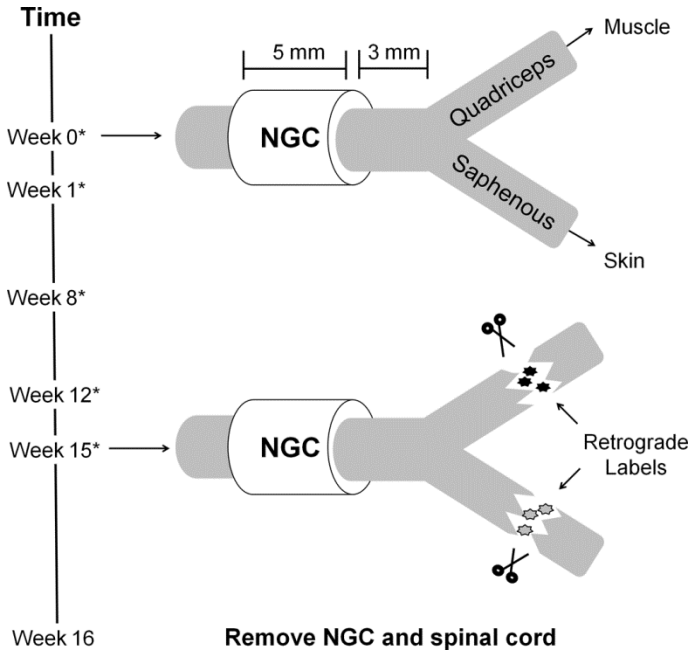

Figure 3.1 Schematic of femoral nerve injury model. The femoral nerve bifurcates into the quadriceps branch, which is innervated by motor and sensory axons, and the saphenous branch, which is innervated by only sensory axons. At week 0, the intact nerve was transected 3 mm proximal to the point of bifurcation and a prefilled nerve guidance conduit (NGC) was sutured in place with an imposed 5 mm gap. At 15 weeks post injury, retrograde labels were introduced into the branches 5 mm distal to the point of bifurcation to evaluate if regenerating motor axons selected the correct branch. One week later, the animal was sacrificed and the regenerated nerve and spinal cord were excised. An asterisk (*) signifies weeks in which animals were filmed to assess functional recovery.

3.2 METHODS

3.2.1 Functionalization of Collagen

From sequences identified previously as functional glycomimetics [19, 20], one linear glycomimetic peptide was selected for HNK-1 (FLHTRLFV, MW: 1032.24) and for PSA (SSVTAWTTG, MW: 908.97). A scrambled version of the HNK-1 peptide (TVFHFRLL) served as a control. All peptides were acquired from a commercial vendor (Genscript, Piscataway, NJ).

Peptides were covalently conjugated onto oligomeric type I collagen using the heterobifunctional crosslinker 1-ethyl-3-(3-dimethylaminopropyl) carbodiimide (EDC) as previously described [28]. Briefly, fetal calf type I collagen (EPC, Owensville, MO) was reconstituted to 3 mg/ml in 0.02 N acetic acid to make an oligomeric collagen solution. To activate carboxyl groups, 2 mg of peptide were dissolved in 2 ml of MES buffer (Fluka) containing 1 mM EDC (Pierce) and reacted for 15 minutes at 37°C. Following this incubation, the activated peptide was added to 5 ml oligomeric collagen solution and rotated overnight at 4°C. The peptide/collagen solution was dialyzed overnight to remove unattached peptide with two dialysate changes. Finally, the purified solution was lyophilized and reconstituted to 3 mg/ml in 0.02 N acetic acid. In a previous study using this conjugation technique, we confirmed that the resulting coupling efficiency is between 50-60%, which translates to 200 - 240 μg of coupled peptide per ml collagen. Additionally, the grafting process does not significantly change the mechanical properties, fiber diameter, or fiber density of the hydrogel [28].

3.2.2 Preparation of Conduits

Collagen hydrogels at 2.0 mg/ml were prepared as previously described [29]. Native or functionalized oligomeric collagen solutions at 3 mg/ml were neutralized on ice using solutions in the following ratios: 2% 1 M Hepes (Fluka), 14% 0.1 N NaOH, 10% 10X Minimum Essential Medium (Sigma), 5.2% M199 (Sigma), 0.1% penicillin/streptomycin (P/S; Sigma), 1% L-glutamine (L-glut; Sigma), 67.7% native or peptide-functionalized collagen. The final concentration of coupled peptide within the hydrogel was between 130 - 160 μg per ml collagen, which was similar to the effective doses given in solution in previous in vivo studies [21, 22]. (For simplicity, hydrogels coupled with the HNK-1 glycomimetic peptide are referred to as HNK-coupled hydrogels, and hydrogels coupled with the PSA glycomimetic peptide are referred to as PSA-coupled hydrogels.) For composite PSA/HNK-coupled hydrogels containing both of the glycomimetics, 33.85% of each of the HNK- and PSA- coupled collagen solutions were neutralized using the formulation above. Glycomimetic peptide-coupled hydrogels refers to the hydrogels coupled with PSA, HNK, or PSA/HNK.

Polyethylene (PE) tubes (0.6mm ID/1mm OD) were pre-cut to a 5.5 mm length and UV sterilized. Native and functionalized collagen solutions were injected in excess to ensure complete void filling into PE tubes using a 22 gauge syringe. The tubes were incubated at 37°C to allow self-assembly of the hydrogel. Control tubes were filled with a sterile PBS solution immediately prior to implantation.

3.2.3 Animals and Surgical Procedure

All procedures were conducted in accordance with approved protocols from the Institutional Animal Care and Use Committee (IACUC). Ten week old C57/B6 female mice (Taconic Farms) were heavily anesthetized by intraperitoneal injections of a

ketamine (80 mg/kg) and xylazine (12 mg/mg) mixture. The surgical area was shaved and cleaned with a Betadine scrub and alcohol. The left femoral nerve was exposed, and a nerve transection was performed at a distance about 3 mm proximal to the bifurcation of the nerve. The cut ends of the nerve were inserted into the pre-filled PE tube fixed with single epineural 10-0 nylon stitches (Ethicon) so that a 5 mm gap was present between the proximal and distal stump. The incised skin was closed with wound clips, which were then removed one week post-surgery.

3.2.4 Measures of Functional Recovery

Injury to the femoral nerve proximal to the point of bifurcation deinnervates the quadriceps muscle. During gait, the quadriceps muscle maintains knee extension in single support phases thereby allowing the contralateral leg to swing forward. Given this distinct biomechanical role, Irintchev et al. [27] developed an approach to quantify the kinematic effects of this type of injury. We used two of Irintchev's defined parameters to evaluate functional recovery: the foot base angle (FBA) and the protraction limb ratio (PLR).

3.2.4.1 Foot Base Angle

Following femoral nerve injury, impaired bending of the knee results in plantar flexion of the ankle joint during load bearing movements. With the classical beam-walk test, this response can be quantified by measuring the angle at which the sole of the hindpaw meets the surface when the contralateral leg is lifted, termed the foot base angle (FBA) [30]. As shown in **Figure 3.2**, during complete load bearing movements, the hindpaw is externally rotated in the transverse plane in intact animals. However, one

week following injury, the hindpaw is externally rotated due to a loss in quadriceps innervation. Animals (n = 10 – 12 per experimental condition) were trained to walk across a 1 meter long wooden beam towards their home cage. Mice were filmed from the rear using a high speed camera (A602fc, Basler) prior to injury and at 1, 8, 12, and 15 weeks following injury. The locomotion videos were analyzed using single frame motion analysis (SFMA) using SimiMotion (SIMI Reality Motion Systems). The FBA was measured at a specific stage of the gait cycle where the contralateral leg was at its highest point, which is when the injured leg bears the most weight. The FBA was determined by dividing the left hind sole into two halves and measuring the angle of that line with the horizontal.

3.2.4.2 Protraction Limb Ratio

The protraction limb ratio (PLR) is measured using a pencil grip test and provides analysis of voluntary movement and proprioceptive ability that is more dependent on supraspinal control compared to gait. Additionally, these pursuits do not require weight support. At weeks 0, 1, 8, and 15, a subset of animals (n = 6 – 7 per experimental condition) were held by their tail and allowed to grab a pencil fixed vertically below them with their forelimbs. The hind limbs will alternate between flexion and extension in an attempt to grab the pencil tip. As shown in **Figure 3.2**, frames during the extension phase were used to measure the PLR, defined as the distance between the anus and the longest digit on the paw [30]. Before injury, limb extension is symmetric and the ratio of the extension for the right/left hind limb is approximately 1. After injury, this ratio increases due to the inability for the injured hind limb to extend completely. As successful regeneration proceeds, the ratio approaches unity once again.

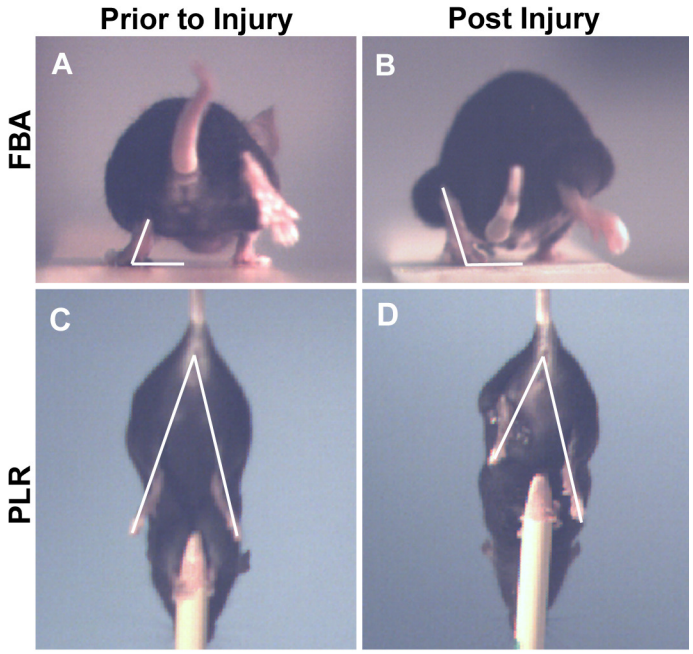

Figure 3.2 Single frame motion analysis. Representative single frames extracted from high-speed videos where individual frames were used to assess effective quadriceps function at specific points within each movement cycle. (A-B): The foot base angle (FBA) was measured at the point where the ipsilateral leg is at its highest point. (C-D) The protraction limb ratio (PLR) was measured when there is complete vertical extension towards the fixed object below. Measurements are taken prior to injury (A, C) and periodically during the first 15 weeks following injury (B, D).

3.2.4.3 Recovery Index Calculation

The recovery index (RI) was used as a relative score of functional recovery normalized to the week one FBA or PLR. The RI was calculated as a percent using the following equation:

$$RI = \frac{X_{reinn} - X_{den}}{X_{pre} - X_{den}} x100$$

Where X_{pre}, X_{den}, X_{reinn} were the values of the FBA or PLR prior to injury, one week following transaction, and at 15 weeks post injury, respectively [30].

3.2.5 Retrograde Labeling and Analysis

Fifteen weeks post-injury, a subset of mice underwent a secondary surgery to introduce retrograde labels into the branches of the femoral nerve (**Figure 3.1**). Under ketamine/xylazine-induced anesthesia (see above), the left femoral nerve was exposed. The quadriceps and saphenous branches were transected approximately 5 mm distal to the point of bifurcation. Two fluorescent retrograde tracers were applied in crystal form to the proximal nerve stumps: 10,000 MW dextran labeled with Alexa Fluor 488 in the saphenous branch, and 10,000 MW dextran labeled with Alexa Fluor 546 in the quadriceps branch (Invitrogen). After thirty minutes, excess dye was removed, nerve stumps were rinsed with PBS, and the incision was closed with wound clips. The labels were allowed to passively traverse back into the spinal cord for one week. Animals were then heavily anaesthetized and perfused through the left ventricle with 4% paraformaldehyde. The lumbar spinal cord was removed and post-fixed overnight in 4% paraformaldehyde and then immersed in a 20% sucrose-saline solution. The entire lumbar

enlargement was then serially sectioned transversely at a thickness of 50 µm. All labeled motoneurons fell within a stack of approximately 40 serial cross-sections and each of these sections generally contained 1 - 5 retrograde-labeled motoneurons. To prevent double-counting of labeled motoneurons, sections spaced 250 µm apart were examined (between 7-10 serial cross-sections per animal) with an inverted epifluorescence microscope (Olympus IX81) for labeled motoneurons using a 20X objective. Labeled motoneurons were only visible in the ventral horn, the motoneuron rich region of the spinal cord. The number of correctly targeted, Alexa Fluor 546+ motoneurons and the number of incorrectly targeted, Alexa Fluor 488+ motoneurons were counted for each animal.

3.2.6 Histomorphometry of Regenerated Nerve

In addition to the lumbar spinal cord, the implanted conduits were also removed post-sacrifice. Samples were post fixed overnight in 4% paraformaldehyde and then immersed in a 20% sucrose-saline solution. A 2 mm segment from the middle of the regenerated nerve was treated with 1% osmium tetroxide solution in 0.1 M sodium cacodylate buffer for one hour at room temperature. Osmium fixed samples were then dehydrated, embedded in an epoxy resin, and cut into 1 µm-thick cross-sections. Sections were counter-stained with 1% toluidine blue in 1% borax in distilled water to enhance contrast. Composite images were captured in bright field using a 100X oil immersion objective. Excised nerves with preserved epineurial sheaths (n = 8 – 10 per experimental condition) were used to manually count the number of myelinated axons per regenerated nerve cross-section using Image J (NIH). These samples were also used to calculate the percent nerve tissue regeneration by dividing the area of nerve tissue regeneration by the

total tissue area. The area of nerve tissue regeneration was defined as the fascicular area containing myelinated axons. Within a subset of these nerves (n = 6 per experimental condition), for each myelinated axon, the mean orthogonal diameter of the axon and of the fiber (axon + myelin sheath) was measured. The mean orthogonal diameter was defined as the average of the length the longest axis of the axon and the perpendicular of that line. The g-ratio, a measure of the quality of myelination, was then calculated as the ratio of the axon-to-fiber diameter. The g-ratio scores were then binned with respect to axon size using a 1 μm bin size [31] .

3.2.7 Statistical Analysis

The study was designed to allow comparison of saline and hydrogel treated conditions, glycomimetic peptide-coupled and non-glycomimetic treated conditions, and within glycomimetic peptide-coupled treated conditions. Variance analysis using a one-way ANOVA was used followed by post-hoc planned comparisons with Tukey's test. Differences were considered significant at $p < 0.05$.

3.3 RESULTS

3.3.1 Functional Recovery

3.3.1.1 Foot Base Angle (FBA)

Injury to the femoral nerve results in abnormal external rotation of the hindpaw, which can be quantified using the FBA (**Figure 3.2**). Prior to injury, the FBA did not differ significantly among groups, and was approximately 68 degrees (**Figure 3.3 A**). One week post-injury, this angle increased to approximately 99 degrees, and was again not significantly different among groups. At eight, twelve, and fifteen weeks post-injury,

the angle for all collagen hydrogel treated groups decreased towards the original values, and significantly outperformed saline treated groups ($p < 0.0001$ for all weeks). Glycomimetic peptide-coupled collagen outperformed native and scrambled peptide-coupled collagen at all measured time points ($p = 0.00141$, $p < 0.0001$, and $p = 0.00011$, respectively). However, no significant differences were found among the glycomimetic peptide-coupled groups or between native and scrambled peptide-coupled collagen at any of these time points.

The recovery index (RI) was used to normalize the degree of functional recovery to the injury at week one (**Figure 3.3 B**). At eight, twelve, and fifteen weeks post-injury, the RI for collagen hydrogel treated groups was significantly greater than for saline treated groups ($p = 0.00017$, $p = 0.00023$, and $p < 0.0001$, respectively). Within hydrogel treated groups, the RI for glycomimetic peptide-coupled collagen was significantly greater than for native and scrambled peptide-coupled collagen ($p = 0.00518$, $p = 0.0006$, and $p < 0.0001$, respectively). At eight weeks post-injury, no significant differences in the RI were noted between scrambled peptide- and glycomimetic peptide-coupled groups. However at twelve and fifteen weeks, glycomimetic peptide-coupled collagen significantly outperformed scrambled peptide-coupled collagen ($p = 0.02321$ and $p = 0.00197$, respectively). Once again, no significant differences were found among glycomimetic peptide-coupled groups or between native and scrambled peptide-coupled groups at any of these time points.

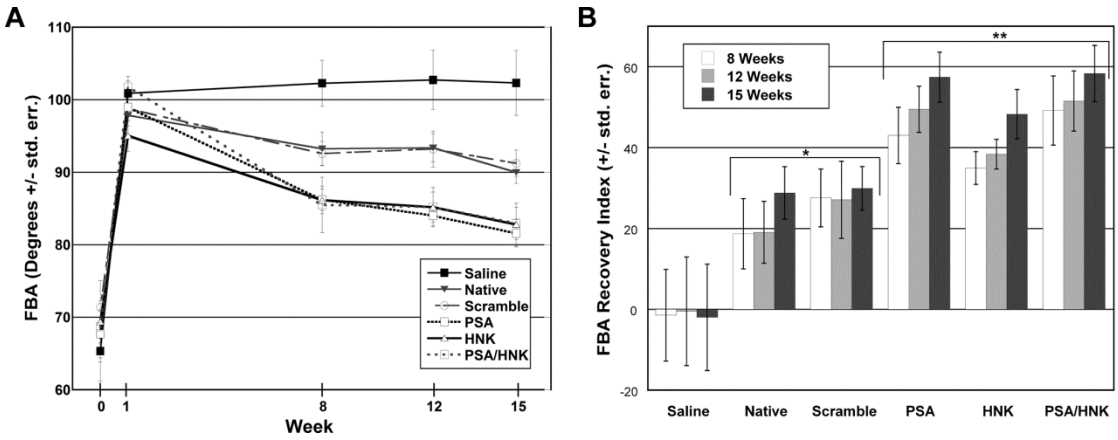

Figure 3.3 Functional evaluation of quadriceps branch reinnervation as assessed using foot base angle (FBA). (A) Evaluation of FBA measurements over time revealed significantly reduced angles at weeks 8, 12, and 15 between collagen and saline treated groups, and glycomimetic peptide-coupled and non-glycomimetic peptide-coupled groups. No statistical differences were found among groups treated with glycomimetic peptide-coupled collagen or between and native collagen and scrambled peptide-coupled groups at any of these time points. (B) When FBA measurements were normalized to the extent of injury at week 1 using the recovery index, statistically significant differences are seen at weeks 8, 12, and 15 between collagen and saline treated groups. No statistical differences were found between glycomimetic treated groups or between native and scrambled peptide-coupled groups at any of these time point. An asterisk (*) signifies statistically significant differences verses saline when compared to its respective time point. A double asterisk (**) signifies statistically significant differences versus saline, native, and scrambled peptide-coupled collagen when compared to its respective time point. Means are reported +/- standard error. Differences were considered significant at $p < 0.05$ using one-way analysis of variance.

3.3.1.2 Protraction Limb Ratio (PLR)

The PLR quantifies the animal's ability to grasp a stationary item fixed below it. More so than ground locomotion, these target-reaching, voluntary movements are generally dependent on supraspinal and propioceptive involvement. Following femoral nerve injury, the quadriceps cannot fully extend the knee, which results in an impaired ability to complete this pursuit (**Figure 3.2**). The ipsilateral and contralateral extensions are compared to generate the PLR.

The PLR increased from approximately 1.0 pre-injury to approximately 1.45 post-injury, with no statistically significant differences among the treatment groups (**Figure 3.4 A**). At eight and fifteen weeks post injury, the PLR for saline groups was significantly higher than for hydrogel treated groups ($p = 0.00121$ and $p < 0.0001$, respectively). However, there were no statistically significant differences noted at either of these time points among collagen hydrogel treated groups. Based on the RI (**Figure 3.4 B**), collagen hydrogel treated groups outperformed saline treated animals at eight and fifteen weeks post-injury ($p = 0.00119$ and $p < 0.0001$, respectively). No significant differences were found among glycomimetic peptide-coupled groups or between native and scrambled peptide-coupled groups at either eight or fifteen weeks post-injury.

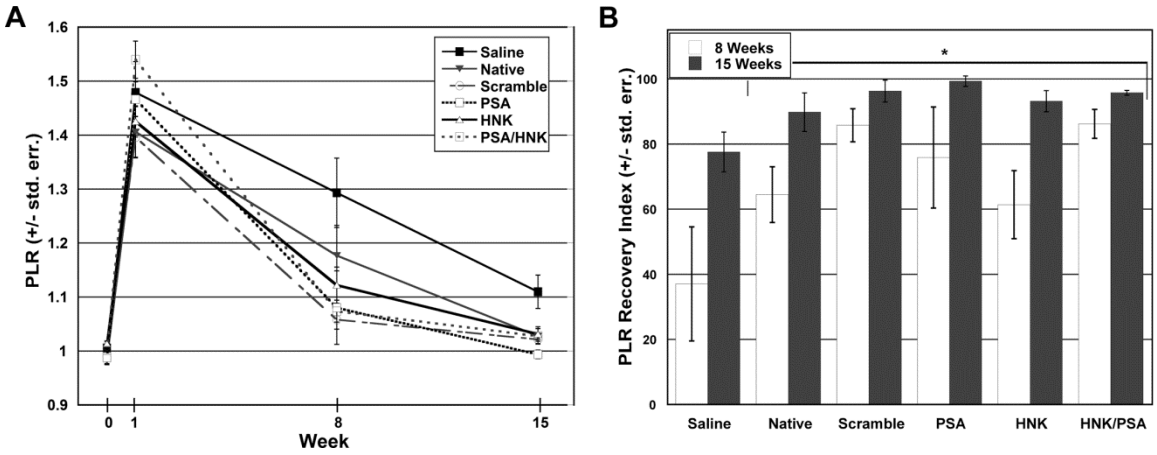

Figure 3.4 Functional evaluation of quadriceps branch reinnervation as assessed using protraction limb ratio (PLR). Evaluation of PLR measurements over time (A) and after normalizing to the extent of injury using the recovery index (B) revealed statistically significant differences at weeks 8 and 15 between collagen and saline treated groups as signified by an asterisk (*). However, no significant differences were found among collagen treated groups at either 8 or 15 weeks post injury. Means are reported +/- standard error. Differences were considered significant at $p < 0.05$ using one-way analysis of variance.

3.3.2 Morphological Analysis

Histological evaluation of osmium tetroxide stained nerve cross-sections showed myelinated axons in all hydrogel treated groups. However, 4 out of 11 saline treated animals had few (< 5) to no distinguishable axons (**Figure 3.5 A-B**). As shown in **Figure 3.5 C**, statistical analysis of axon numbers revealed significantly more axons in hydrogel treated groups than saline ($p = 0.00106$). Within hydrogel conditions, PSA-coupled hydrogels contained significantly more axons than hydrogels without the coupled PSA mimicking peptide ($p = 0.0153$). HNK- coupled hydrogels did not show significant differences in axon count when compared to hydrogels without the coupled HNK-1 mimicking peptide. As shown in **Figure 3.5 D**, all hydrogel treated conditions had a greater percent of regeneration compared to saline treated animals ($p = 0.01705$). There were no statistically significant differences in percentage of nerve regeneration among hydrogel treated groups.

The distribution of myelin within regenerated nerves was analyzed by quantifying the g-ratio, which is the ratio of the axon-to-fiber diameter (**Figure 3.6**). A smaller g-ratio represents an increase in the amount of myelin surrounding the axon. G-ratios were binned with respect to axon size and then tested for statistical significance. In general, HNK-coupled hydrogels yielded the smallest g-ratio while other hydrogels did not differ significantly across axon sizes. For simplicity, the discussion below is restricted to HNK-coupled hydrogels. For a complete statistical analysis of groups tested, the reader is referred to **Table 3.1**.

Within axons up to 4 μm in diameter, HNK-coupled hydrogels yielded significantly lower g-ratios when compared to all other injury conditions ($p < 0.01$) Between 4 and 5 μm, HNK-coupled hydrogels had significantly lower g-ratios than all other hydrogel treated groups but were not statistically significant different from saline treated nerves or intact, unoperated nerves ($p < 0.01$). Finally, nerves treated with HNK-coupled hydrogels were not significantly different than other regenerated nerves for axons larger than 5 μm. For these larger axons (< 5μm), intact nerves yielded significantly lower g-rations compared to all regenerated nerves ($p < 0.0001$). Notably, mean g-ratios of all regenerated nerves fell between 0.6 and 0.8, which has been shown to be physiologically healthy values for nerve conduction [32].

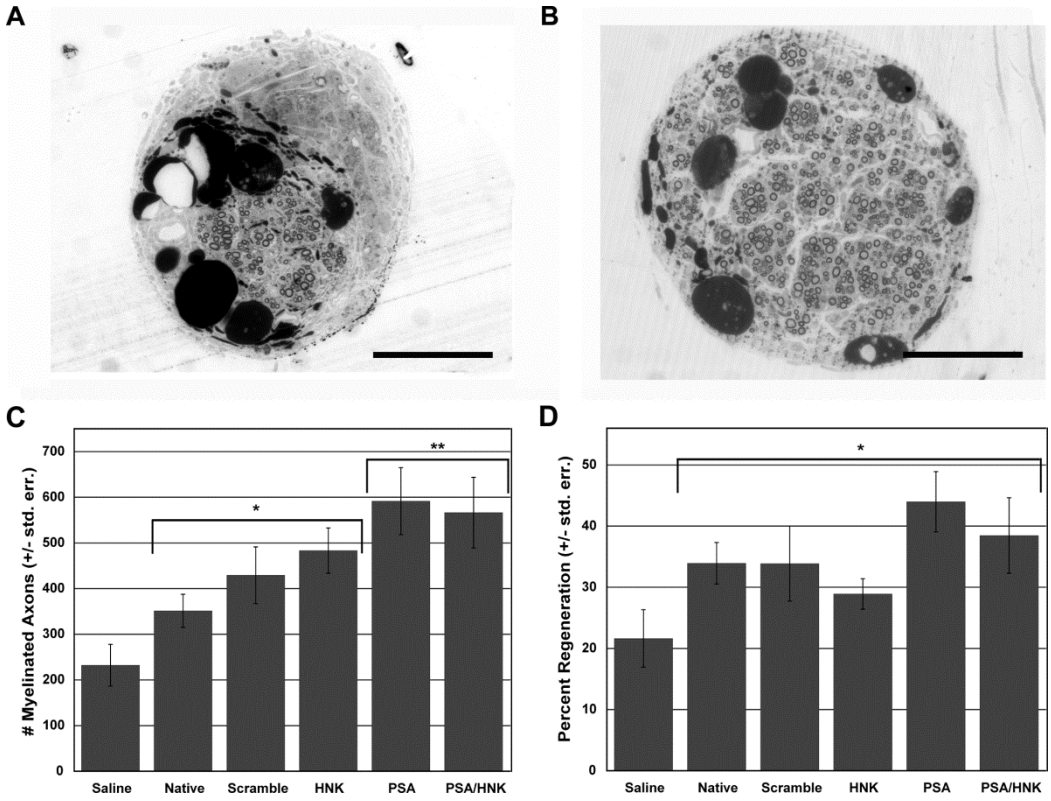

Figure 3.5 Histomorphometry of regenerated nerve. Representative images of osmium tetroxide stained saline (A) and glycomimetic peptide-coupled collagen (B) treated cross-sections from the middle of regenerated nerves at 16 weeks post-injury. (C) Evaluation of myelinated axon number revealed significantly more axons in collagen hydrogel verses saline treated groups, and between PSA containing hydrogels and non-PSA containing hydrogels. (D) Grafts with collagen hydrogels yielded a significantly greater percentage of nerve regeneration compared to saline treated animals. No statistical differences were noted between collagen treated groups. An asterisk (*) signifies statistically significant differences when compared to saline. A double asterisk (**) signifies statistically significant differences when compared to native, scrambled peptide-coupled, and HNK-coupled groups. Means are reported +/- standard error. Differences were considered significant at $p < 0.05$ using one-way analysis of variance. Scale bar represents 200 µm.

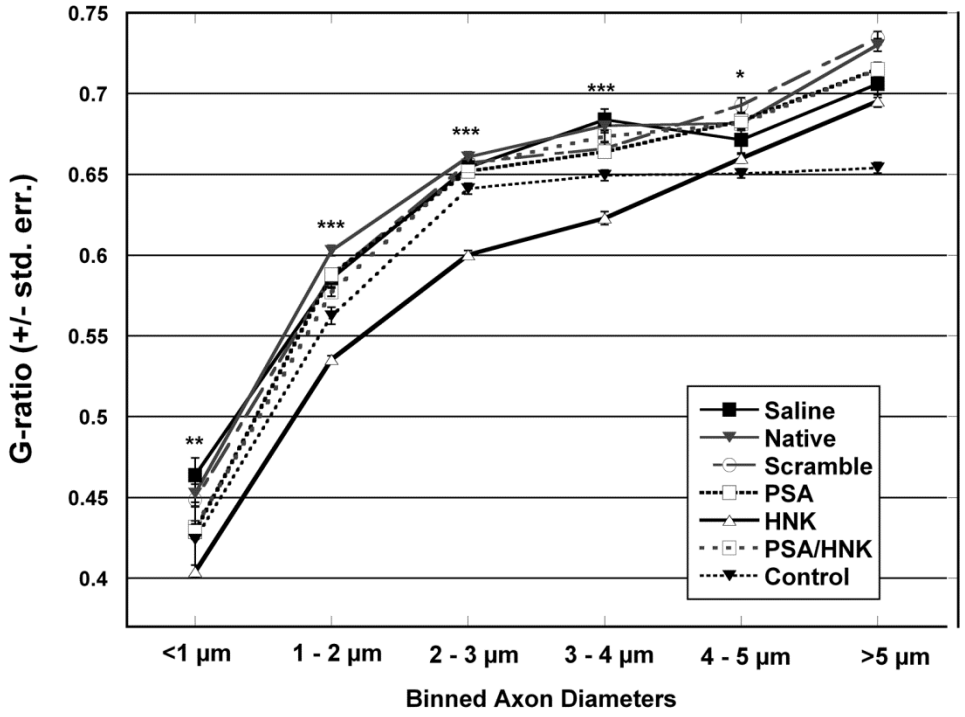

Figure 3.6 Effect of HNK-1 grafted hydrogels on g-ratio distribution in femoral nerve cross-sections. Measured g-ratios were binned with respect to axon size. Each bin was tested for statistical significance using a one-way ANOVA. Small caliber axons (< 1 µm) treated with HNK-coupled hydrogels yield significantly lower g-ratios compared to all other groups (**). Axons between 1 and 4 µm in diameter yielded significantly lower g-ratios in HNK-coupled collagen treated nerves compared to both intact and regenerated nerves (***). Axons between 4 and 5 µm in diameter yielded significantly lower g-ratios than other collagen-treated groups, but not saline-treated or intact nerves (*). No significant differences were found with inclusion of HNK-grafted hydrogels for large caliber axons (> 5 µm). Means are reported +/- standard error. Differences were considered significant at $p < 0.05$ using one-way analysis of variance.

<1μm	**Saline**	**Native**	**Scrambled**	**PSA**	**HNK**	**PSA/HNK**
Native	0.9548	x	x	x	x	x
Scrambled	0.7914	0.999	x	x	x	x
PSA	**0.0133**	**0.0245**	**0.0277**	x	x	x
HNK	**<0.0001**	**<0.0001**	**<0.0001**	**0.0014**	x	x
PSA/HNK	**0.0303**	0.0695	0.0909	0.9994	**0.0002**	x
Intact	0.2344	0.5236	0.6519	0.9999	0.841	0.9988

1 – 2 μm	**Saline**	**Native**	**Scrambled**	**PSA**	**HNK**	**PSA/HNK**
Native	**<0.0001**	x	x	x	x	x
Scrambled	0.999	**0.003**	x	x	x	x
PSA	0.9995	**0.005**	1	x	x	x
HNK	**<0.0001**	**<0.0001**	**<0.0001**	**<0.0001**	x	x
PSA/HNK	0.65	**<0.0001**	0.0798	0.0501	**<0.0001**	x
Intact	**0.0069**	**<0.0001**	**<0.0001**	**<0.0001**	**<0.0001**	0.0935

2 – 3 μm	**Saline**	**Native**	**Scrambled**	**PSA**	**HNK**	**PSA/HNK**
Native	**<0.0001**	x	x	x	x	x
Scrambled	**<0.0001**	0.9988	x	x	x	x
PSA	**<0.0001**	0.8831	0.9887	x	x	x
HNK	**<0.0001**	**<0.0001**	**<0.0001**	**<0.0001**	x	x
PSA/HNK	**<0.0001**	0.9898	1	0.9983	**<0.0001**	x
Intact	**<0.0001**	0.1262	0.2858	0.74	**<0.0001**	0.3865

3 – 4 μm	**Saline**	**Native**	**Scrambled**	**PSA**	**HNK**	**PSA/HNK**
Native	0.9989	x	x	x	x	x
Scrambled	0.192	0.333	x	x	x	x
PSA	0.0832	0.1495	0.9999	x	x	x
HNK	**<0.0001**	**<0.0001**	**<0.0001**	**<0.0001**	x	x
PSA/HNK	0.775	0.9438	0.8941	0.623	**<0.0001**	x
Intact	**<0.0001**	**<0.0001**	**0.0313**	**0.0466**	**<0.0001**	**<0.0001**

4 – 5 μm	**Saline**	**Native**	**Scrambled**	**PSA**	**HNK**	**PSA/HNK**
Native	0.9153	x	x	x	x	x
Scrambled	0.1826	0.7322	x	x	x	x
PSA	0.8279	1	0.7723	x	x	x
HNK	0.8463	**0.0355**	**<0.0001**	**0.0074**	x	x
PSA/HNK	0.9002	1	0.6404	1	**0.0158**	x
Intact	0.102	**<0.0001**	**<0.0001**	**<0.0001**	0.524	**<0.0001**

>5 μm	**Saline**	**Native**	**Scrambled**	**PSA**	**HNK**	**PSA/HNK**
Native	0.2799	x	x	x	x	x
Scrambled	0.1129	0.9993	x	x	x	x
PSA	0.9762	0.586	0.2622	x	x	x
HNK	0.9414	**0.0015**	**<0.0001**	0.1771	x	x
PSA/HNK	0.9724	0.5423	0.2205	1	0.1364	x
Intact	**<0.0001**	**<0.0001**	**<0.0001**	**<0.0001**	**<0.0001**	**<0.0001**

Table 3.1 Statistical analysis of binned g-ratios as a function of axon size using one-way ANOVA followed by Tukey's post-hoc analysis. Values were considered significant at $p < 0.05$ and are denoted in bold.

3.3.3 Retrograde Labeling

To assess the effect of the coupled glycomimetics on targeting efficiency, different fluorescently tagged retrograde labels were introduced into the quadriceps and saphenous branch 15 weeks post injury (**Figure 3.1**). One week following introduction of the dyes, animals were sacrificed and spinal cords were excised for motoneuron counts (**Figure 3.7 A**). Statistical evaluation of motoneuron counts revealed significantly more correctly labeled motoneurons in hydrogel treated groups verse saline ($p = 0.01341$; **Figure 3.7 B**). Within hydrogels treated groups, HNK- coupled hydrogels contained significantly more correctly labeled motoneurons than hydrogels without the HNK mimicking peptide ($p = 0.02$). No significant differences were noted between hydrogels with or without the coupled PSA mimicking peptide. No statistically significant differences were found between conditions with regard to numbers of incorrectly labeled motoneurons or the total number of labeled motoneurons (correct and incorrect).

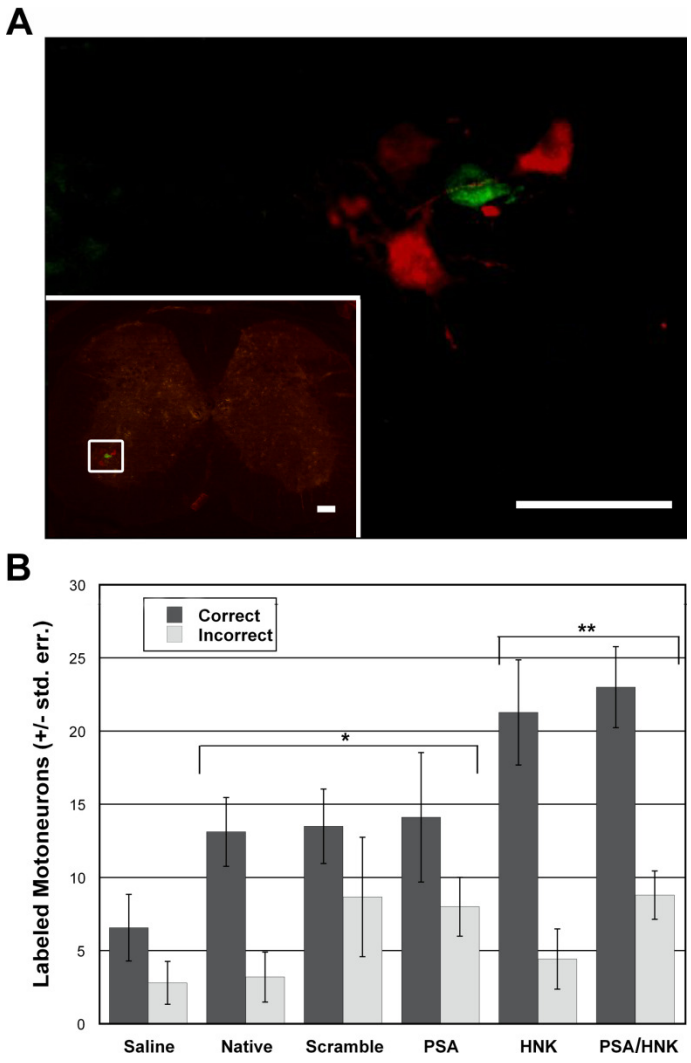

Figure 3.7 Analysis of retrogradely-labeled motoneurons. (A) Representative optical slice of correctly (red) and incorrectly (green) labeled motoneuronal cell bodies in cross-sections from spinal cords within the lumbar enlargement. Inset shows that fluorescently tagged retrograde labels were restricted to the motoneuron-rich ventral horn ipsilateral to the injured side. Longer exposure times were used to enhance autofluoresence in order to visualize the spinal cord structure in the inset. The higher magnification image shows distinguishable cell bodies used for motoneuron counts. Scale bars represent 100 µm. (B) Statistical analysis revealed significantly more correctly labeled motoneurons in all

collagen-treated versus saline treated groups. Within hydrogel-treated conditions, groups containing coupled HNK peptide resulted in significantly more correctly labeled motoneurons than groups without coupled HNK. No statistically significant differences were found between PSA and non-PSA containing collagen-treated animals, number of incorrectly labeled motoneurons, and total number of motoneurons. An asterisk (*) represents statistically significant differences compared to saline treated groups in number of correctly labeled motoneurons. A double asterisk (**) represents statistically significant differences of HNK- and PSA/HNK-coupled hydrogels compared to saline, native, scrambled peptide-coupled, and PSA-coupled in number of correctly projecting motoneurons. Means are reported +/- standard error. Differences were considered significant at $p < 0.05$ using one-way analysis of variance.

3.4 DISCUSSION

Despite the innate regenerative potential of the PNS, functional recovery remains incomplete with increasing severity of injury. This has been attributed to a number of reasons including the local inflammatory response, ingrowth of fibrous scar tissue, lack of mechanical support for emerging neurites, and more recently the malrouted regrowth of axons. We have previously shown that covalent conjugation of glycomimetic HNK-1 and PSA peptides to type I collagen results in neural cell type-specific responses in vitro [27]. Given these unique, modality-defined effects, we investigated the potential for glycomimetic functionalized collagen to promote axonal regeneration and targeting in a challenging, 5 mm gap size femoral nerve injury model. While these peptides have previously been shown to be efficacious in smaller gap sizes [22, 23, 33], this is the first successful study utilizing the peptide mimics within a critical gap.

Following implantation of a polyethylene tube filled with glycomimetic functionalized collagen after injury, we observed significant improvement in functional and morphological recovery as summarized in **Table 3.2**. These positive effects are due to the structural similarity between the glycomimetic peptides and their respective carbohydrate epitope. Previous studies have shown that the peptides have specific binding affinity for anti-PSA and anti-HNK antibodies [19, 20, 33]. Additionally, the scrambled peptide-coupled collagen did not elicit any more benefit than native collagen, which also indicates that these effects are sequence specific.

	Functional Scores		Morphological Scores			
	FBA	**PLR**	**Axon #**	**% Reg.**	**G-ratio**	**Motoneurons**
Saline	-	+	-	-	+	-
Native	+	++	+	+	+	+
Scrambled	+	++	+	+	+	+
PSA	++	++	++	++	+	+
HNK	++	++	+	+	++	++
PSA/HNK	++	++	++	++	+	++

Table 3.2 Summary of functional and morphological results as assessed sixteen weeks post injury. A '-'denotes no improvement from week one scores, a '+' denotes moderate improvement, and '++' denotes greatest improvement relative to other conditions.

3.4.1 Utility of the Femoral Nerve Injury Model

The femoral nerve injury paradigm was used to test the in vivo efficacy of our modified collagen hydrogels, as it particularly well suited to assess functional and morphological recovery [34]. Although the sciatic nerve model is most widely used for peripheral nerve injury, it has been criticized as having limited reliability in quantifying functional recovery. In the sciatic model, a single behavior is generally used to represent the relative contributions of numerous muscles affected by sciatic nerve transection. Further, return of function is often measured using ink prints of the hindpaw. This approach is frequently difficult to interpret due to smearing, incomplete steps, and self-mutilation which limit the precision of this paradigm [35-37]. In contrast, the femoral model allows for objective, sensitive measurement of quadriceps reinnervation over the course of regeneration using FBA and PLR scores.

Perhaps the most interesting use of the femoral nerve paradigm stems from its unique anatomy that allows for quantitative evaluation of motoneuron targeting. Near the inguinal ligament, the mixed femoral nerve divides into two branches of similar diameters - the sensory saphenous branch and the mixed quadriceps branch (**Figure 3.1**). If the femoral nerve is injured prior to the point of bifurcation, regenerating motor axons have equal opportunity to grow into the incorrect, saphenous branch or the correct quadriceps branch. When PMR occurs, more motor axons will be located in the correct pathway as assessed with retrograde labeling. Collectively, the model allows for insights into the mechanisms underlying motor axon targeting and evaluation of methods to improve its propensity of occurring.

3.4.2 Collagen as an Intraluminal Filler

The present study demonstrates that native and grafted collagen hydrogels provide significant functional and morphological benefits compared to saline filled conduits. These findings are in agreement with increasing evidence that suggests that a nerve guidance conduit for longer, clinically relevant gap sizes will likely involve optimization of the inner lumen in addition to improving the chemistry of outer tube [38]. The intraluminal filling serves to replace the fibrin cable which often fails to form in the case of larger injuries [39]. In doing so, the matrix provides a supportive substrate for the ingrowth of Schwann cells and regenerating axons [40].

3.4.3 Glycomimetic Functionalized Collagen Hydrogels

The greatest overall improvement in functional and morphological recovery was observed in groups treated with glycomimetic peptide-functionalized collagen. By covalent conjugation of the glycomimetics to the collagen backbone, it is possible that peptidase-mediated degradation is limited and time of local availability is increased. Further, since PSA and HNK-1 glycans in their native configuration are tethered to the extracellular matrix or presented on the cell surface in vivo, the mode of presentation may be more physiologically relevant when compared to administration in their soluble forms.

Functional recovery was assessed using two methods: the FBA and PLR. When measured using the FBA, glycomimetic peptide-coupled hydrogels significantly outperformed non-glycomimetic peptide-coupled hydrogels. On the other hand, there were no significant differences noted between any of the hydrogel treated groups when

measured using the PLR. The differences in functional outcomes between these two tests are likely related to the importance of quadriceps reinnervation in the successful completion of the task. The PLR is a non-weight bearing pursuit and therefore may not have adequate sensitivity to negotiate differences in quadriceps function between treatment groups. Additionally, other muscles involved in lower limb extension, including the biceps femoris, may provide compensation during the reaching pursuit. The FBA quantifies changes during the stance phase of the gait cycle where the affected quadriceps muscle bears body weight. Other muscle groups would provide minimal compensation as the quadriceps is solely responsible for the knee extension. The functional scores at eight weeks post injury provide evidence that the FBA may be a more appropriate metric to assess changes in quadriceps reinnervation. Whereas the PLR RI scores for the hydrogel treated groups were between 60 and 80%, the FBA RI scores for the FBA were between 20 and 40%. It is unlikely that at this time point the quadriceps has up to 80% successful reinnervation as suggested by the PLR scores. However, it should be noted that the PLR may provide an early screening tool to assess quadriceps reinnervation.

Although both PSA- and HNK-coupled hydrogels resulted in similar functional recovery, the morphological outcomes indicate that distinct cellular mechanisms may be involved (**Table 3.2**). Mice treated with PSA-coupled collagen had significantly higher axon counts, while mice treated with HNK-coupled collagen showed increased myelin and motor axon targeting compared to saline and other hydrogel-treated conditions. The different outcomes in the morphological parameters add evidence that the mode of action of the peptides is likely related to their functions as glycan homologs.

Following peripheral nerve injury, axons will extend several exploratory collateral sprouts towards distal nerve branches. Franz et al. have demonstrated that PSA is an important determinant of this phenomenon [9]. PSA is generally found tethered to the neural cell adhesion molecule (NCAM), and has been suggested to promote axon regrowth by sterically limiting heterophilic and homophilic NCAM interactions [41]. When enzymatically removed or genetically interrupted, PSA-deficient mice have significantly reduced axon numbers within regenerated nerve cables [9]. These findings are in agreement with our results, which show an increase in axon count in nerves treated with PSA-coupled collagen. The differences in axon count are not related to an increase in the area of regeneration, but reflect an increase in the density of axonal sprouts. Since the total number of labeled motoneurons was not significantly different between hydrogel treated groups, it is likely that the increase in axon count reflects an increase in collateral sprouts and not an increase in motoneurons. Thus, these axonal projections likely create more chances for the regenerating axons to reach their appropriate target and may account for an increase in locomotor recovery. We did not observe improvement in axonal targeting underlying PMR with PSA, which is consistent with previous work from Mehanna et al. [21].

The increased myelin production resulting from incorporation of the HNK-1 mimicking peptide is also in agreement with studies on the function of its glycan counterpart. In the canine, HNK-1 was recently found to be associated with myelinating Schwann cells with limited-to-no expression on non-myelinating Schwann cells, which supports the view that the glycan is related to myelin production [42]. Interestingly, Simova et al. demonstrated that soluble administration of the HNK-1 mimicking peptide

resulted in an increase in HNK-1 expression in the quadriceps branch of the injured mouse femoral and an increase in myelin thickness [22]. Although evaluating changes in myelin production as a function of axon phenotype was beyond the scope of this study, future work will explore if introduction of HNK-coupled hydrogels differentially affects myelination of motor versus sensory axons.

The targeting results with HNK-coupled collagen are in agreement with previous results in the 2 mm gap paradigm in mouse and monkey where the peptide was presented in solubilized form [22, 43]. In vivo, HNK-1 has an unusual, highly specific expression pattern on mouse motor-associated Schwann cells [11], and its expression is increased following administration of the peptide [22]. This may lead to a more permissive environment for proliferating Schwann cells and regenerating motor axons and 'prime' them for other downstream trophic cues. More specifically, recent evidence has suggested that the HNK-1 glycan causes activation of the receptor for the advanced glycation end products (RAGE) through its interaction with HMGB1 (amphoterin). The activation of this pathway leads to increased neurite outgrowth and survival, and impairment of RAGE signaling significantly reduces nerve regeneration [44-46]. Other molecular mechanisms underlying the observed effects could be due to the ability of HNK-1 to bind to laminin. [47]

Given these distinct responses, using a combination of the two glycomimetics could potentially provide synergistic benefit. In this study, however, we did not see any significant increase in functional or morphological improvement from presentation of both of these cues simultaneously. We speculate that this may be due to an inadequate concentration of the conjugated peptides. To maintain equal total peptide concentration

between coupled collagen conditions, the PSA/HNK-coupled hydrogels were made in 50/50 ratios. Future work will evaluate varied concentrations of PSA/HNK-coupled hydrogels to find optimal concentrations using in vitro methods. The ratios which elicit maximal benefit can then be translated to in vivo use. It is also possible that functional recovery was maximized for this time point or this model. Thus, future work will evaluate the performance of the materials in larger animals, later time points, and other nerve injury models. In addition to peptide grafting, collagen is amenable to other higher order modifications including gradient generation [48] and longitudinal fiber alignment [49, 50]. Future studies will evaluate the benefit of introducing structural and haptotactic anisotropy to our biomaterial.

3.5 CONCLUSION

The peptide glycomimetics of PSA and HNK-1 represent interesting target molecules to improve the efficiency of synaptic reconnection. In this study, the efficacy of glycomimetic-functionalized collagen hydrogels as a strategy for repair following peripheral nerve injury (PNI) is described. Although both PSA- and HNK-coupled hydrogels encouraged functional recovery following femoral nerve transection, the distinct morphological outcomes indicates the peptides likely function through different mechanisms related to their glycan homolog. Specifically, PSA-coupled collagen improved axon number, HNK-coupled collagen improved motoneuron targeting and myelination of axons. Collectively, this study represents a biomaterial approach at improving the efficiency of synaptic reconnection and functional recovery following PNI.

3.6 ACKNOWLEDGEMENTS

Funding for these studies was provided by the National Institutes of Health (NIH 1R21EB009245-01A1) and US Army contract #W81XWH-04-2-0031, and fellowships from the Rutgers-UMDNJ Biotechnology Training Program (NIH Grant Number 5T32GM008339-20), the National Science Foundation (NSF DGE 0801620, IGERT on the Integrated Science and Engineering of Stem Cells), and the Aresty Research Center for Undergraduates. MS is a New Jersey Professor of Spinal Cord Research. We confirm that all studies involving experimental animals were conducted under the ethical approval of all relevant bodies.

3.7 REFERENCES

1. Huang YC, Huang YY. Biomaterials and strategies for nerve regeneration. Artif Organs. 2006;30(7):514-22. Epub 2006/07/14.
2. Hudson TW, Evans GR, Schmidt CE. Engineering strategies for peripheral nerve repair. Clin Plast Surg. 1999;26(4):617-28, ix. Epub 1999/11/30.
3. Sumner AJ. Aberrant reinnervation. Muscle Nerve. 1990;13(9):801-3. Epub 1990/09/01.
4. Sunderland S. Nerves and nerve injuries. 2d ed. Edinburgh ; New YorkNew York: Churchill Livingstone ; distributed by Longman; 1978. xii, 1046 p. p.

5. Brushart TM, Seiler WAt. Selective reinnervation of distal motor stumps by peripheral motor axons. Exp Neurol. 1987;97(2):289-300. Epub 1987/08/01.
6. Brushart TM. Preferential reinnervation of motor nerves by regenerating motor axons. J Neurosci. 1988;8(3):1026-31. Epub 1988/03/01.
7. Brushart TM. Motor axons preferentially reinnervate motor pathways. J Neurosci. 1993;13(6):2730-8. Epub 1993/06/01.
8. Madison RD, Archibald SJ, Brushart TM. Reinnervation accuracy of the rat femoral nerve by motor and sensory neurons. J Neurosci. 1996;16(18):5698-703. Epub 1996/09/15.
9. Franz CK, Rutishauser U, Rafuse VF. Polysialylated neural cell adhesion molecule is necessary for selective targeting of regenerating motor neurons. J Neurosci. 2005;25(8):2081-91. Epub 2005/02/25.
10. Martini R, Bollensen E, Schachner M. Immunocytological Localization of the Major Peripheral Nervous-System Glycoprotein P0 and the L2/Hnk-1 and L3 Carbohydrate Structures in Developing and Adult-Mouse Sciatic-Nerve. Developmental Biology. 1988;129(2):330-8.
11. Martini R, Schachner M, Brushart TM. The L2/Hnk-1 Carbohydrate Is Preferentially Expressed by Previously Motor Axon-Associated Schwann-Cells in Reinnervated Peripheral-Nerves. Journal of Neuroscience. 1994;14(11):7180-91.

12. Martini R, Xin Y, Schmitz B, Schachner M. The L2/Hnk-1 Carbohydrate Epitope Is Involved in the Preferential Outgrowth of Motor Neurons on Ventral Roots and Motor Nerves. European Journal of Neuroscience. 1992;4(7):628-39.
13. Eberhardt KA, Irintchev A, Al-Majed AA, Simova O, Brushart TM, Gordon T, et al. BDNF/TrkB signaling regulates HNK-1 carbohydrate expression in regenerating motor nerves and promotes functional recovery after peripheral nerve repair. Exp Neurol. 2006;198(2):500-10. Epub 2006/02/08.
14. Luo J, Bo X, Wu D, Yeh J, Richardson PM, Zhang Y. Promoting survival, migration, and integration of transplanted Schwann cells by over-expressing polysialic acid. Glia. 2010. Epub 2010/12/31.
15. El Maarouf A, Petridis AK, Rutishauser U. Use of polysialic acid in repair of the central nervous system. Proc Natl Acad Sci U S A. 2006;103(45):16989-94. Epub 2006/11/01.
16. Franz CK, Rutishauser U, Rafuse VF. Intrinsic neuronal properties control selective targeting of regenerating motoneurons. Brain. 2008;131(Pt 6):1492-505. Epub 2008/03/13.
17. Magnani JL, Ernst B. Glycomimetic drugs - a new source of therapeutic opportunities. Discov Med. 2009;8(43):247-52. Epub 2009/12/31.
18. Ernst B, Magnani JL. From carbohydrate leads to glycomimetic drugs. Nat Rev Drug Discov. 2009;8(8):661-77. Epub 2009/07/25.
19. Simon-Haldi M, Mantei N, Franke J, Voshol H, Schachner M. Identification of a peptide mimic of the L2/HNK-1 carbohydrate epitope. J Neurochem. 2002;83(6):1380-8. Epub 2002/12/11.
20. Torregrossa P, Buhl L, Bancila M, Durbec P, Schafer C, Schachner M, et al. Selection of poly-alpha 2,8-sialic acid mimotopes from a random phage peptide library and analysis of their bioactivity. J Biol Chem. 2004;279(29):30707-14. Epub 2004/05/08.
21. Mehanna A, Mishra B, Kurschat N, Schulze C, Bian S, Loers G, et al. Polysialic acid glycomimetics promote myelination and functional recovery after peripheral nerve injury in mice. Brain. 2009;132(Pt 6):1449-62. Epub 2009/05/21.
22. Simova O, Irintchev A, Mehanna A, Liu J, Dihne M, Bachle D, et al. Carbohydrate mimics promote functional recovery after peripheral nerve repair. Ann Neurol. 2006;60(4):430-7. Epub 2006/09/08.
23. Irintchev A, Wu MM, Lee HJ, Zhu H, Feng YP, Liu YS, et al. Glycomimetic improves recovery after femoral injury in a non-human primate. J Neurotrauma.28(7):1295-306. Epub 2011/04/06.
24. Satou T, Nishida S, Hiruma S, Tanji K, Takahashi M, Fujita S, et al. A morphological study on the effects of collagen gel matrix on regeneration of severed rat sciatic nerve in silicone tubes. Acta Pathol Jpn. 1986;36(2):199-208. Epub 1986/02/01.
25. Rosen JM, Padilla JA, Nguyen KD, Padilla MA, Sabelman EE, Pham HN. Artificial Nerve Graft Using Collagen as an Extracellular-Matrix for Nerve Repair Compared with Sutured Autograft in a Rat Model. Annals of Plastic Surgery. 1990;25(5):375-87.
26. Sundararaghavan HG, Monteiro GA, Firestein BL, Shreiber DI. Neurite growth in 3D collagen gels with gradients of mechanical properties. Biotechnol Bioeng. 2009;102(2):632-43. Epub 2008/09/04.
27. Masand SN, Perron IJ, Schachner M, Shreiber DI. Neural cell type-specific responses to glycomimetic functionalized collagen. Biomaterials.33(3):790-7. Epub 2011/10/27.
28. Monteiro GA, Fernandes AV, Sundararaghavan HG, Shreiber DI. Positively and Negatively Modulating Cell Adhesion to Type I Collagen Via Peptide Grafting. Tissue Eng Part A. 2009. Epub 2009/02/07.

29. Shreiber DI, Barocas VH, Tranquillo RT. Temporal variations in cell migration and traction during fibroblast-mediated gel compaction. Biophys J. 2003;84(6):4102-14. Epub 2003/05/29.
30. Irintchev A, Simova O, Eberhardt KA, Morellini F, Schachner M. Impacts of lesion severity and tyrosine kinase receptor B deficiency on functional outcome of femoral nerve injury assessed by a novel single-frame motion analysis in mice. Eur J Neurosci. 2005;22(4):802-8. Epub 2005/08/24.
31. McCreery DB, Yuen TG, Agnew WF, Bullara LA. A quantitative computer-assisted morphometric analysis of stimulation-induced injury to myelinated fibers in a peripheral nerve. J Neurosci Methods. 1997;73(2):159-68. Epub 1997/05/16.
32. Chomiak T, Hu B. What is the optimal value of the g-ratio for myelinated fibers in the rat CNS? A theoretical approach. PLoS One. 2009;4(11):e7754. Epub 2009/11/17.
33. Mehanna A, Jakovcevski I, Acar A, Xiao M, Loers G, Rougon G, et al. Polysialic acid glycomimetic promotes functional recovery and plasticity after spinal cord injury in mice. Mol Ther.18(1):34-43. Epub 2009/10/15.
34. Irintchev A. Potentials and limitations of peripheral nerve injury models in rodents with particular reference to the femoral nerve. Ann Anat.193(4):276-85. Epub 2011/04/13.
35. Monte-Raso VV, Barbieri CH, Mazzer N, Yamasita AC, Barbieri G. Is the Sciatic Functional Index always reliable and reproducible? J Neurosci Methods. 2008;170(2):255-61. Epub 2008/03/08.
36. Shenaq JM, Shenaq SM, Spira M. Reliability of sciatic function index in assessing nerve regeneration across a 1 cm gap. Microsurgery. 1989;10(3):214-9. Epub 1989/01/01.
37. Varejao AS, Melo-Pinto P, Meek MF, Filipe VM, Bulas-Cruz J. Methods for the experimental functional assessment of rat sciatic nerve regeneration. Neurol Res. 2004;26(2):186-94. Epub 2004/04/10.
38. Bellamkonda RV. Peripheral nerve regeneration: an opinion on channels, scaffolds and anisotropy. Biomaterials. 2006;27(19):3515-8. Epub 2006/03/15.
39. Zhao Q, Dahlin LB, Kanje M, Lundborg G. Repair of the transected rat sciatic nerve: matrix formation within implanted silicone tubes. Restor Neurol Neurosci. 1993;5(3):197-204. Epub 1993/01/01.
40. Pfister LA, Papaloizos M, Merkle HP, Gander B. Nerve conduits and growth factor delivery in peripheral nerve repair. J Peripher Nerv Syst. 2007;12(2):65-82. Epub 2007/06/15.
41. Johnson CP, Fujimoto I, Rutishauser U, Leckband DE. Direct evidence that neural cell adhesion molecule (NCAM) polysialylation increases intermembrane repulsion and abrogates adhesion. J Biol Chem. 2005;280(1):137-45. Epub 2004/10/27.
42. Bock P, Beineke A, Techangamsuwan S, Baumgartner W, Wewetzer K. Differential expression of HNK-1 and p75(NTR) in adult canine Schwann cells and olfactory ensheathing cells in situ but not in vitro. J Comp Neurol. 2007;505(5):572-85. Epub 2007/10/11.
43. Irintchev A, Wu MM, Lee HJ, Zhu H, Feng YP, Liu YS, et al. Glycomimetic improves recovery after femoral injury in a non-human primate. J Neurotrauma. 2011;28(7):1295-306. Epub 2011/04/06.
44. Chou DK, Zhang J, Smith FI, McCaffery P, Jungalwala FB. Developmental expression of receptor for advanced glycation end products (RAGE), amphoterin and sulfoglucuronyl (HNK-1) carbohydrate in mouse cerebellum and their role in neurite outgrowth and cell migration. J Neurochem. 2004;90(6):1389-401. Epub 2004/09/03.
45. Rong LL, Trojaborg W, Qu W, Kostov K, Yan SD, Gooch C, et al. Antagonism of RAGE suppresses peripheral nerve regeneration. FASEB J. 2004;18(15):1812-7. Epub 2004/12/04.
46. Fang P, Schachner M, Shen YQ. HMGB1 in Development and Diseases of the Central Nervous System. Mol Neurobiol. 2012;45(3):499-506. Epub 2012/05/15.

47. Hall H, Liu L, Schachner M, Schmitz B. The L2/HNK-1 carbohydrate mediates adhesion of neural cells to laminin. Eur J Neurosci. 1993;5(1):34-42. Epub 1993/01/01.
48. Sundararaghavan HG, Masand SN, Shreiber DI. Microfluidic generation of haptotactic gradients through 3D collagen gels for enhanced neurite growth. J Neurotrauma. 2011;28(11):2377-87. Epub 2011/04/09.
49. Lee P, Lin R, Moon J, Lee LP. Microfluidic alignment of collagen fibers for in vitro cell culture. Biomed Microdevices. 2006;8(1):35-41. Epub 2006/02/24.
50. Verdu E, Labrador RO, Rodriguez FJ, Ceballos D, Fores J, Navarro X. Alignment of collagen and laminin-containing gels improve nerve regeneration within silicone tubes. Restor Neurol Neurosci. 2002;20(5):169-79. Epub 2003/01/08.

CHAPTER 4. IMPROVING THE USE OF GLYCOMIMETIC FUNCTIONALIZED COLLAGEN FOR PERIPHERAL NERVE REPAIR

4.1 INTRODUCTION

In Chapter 3, the efficacy of using glycomimetic functionalized collagen as an intraluminal filler for a nerve guidance conduit (NGC) was explored. While the functional and morphological outcomes of animals treated with PSA- and HNK-functionalized collagen were significantly improved when compared to saline or native collagen conditions, there were no observed benefits of using HNK/PSA composite hydrogels. The lack of synergy with the use of both glycomimetics was somewhat surprising as the differences in morphological outcomes indicated that distinct mechanisms may be involved in their action. More specifically, the use of PSA-functionalized hydrogels led to an increase in axon count, whereas HNK-functionalized hydrogels showed an increase in myelination and number of correctly projecting motoneurons [1].

In our previous work, the total concentration of grafted peptide was maintained between groups. In order to do this, the HNK/PSA composite hydrogels had half of the amount of each peptide. In the composite hydrogels, the concentration of each of the glycomimetics was between 65 - 80 µg per ml collagen, whereas the initial studies evaluating the efficacy of the peptides used a concentration of 200 µg per ml [2, 3]. It is therefore possible that the concentration of each peptide in the composite hydrogels was below the effective 'dose' required to elicit any additional biological response.

Another study limitation of our previous work was the use of a non-degradable polyethylene outer tube. An ideal NGC will likely incorporate a bioresorbable or degradable outer conduit to reduce the likelihood of nerve compression and the requirement for a secondary surgery [4]. While there are several clinically approved degradable NGCs, they have been met with several limitations. For one, these tubes are not indicated for use for larger gap sizes. Further, none of these approved NGCs have incorporated intraluminal fillers or neurotrophic agents. Except for polylactic acid (PLA)-poly(caprolactone) conduit, the available conduits have fixed degradation profiles which cannot be adjusted to match the regenerative requirements of the particular nerve. While the current options for NGCs generally provide a physical guide for regenerating axons, the next generation of conduits will likely incorporate higher level cues to encourage increased recovery. Thus, it is an important requirement for any potential intraluminal filler to be able to interface successfully with a degradable conduit.

To this end, in this chapter we explore two potential improvements in the use of glycomimetic functionalized collagen- 1) within a degradable NGC and 2) higher concentrations of functionalized glycomimetics. Two formulations of degradable conduits were used in this study, a salicylic acid based poly(anhydride-ester), PAE and PLAA blends from the Uhrich group and tyrosine-derived polycarbonates from the Kohn group. While the use of tyrosine-derived polycarbonates with glycomimetic-functionalized collagen yielded promising results, we limit our discussion to the PAE/PLAA NGCs in this thesis.

4.2 METHODS

4.2.1 Collagen Functionalization

Type I collagen was functionalized as previously described [5]. For high concentration glycomimetic-functionalized collagen, 1 mg of glycomimetic peptide was added to 1 mL of collagen. The final concentration of individual peptide in the composite high concentration hydrogels was between 170 - 200 µg per ml collagen. For simplicity, composite hydrogels with increased amounts of peptides are referred to as HP High and those containing the previously studied doses are referred to as HP.

4.2.2 Preparation of Conduits

NGCs by the Uhrich group (Jeremy Griffin) were fabricated by dip-coating Teflon needles into solutions of poly(lactic-anhydride) and poly(anhydride-ester). For simplicity, this polymer blend will be referred to as PS conduits. Commercially available, non-degradable polyethylene (PE) tubes (0.6mm ID/1mm OD) were pre-cut to a 5.5 mm length and UV sterilized.

Collagen hydrogel solutions at 2.0 mg/ml were prepared as previously described [6]. Native and functionalized collagen solutions were injected in excess to ensure complete void filling into all NGCs tubes using a 22 gauge syringe. The tubes were incubated at 37°C to allow self-assembly of the hydrogel. Control tubes were filled with a sterile PBS solution immediately prior to implantation.

4.2.3 Animals and Surgical Procedure

All surgical procedures (completed by Jian Chen), functional measures, and morphological measures were similar to those conducted in Chapter 3 of this thesis. Functional metrics included the foot base angle (FBA) and the protraction limb ration (PLR). The acquision of the video and analysis were primarily completed by Yong Soo

Lee of the Uhrich group. Morphological metrics included axon count and percent regeneration. The number of samples used for each analysis per condition are summarized in **Table 4.1** below:

	Functional Recovery		**Morphological Recovery**	
Condition	FBA	PLR	Axon Count	% Regeneration
PS Saline (Cohort III)	6	6	2*	2*
PS Native (Cohort III)	6	6	4	4
PS HP (Cohort III)	6	6	2*	2*
PE HP High (Cohort III)	11	11	8	7

Table 4.1 Summary of experimental conditions * Not included in statistical analysis

4.3 RESULTS

4.3.1 Functional Recovery

4.3.1.1 Degradable Tubes

Foot base angle (FBA) measurements were collected for all animals treated with PS conduits at 0, 1, 8, and 15 weeks post-injury (**Figure 4.1 A**). Prior to injury, the FBA did not differ significantly among PS-treated groups and was approximately 72 degrees. One week post-injury, the average FBA increased to approximately 109 degrees in PS-treated conditions and nearly approached statistically significant differences between groups ($p = 0.053$). Between PE- and PS- cohorts, no significant differences were found at week 0, however were noted at week 1 ($p < 0.0001$). Given the disparity among PS-treated conditions and between PE and PS cohorts at week 1, the utility of analyzing raw FBA scores is limited. In other words, the raw recovery scores are dependent on the extent of injury at week 1. As the angles at week 1 are different, the angles at week 15 are not comparable. Therefore, further analysis of PS conduits and their comparison to PE conduits from previous cohorts was completed using the recovery index (RI, **Figure 4.1 B**). At both 8 and 15 weeks post injury, there were no significant differences found between the use of PE or PS when compared to use with its respective filler (ie PS Saline vs PE Saline, PS Native vs PE Native).

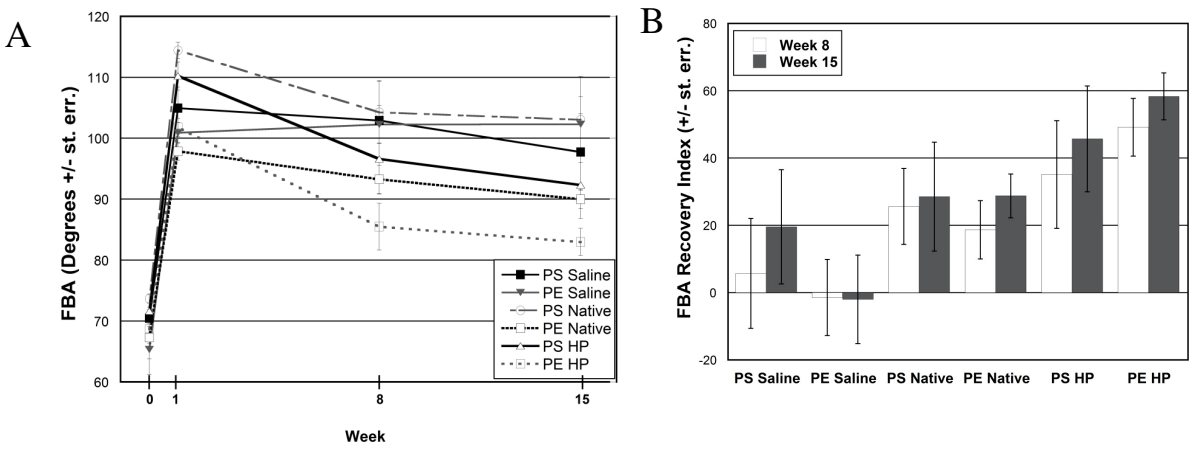

Figure 4.1 Functional evaluation of quadriceps branch reinnervation as assessed using foot base angle (FBA) for degradable PS and non-degradable PE conduits. (A) Evaluation of FBA measurements over time revealed significantly different scores between PE and PS containing cohorts at Week 1, precluding the use of raw FBA scores. (B) When FBA measurements were normalized to the extent of injury at week 1 using the recovery index, no statistical differences were found PE and PS tubes when using the same intraluminal filler. Means are reported +/− standard error. Differences were considered significant at $p < 0.05$ using one-way analysis of variance.

PS-treated animals were also subjected to the pencil grip analysis on weeks 0, 1, 8, and 15 post injury (**Figure 4.2 A**). The PLR increased from approximately 1.0 pre-injury to approximately 1.53 post-injury, with no statistically significant differences among the treatment groups or between cohorts at either time point. At weeks 8 and 15, no statistically significant differences were found in the PLR between the use of PE or PS when the same intraluminal filler was used. Similarly, no significant differences were found between PE and PS when the PLR RI was compared between groups with the same intraluminal filler (**Figure 4.2 B**).

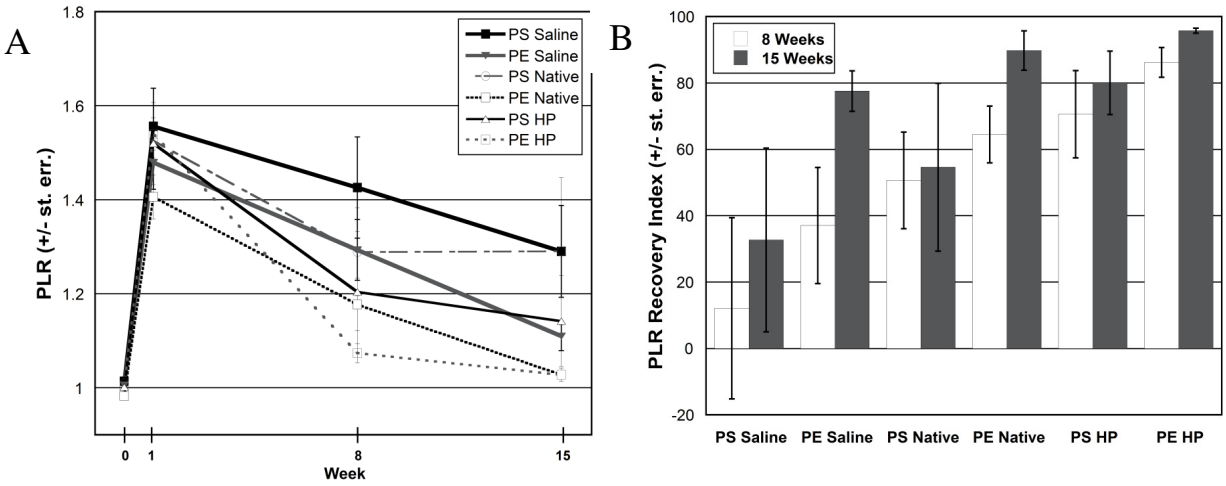

Figure 4.2 Functional evaluation of quadriceps branch reinnervation as assessed using protraction limb ratio (PLR) for degradable PS and non-degradable PE conduits. Evaluation of PLR measurements over time (A) and after normalizing to the extent of injury using the recovery index (B) revealed no statistically significant differences between PE and PS conduits when compared to its respective intraluminal filler at 8 or 15 weeks post injury. Means are reported +/− standard error. Differences were considered significant at $p < 0.05$ using one-way analysis of variance.

4.3.1.2 High Concentration Glycomimetic Functionalized Collagen

Within this cohort, FBA measurements were collected for all PE conduits at 0, 1, 8, and 15 weeks post-injury (**Figure 4.3 A**). Prior to injury, the FBA did not differ significantly among PE-treated groups and was approximately 69 degrees. One week post-injury, the average FBA for HP High- treated groups increased to 108 degrees, which was significantly higher than the scores from the previous cohort using PE tubes at week 1 ($p < 0.0001$). Once again, this limits the utility of using raw FBA angles to assess overall recovery since there are discrepancies in the degree of initial injury between cohorts.

As shown in **Figure 4.3 B**, when comparing the FBA RI at 8 and 15 weeks post-injury, significant differences were found between saline and hydrogel conditions ($p = 0.00025$ and $p < 0.0001$, respectively) and native and scrambled-coupled versus glycomimetic-functionalized collagen hydrogels ($p = 0.02027$ and $p = 0.00055$, respectively). However, no significant differences were found within glycomimetic-functionalized conditions for either time point.

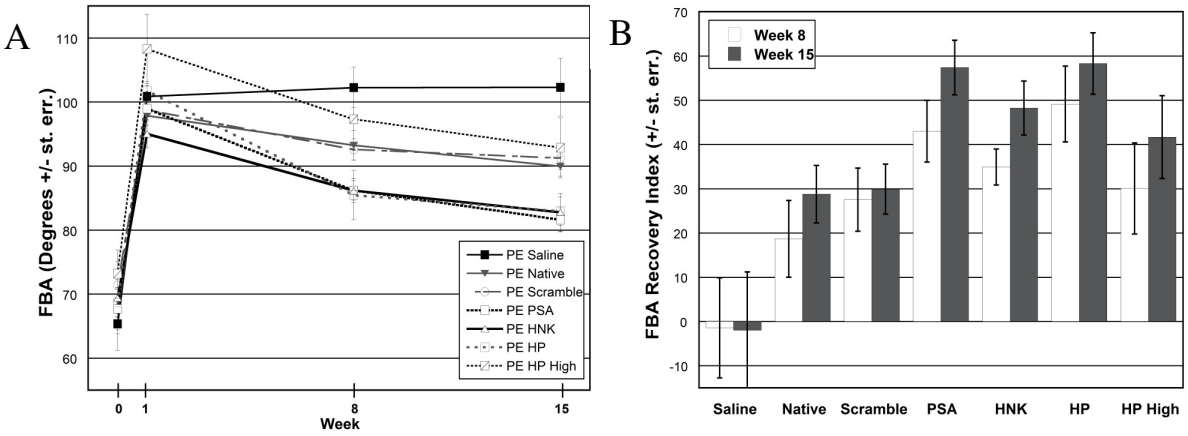

Figure 4.3 Functional evaluation of quadriceps branch reinnervation as assessed using FBA for PE conduits. (A) Evaluation of FBA measurements over time revealed significantly different scores between PE conduits at Week 1, precluding the use of raw FBA scores. (B) When FBA measurements were normalized to the extent of injury at week 1 using the recovery index, statistically significant differences were found between saline and hydrogel containing groups and glycomimetic-functionalized versus non-glycomimetic-functionalized groups. However, no statistical differences were noted within groups treated with glycomimetic-functionalized collagen. Means are reported +/− standard error. Differences were considered significant at $p < 0.05$ using one-way analysis of variance.

Functional recovery was also assessed using the pencil grip for hydrogels containing higher concentrations of the grafted glycomimetic (**Figure 4.4 A**). At 0 and 1 week post injury, the PLR was not significantly different between groups and increased from unity to approximately 1.45. At 8 weeks post injury, animals treated with collagen hydrogels outperformed saline treated groups ($p = 0.01932$), but no significant differences were noted between hydrogel treated groups. No significant differences were noted between any groups at 15 weeks post injury. When scores were normalized to the extent of injury using the recovery index (**Figure 4.4 B**), collagen hydrogels outperformed saline treated groups at week 8 ($p = 0.05$), but no significant differences were noted between hydrogel treated groups. Once again, no differences were noted between any of the treatment groups at 15 weeks post injury.

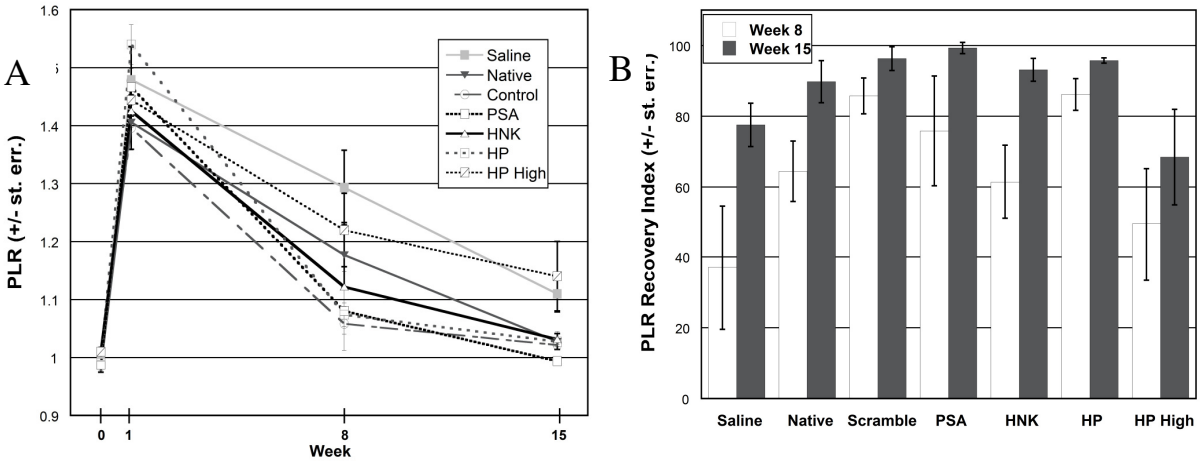

Figure 4.4 Functional evaluation of quadriceps branch reinnervation as assessed using PLR for PE conduits. Evaluation of PLR measurements over time (A) and after normalizing to the extent of injury using the recovery index (B) revealed statistically significant differences at 8 weeks between collagen and saline treated groups. However, no significant differences were found among any groups at 15 weeks post injury. Means are reported +/− standard error. Differences were considered significant at $p < 0.05$ using one-way analysis of variance.

4.3.1.3 Analysis for Statistical Outliers

Further evaluation of the Week 15 FBA recovery index as a dot plot for PS conduits revealed a large variance in the data set (**Figure 4.5**). Therefore, the data was tested for statistical outliers using the Grubb's test. Within all PS treated groups, only the lowest point in the PS HP was considered a statistical outlier at the significance level of $p = 0.05$.

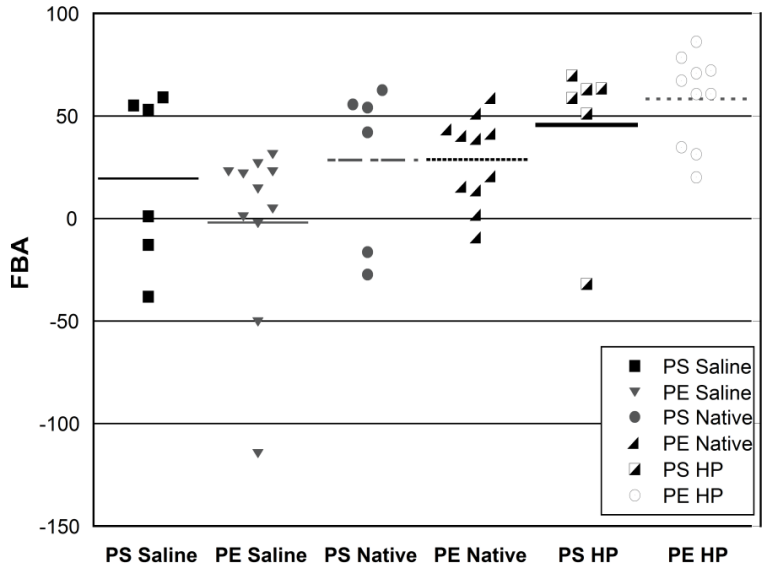

Figure 4.5 Dot plot of degradable PS conduits and non-degradable PE conduits. Individual conditions were subjected to Grubb's Test, where it was reveled that the lowest point in the PS HP was a statistical outlier.

4.3.2 Morphological Recovery

4.3.2.1 Degradable Tubes

Regenerated nerve samples were transected from sacrificed animals at 16 weeks post injury. For several of the samples, technical difficulties in the processing of the tissue prohibited further histomorphometric analysis. Within the samples that were stained and processed successfully, evaluation revealed that a portion of the PS tubes had failed in vivo as made evident by an undefined epineurium surrounding the nerve. Only the PS Native condition had a large enough sample size (n = 4) to merit further statistical analysis (**Figure 4.6 A, B**). While there the percentage of fascicular regeneration was greater in the PS Native condition versus PE Native ($p = 0.01$), there were no significant differences in the number of axons between the two groups.

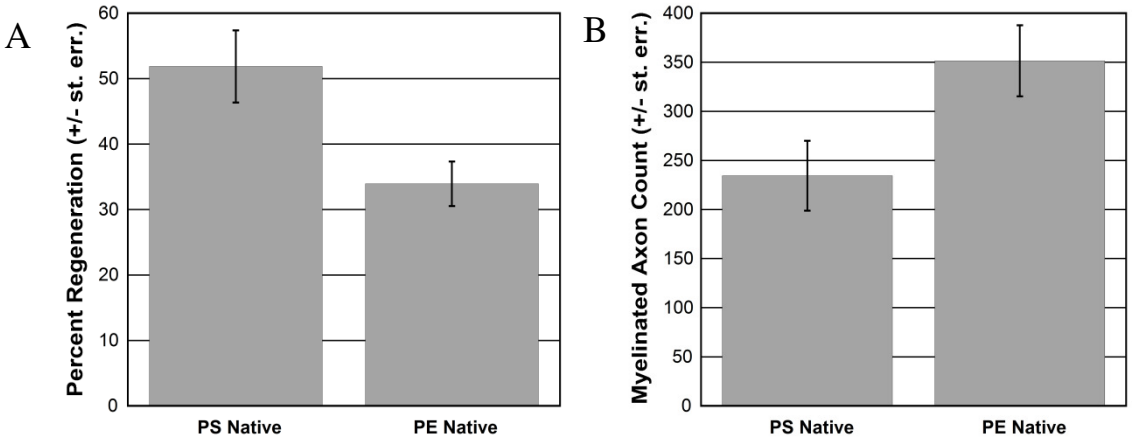

Figure 4.6 Histomorphometry of regenerated nerves from degradable PS conduits and non-degradable PE conduits filled with native collagen. (A) PS conduits yielded a significantly higher percentage of fascicular regeneration. (B) No statistical differences in myelinated axon counts were noted between PE and PS. Means are reported +/– standard error. Differences were considered significant at $p < 0.05$ using one-way analysis of variance.

4.3.2.2 High Concentration Glycomimetic Functionalized Collagen

Hydrogel treated axons had significantly greater percentage of fascicular regeneration than saline treated animals (**Figure 4.7 A**; p = 0.00861). Within hydrogel treated groups, high concentration composite hydrogels outperformed HNK-functionalized hydrogels (p = 0.0164).

When the number of myelinated axons in the regenerated nerve were analyzed as shown in **Figure 4.7 B**, significant differences were found between saline verse hydrogel treated conditions (p = 0.00112). Within peptide grafted hydrogels, PSA containing hydrogels outperformed non-PSA containing hydrogels (p = 0.011). On the other hand, HNK-functionalized hydrogels were not significantly different than non-HNK functionalized hydrogels. While there were no statistically significant differences between PSA containing hydrogels, HP high hydrogels had the highest myelinated axon count on average.

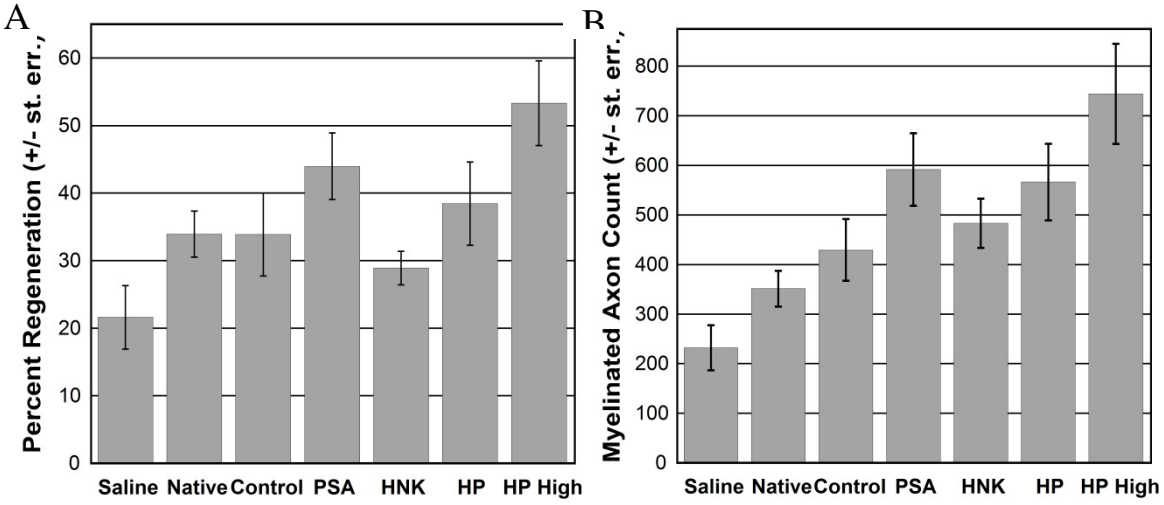

Figure 4.7 Histomorphometry of regenerated nerves. (A) Hydrogel-treated conditions yielded significantly higher percentage of fascicular regeneration compared to saline. Within hydrogel-treated groups, HP High-functionalized hydrogels outperformed HNK-functionalized hydrogels. (B) Significantly more myelinated axons were found in hydrogel treated groups verse saline. PSA-containing hydrogels also had significantly greater axon counts when compared to non-PSA containing hydrogels. No differences were found between HNK and non-HNK containing hydrogels. Means are reported +/– standard error. Differences were considered significant at $p < 0.05$ using one-way analysis of variance.

4.4 DISCUSSION

In our previous in vivo work, we have shown that the use of glycomimetic-functionalized collagen results in improvement in functional and morphological recovery following peripheral nerve injury. Given these promising results, in this study we attempted to further improve the utility of HNK/PSA glycomimetic-functionalized collagen using two methods- interfacing with a degradable outer conduit and increasing the concentration of the individual glycomimetics in composite hydrogels.

4.1 Degradable Tubes

One formulation for a degradable NGC that we used is a salicylic acid based poly(anhydride-ester), PAE and PLAA blend from the Uhrich group. The novelty of this polymer is that one of the degradation products includes salicylic acid, the active component of aspirin, and a biocompatible linker [7-9]. The non-steroidal anti-inflammatory (NSAID) has been shown to maintain bioactivity after incorporation into and release from the polymeric backbone [10]. As the salicylic acid is released locally, it may be possible to achieve high tissue specific concentrations of the NSAID and thereby mitigate local pain, swelling, and infection.

When the functional recovery of PS conduits was compared to PE conduits, no statistical differences were found between either NGC. While surprising, there are several possible explanations for this outcome. For one, the intraluminal filler may be a greater determinant of functional outcome than the material which makes up the outer conduit. The outer conduit generally provides protection from infiltrating fibroblasts, and likely both conduits perform similarly in this role. Additionally, it should be noted that the

original studies with PE were conducted in a different cohort which may add inherent variability to the functional scores. This possibility is supported by the large variance in the raw FBA scores at week one, whose range should be relatively narrow. However, it should be noted, that while there were no significant differences between PE and PS groups, the trends noted with the addition of the intraluminal filler were preserved. In other words, the addition of collagen to a hollow conduit, either PS or PE, increased the FBA.

As this was a pilot study with the PS conduits, the sample numbers were relatively small (n = 6). Therefore while statistical significance may not have been reached, it is important to note emerging trends in the data. One particularly interesting outcome was the increase in functional recovery with PS Saline verse PE Saline. While this may be attributed to the therapeutic effect of the NSAID degradation products, more work is required to more accurately support this hypothesis.

4.2 High Concentration Glycomimetic Functionalized Collagen

Given the distinct morphological results seen in our previous in vivo work with the use of PSA and HNK- functionalized hydrogels, we speculated that different mechanisms may be involved in their individual action. Since we did not see any functional or morphological benefit in our composite hydrogel, we speculated that this may be a result of an inadequate amount of the each peptide. To this end we generated composite hydrogels containing higher doses of functionalized glycomimetic to assess if there would be any increase in functional or morphological outcomes.

While there were no differences noted with the FBA and PLR scores with the higher concentration hydrogels, there were some interesting differences noted in the morphological results. For one, the HP High hydrogels had a significantly higher percentage of fascicular regeneration when compared to other hydrogel treated groups. Additionally, the HP High hydrogels yielded the largest myelinated axon count on average. The increase in axon count is in agreement with our previous work which also showed that inclusion of grafted PSA leads to an increase in axon counts, perhaps through collateralization. Currently, we are investigating whether inclusion of the HP High hydrogels results in an increase in myelination profiles and motoneuron targeting.

Although there was an improvement in morphological recovery, we did not any significant changes in functional recovery. This outcome may be attributed to several sources. For one, it is possible that we have reached the maximum possible recovery for this injury model. It may be necessary to use a different nerve injury model, like the sciatic nerve, to distinguish differences between glycomimetic-functionalized collagen hydrogels. Also, since the differences between the conditions are likely to be less pronounced between glycomimetic-functionalized hydrogels, an increased sample size may be required to elucidate any improvement in functional recovery.

4.5 REFERENCES

1. Masand SN, Chen J, Perron IJ, Hammerling BC, Loers G, Schachner M, et al. The effect of glycomimetic functionalized collagen on peripheral nerve repair. Biomaterials. 2012. Epub 2012/08/25.
2. Mehanna A, Mishra B, Kurschat N, Schulze C, Bian S, Loers G, et al. Polysialic acid glycomimetics promote myelination and functional recovery after peripheral nerve injury in mice. Brain. 2009;132(Pt 6):1449-62. Epub 2009/05/21.
3. Simova O, Irintchev A, Mehanna A, Liu J, Dihne M, Bachle D, et al. Carbohydrate mimics promote functional recovery after peripheral nerve repair. Ann Neurol. 2006;60(4):430-7. Epub 2006/09/08.
4. Nectow AR, Marra KG, Kaplan DL. Biomaterials for the development of peripheral nerve guidance conduits. Tissue Eng Part B Rev. 2012;18(1):40-50. Epub 2011/08/05.
5. Masand SN, Perron IJ, Schachner M, Shreiber DI. Neural cell type-specific responses to glycomimetic functionalized collagen. Biomaterials. 2012;33(3):790-7. Epub 2011/10/27.
6. Shreiber DI, Barocas VH, Tranquillo RT. Temporal variations in cell migration and traction during fibroblast-mediated gel compaction. Biophys J. 2003;84(6):4102-14. Epub 2003/05/29.
7. Erdmann L, Uhrich KE. Synthesis and degradation characteristics of salicylic acid-derived poly(anhydride-esters). Biomaterials. 2000;21(19):1941-6. Epub 2000/08/15.
8. Griffin J, Delgado-Rivera R, Meiners S, Uhrich KE. Salicylic acid-derived poly(anhydride-ester) electrospun fibers designed for regenerating the peripheral nervous system. Journal of biomedical materials research Part A. 2011;97(3):230-42. Epub 2011/03/29.
9. Prudencio A, Schmeltzer RC, Uhrich KE. Effect of linker structure on salicylic acid-derived poly(anhydride-esters). Macromolecules. 2005;38(16):6895-901.
10. Erdmann L, Macedo B, Uhrich KE. Degradable poly(anhydride ester) implants: effects of localized salicylic acid release on bone. Biomaterials. 2000;21(24):2507-12.

CHAPTER 5. DEVELOPMENT AND UTILIZATION OF IN VITRO TOOLS TO CHARACTERIZE NEURAL CELL/BIOMATERIAL INTERACTION

5.1 INTRODUCTION

Despite the innate regenerative potential of the peripheral nervous system (PNS), functional recovery is often incomplete with increasing severity of injury. Although this outcome has been attributed to a number of causes, the malrouted reinnervation of emerging neurites may be a significant cause. We have generated glycomimetic-functionalized collagen hydrogels as a potential therapeutic strategy to increase the efficiency of synaptic reconnection [1, 2]. While this novel material has yielded promising results both in vivo and in vitro, there is still limited understanding of its specific mechanism of action.

In our studies we have shown that PSA- and HNK- functionalized hydrogels yield a similar magnitude of functional recovery despite having discrete results morphologically. While PSA-functionalized collagen results in an increase of axon count, HNK-functionalized collagen improves myelination and motoneuron targeting. Composite hydrogels comprising both HNK- and PSA-functionalized collagen can further improve morphological outcome, suggesting there may be a synergistic benefit. This interesting divergence in morphological results led us to speculate that distinct mechanisms may be involved in their action. Unfortunately, while in vivo systems represent the most physiologically relevant method to characterize neural cell/biomaterial interaction in the PNS, they have many limitations. In vivo approaches are cost-prohibitive, labor intensive, and generally have minimal throughput. Therefore, the need for alternative methods to address mechanistic questions exists. In vitro tools have been

developed over the years to overcome some of these drawbacks, however they have generally focused on sensory axon outgrowth since dorsal root ganglia cultures are more easily cultured than their motor counterpart [3].

Herein, we use two distinct methods to culture motoneurons: 1) dissociated embryonic spinal cord cultures and 2) organotypic spinal cord explants. We utilize these cultures to preliminarily examine the effects of a library of kinase inhibitors on native and glycomimetic-functionalized hydrogels. We aim to generate a platform to understand neural cell/biomaterial interaction and to begin to understand the pathways potentially involved in the action of these glycomimetics.

Currently, dissociated embryonic spinal cords are the most utilized technique for the culture of motoneurons. They provide more physiological relevance over the use of immortalized cell lines like PC12, while still maintaining relatively high-throughput with reasonably limited cost.

Organotypic slice cultures have several advantages over traditional in vitro culture techniques. For one, these cultures mimic in vivo cytoarchitecture which is likely important to many physiological processes. Generally, these cultures are biochemically and physiologically more similar to in vivo conditions over traditional in vitro techniques. Additionally, homophilic and heterophilic cell/cell interactions are maintained. In peripheral nerve regeneration, neuron/Schwann cell apposition has been shown to be vital to the regenerative process [4]. However, in vitro methods for their co-culture are limited. Postnatal motoneurons can be cultured from P7 - P10 rat pups since neuronal viability is high and neurite outgrowth is robust without the requirement for end-organs [5]. While most of the work using spinal cord explants have assessed

motoneuron survial [6], Allodi et al. have recently developed methods to assess neurite outgrowth from motoneurons in these preparations [7]. We have used slight modifications of their technique to culture spinal cord explants within our modified collagen hydrogels.

5. 2 METHODS

5.2.1 Isolation of Dissociated Spinal Cord Neurons (SCNs)

SCNs were isolated from E15 Sprague Dawley rats as previously described [8]. Spinal cords were excised and meninges removed. Cords were transferred to a 15 mL centrifuge containing 0.05% trypsin in HBSS and incubated at 37°C for 20 minutes. Following this incubation, the sample was centrifuged and supernatant removed and replaced with a 10% serum-containing media. The tissue pieces were mechanically dissociated via trituration and large pieces of debris were allowed to settle. The supernatant, which contained the single cell suspension, was transferred to a 50 mL centrifuge tube and placed in a 37°C humidified incubator. The remaining tissue pieces were subjected to a second dissociation and were then pooled with dissociated cells from the first. The combined supernatants were filtered through a 40-µm pore-sized nylon mesh. Cells were centrifuged for 5 minutes at 1000 rpm at 4°C, resuspended in 10% serum containing media, and triturated with a fire-polished Pasteur pipette. The cell suspension was transferred to a T-75 tissue culture flask and incubated for 30 minutes at 37 °C to enhance the purity of the culture via differential adhesion of the contaminating glia and fibroblasts vs. neurons. The neuron-enriched supernatant was removed with a serological pipette and transferred to a centrifuge tube. Following centrifugation, the cells

were resuspended in neurobasal media supplemented with B-27, penicillin/streptomyocin, L-glutamine, and beta-mercapoethanol prior to plating.

5.2.2 Isolation of Spinal Cord Explants

Sprague Dawley rats at postnatal day 7 were decapitated and their spinal cords excised and placed in cold Gey's balanced salt solution supplemented with 30% glucose. Meninges and spinal roots were carefully removed. Cords were then sectioned into 350 μm slices using a vibratome and placed in the additional cold Gey's balanced salt solution until plating.

5.2.3 Preparation of Cultures

Glycomimetic-functionalized type I collagen was made as previously described [2]. PSA- and HNK- functionalized hydrogels were used at a concentration of 200 - 240 μg of grafted peptide per ml collagen. Collagen hydrogel solutions were made as previously described [9]. Briefly, native or functionalized oligomeric collagen solutions at 3 mg/mL were neutralized using solutions in the following ratios: 2% 1M Hepes (Fluka), 14% 0.1N NaOH, 10% 10X Minimum Essential Medium (Sigma), 5.2% M199 (Sigma), 0.1% Penicillin/Streptomycin (P/S; Sigma), 1% L-glutamine (L-glut; Sigma), 67.7% native or peptide-functionalized collagen. Solutions were kept on ice to prevent fibrillogenesis.

For spinal cord explant cultures, glass coverslips were pre-coated with PDL and put into individual wells of a 24 well microtiter plates. A 30uL droplet of collagen hydrogel solution was added to each well and incubated to allow self-assembly. Individual explants were placed on each droplet additional collagen hydrogel solution was added to the top. Following gel formation, neurobasal media supplemented with

B27, glucose, P/S, and L-glut was added to each well. For dissociated spinal cord cultures, 50 uL of the collagen hydrogel solution was added to each well of a 48 well microtiter plate and incubated to allow self assembly. Dissociated spinal cord neurons were plated on native or functionalized collagen hydrogels at 75,000 cells per/well.

5.2.4 Kinase Inhibitors for Dissociated SCNs

Various kinase inhibitors, as summarized in **Table 5.1**, were added to SCN cultures at DIV3. Control cultures were supplemented with 0.05% DMSO. Following a 5-day incubation period, cells were fixed and stained using rabbit anti-MAP-2 (Millipore, 1:1000) followed by goat anti-rabbit Alexa Fluor 488. Approximately fifteen images per well were taken using a 20× objective and analyzed using ImageJ. Neurite extension was considered to be the length of the presumptive axon, or the longest neurite. Measurements were only included if the recorded length was longer than the cell body diameter. Neurite extension was compared using ANOVA followed by posthoc pairwise comparisons with Tukey's test. Differences were considered significant at $p < 0.05$.

Kinase Inhibitor	Conc.	Target	Supplier (Catalog)
FAK Inhibitor	1 µM	Prevents Focal Adhesion Kinase (FAK) Autophosphorylation	Calbiochem (324877)
ML 141	10 µM	Inhibitor of Cdc42 GTPase	Tocris (4266)
IPA-3	5 µM	Prevents activation of p21 Kinase	Calbiochem (506106)
Wortmannin	100 nM	Inhibitor of PI3 Kinase	Millipore (12-338)
RAC1 Inhibitor	100 µM	Inhibits Rac1 GDP/GTP exchange activity	Calbiochem (553502)
PD98059	10 µM	Inhibitor of MAP kinase kinase (MEK)	Calbiochem (513000)
SB202190	1 µM	Inhibitor of p38 MAP kinase	Calbiochem (559388)
Rho/SRF Pathway Inhibitor	5 µM	Inhibitor against RhoA- and RhoC	Calbiochem (555558)

Table 5.1 Kinase Inhibitors used in SCN cultures.

5.2.5 Kinase Inhibitors for SC Explant Cultures:

Various kinase inhibitors, were added to SC explant cultures as summarized in Table 5.2. In preliminary experiments, kinase inhibitors were added to SC explant cultures at DIV1. Unfortunately, this ultimately resulted in death of the cultures. We speculated that the early addition of these kinase inhibitors disrupted early cellular processes which are required for Schwann cell migration and neurite extension. In followup experiments, kinase inhibitors were added at DIV4.

Kinase Inhibitor	Conc.	Target	Supplier (Catalog)
SB415286	50 mM	Inhibitor of glycogen synthase kinase-3 (GSK-3)	Tocris (1617)
SP600125	10 µM	Inhibitor of *c*-Jun N-terminal kinase (JNK)	Calbiochem (420119)
U0126	10 µM	Inhibitor of MEK1	Calbiochem (662005)
FAK Inhibitor	30 µM	Prevents Focal Adhesion Kinase (FAK) Autophosphorylation	Calbiochem (324877)
ML 141	10 µM	Inhibitor of Cdc42 GTPase	Tocris (4266)
IPA-3	20 µM	Prevents activation of p21 Kinase	Calbiochem (506106)
Wortmannin	500 nM 50 µM	Inhibitor of PI3 Kinase	Millipore (12-338)
RAC1 Inhibitor	20 µM	Inhibits Rac1 GDP/GTP exchange activity	Calbiochem (553502)
PD98059	1 µM 100 µM	Inhibitor of MAP kinase kinase (MEK)	Calbiochem (513000)
SB202190	20 µM	Inhibitor of p38 MAP kinase	Calbiochem (559388)
Rho/SRF Pathway Inhibitor	100 µM	Inhibitor against RhoA- and RhoC	Calbiochem (555558)

Table 5.2 Kinase Inhibitors used in SC Explant cultures.

Given the thickness of the explant cultures, more involved immunohistochemical techniques were required for staining. Cultures were fixed in 4% paraformaldehyde at DIV6, washed with PBS, and then treated with hot citrate buffer for 1 hour for antigen retrieval. Slices were then methanol dehydrated and incubated with primary antibodies, an anti-neurofilament (mouse RT-97, Developmental Hybridoma Bank, 1:200) and anti-S100 (rabbit ab74161, Abcam), for 48 hours. Following generous washes, explants were then incubated with an anti-mouse AlexaFluor 488 and an anti-rabbit AlexaFluor 568 (Life Technologies) for 24 hours. Slices were then ethanol dehydrated and mounted on glass slides. Montages of the explants were taken on an Olympus IX81 using a 10X objective. Neurite extension and Schwann cell migration from the explant were quantified and compared using ANOVA followed by posthoc pairwise comparisons with Tukey's test. Differences were considered significant at $p < 0.05$.

5.3 RESULTS

5.3.1 Dissociated SCNs

Dissociated SCNs were cultured on native and glycomimetic-functionalized hydrogels for 5 DIV. Similar to our previous in vitro experiments, PSA- and HNK-functionalized hydrogels yielded significantly longer neurite lengths than native hydrogels ($p < 0.0001$ for both conditions). As the kinase inhibitors are solubilized in DMSO, on DIV3 a small amount of DMSO was added to cultures to assess baseline effects on neurite outgrowth. As shown in **Figure 5.1 A**, no significant differences were observed between control and DMSO-supplemented media.

Following the addition of FAK, neurite outgrowth remained significantly greater on PSA and HNK-functionalized hydrogels compared to native hydrogels ($p = 0.0015$

and $p = 0.0141$, respectively). Also, control cultures were not significantly different than FAK-supplemented cultures. These results suggest that FAK is not involved in the behavior of our glycomimetic-functionalized hydrogels (**Figure 5.1 B**).

With addition of ML141 and IPA-3, neurite outgrowth on native, PSA-functionalized, and HNK-functionalized hydrogels dropped significantly when compared to control cultures ($p = 0.0012$, $p < 0.0001$, $p < 0.0001$ for ML141, and $p = 0.00056$, $p < 0.0001$, $p < 0.0001$ for IPA-3, respectively). Additionally, there were no significant differences between hydrogel groups in ML141 or IPA-3 treated conditions. These results suggest that the inhibition pathways of ML141 and IPA-3 result in a global disruption of neurite outgrowth (**Figure 5.1 C**).

Following the addition of RAC1 inhibitor and PD98059, neurite outgrowth on native, PSA-functionalized, and HNK-functionalized hydrogels were not significantly different from one another. While growth on native hydrogels were not significantly affected by the addition of RAC1 and PD98059, growth on PSA- and HNK-functionalized hydrogels was significantly reduced when compared to control cultures (RAC1: $p < 0.0001$ and $p = 0.0149$, respectively; PD98059: $p < 0.0001$ and $p < 0.0001$, respectively). These results suggest that inhibition of the RAC1 and MEK pathways affects glycomimetic-functionalized hydrogels specifically (**Figure 5.1 D**).

As demonstrated in **Figure 5.1 E**, following the addition of and Rho/SRF inhibitor, neurite outgrowth on native and PSA-functionalized hydrogels were not significantly different from one another. HNK-functionalized hydrogels yielded significantly higher neurite lengths when compared to native and PSA-functionalized

hydrogels ($p < 0.0001$ and $p = 0.0071$, respectively). When cultures containing Rho/SRF were compared to cultures without, only PSA-functionalized hydrogels showed a significant decrease in neurite outgrowth ($p < 0.0001$).

Finally, in cultures supplemented with SB202190, PSA- and HNK- functionalized hydrogels yielded significantly longer neurites than native hydrogels ($p = 0.008$ and $p < 0.0001$, respectively). HNK-functionalized hydrogels outperformed PSA-functionalized hydrogels ($p = 0.0024$). When these cultures were compared to their control counterparts (i.e. without inhibitor), only neurites on PSA-functionalized hydrogels were found to be significantly shorter ($p < 0.0001$). The results with Rho/SRF and SB202190 inhibitor suggest that these pathways are involved in the action of PSA-functionalized hydrogels (**Figure 5.1 E**).

For ease of between group comparison, these results are summarized in **Figure 5.2**.

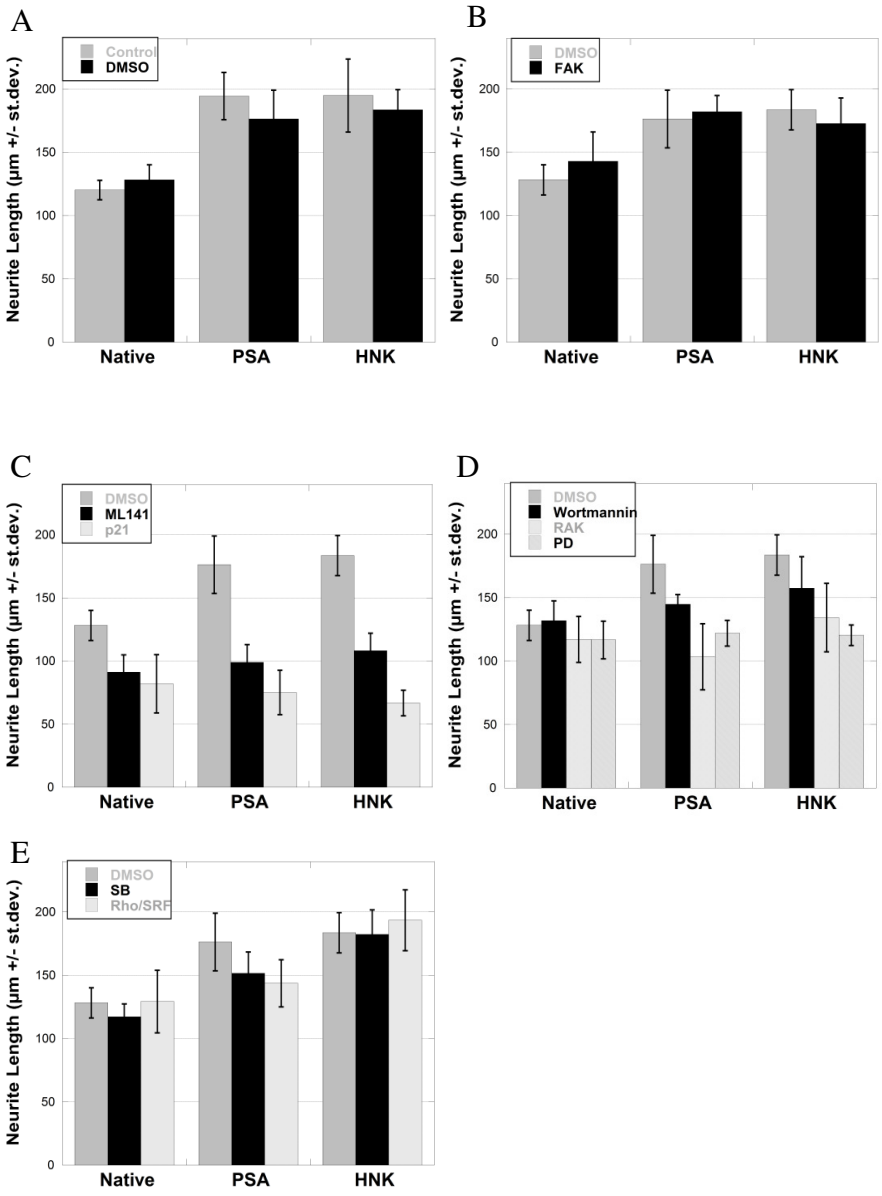

Figure 5.1 The effect of various kinase inhibitors on neurite extension in dissociated spinal cord cultures. (A) PSA- and HNK- functionalized hydrogels yield significantly longer neurites than native hydrogels in control and DMSO supplemented conditions. (B) The addition of FAK Inhibitor does not have a significant effect on neurite length (C) IPA-3 and ML141 significantly reduced neurite length in all conditions when compared to control.(D) Wortmannin, RAC1 Inhibitor, and PD98059 significantly reduced neurite length in glycomimetic-functionalized hydrogels. (E) SB202190 and Rho/SRF Inhibitor significantly reduced neurite lengths in PSA-functionalized hydrogels. Means are reported +/− standard deviation. Differences were considered significant at $p < 0.05$ using one-way analysis of variance.

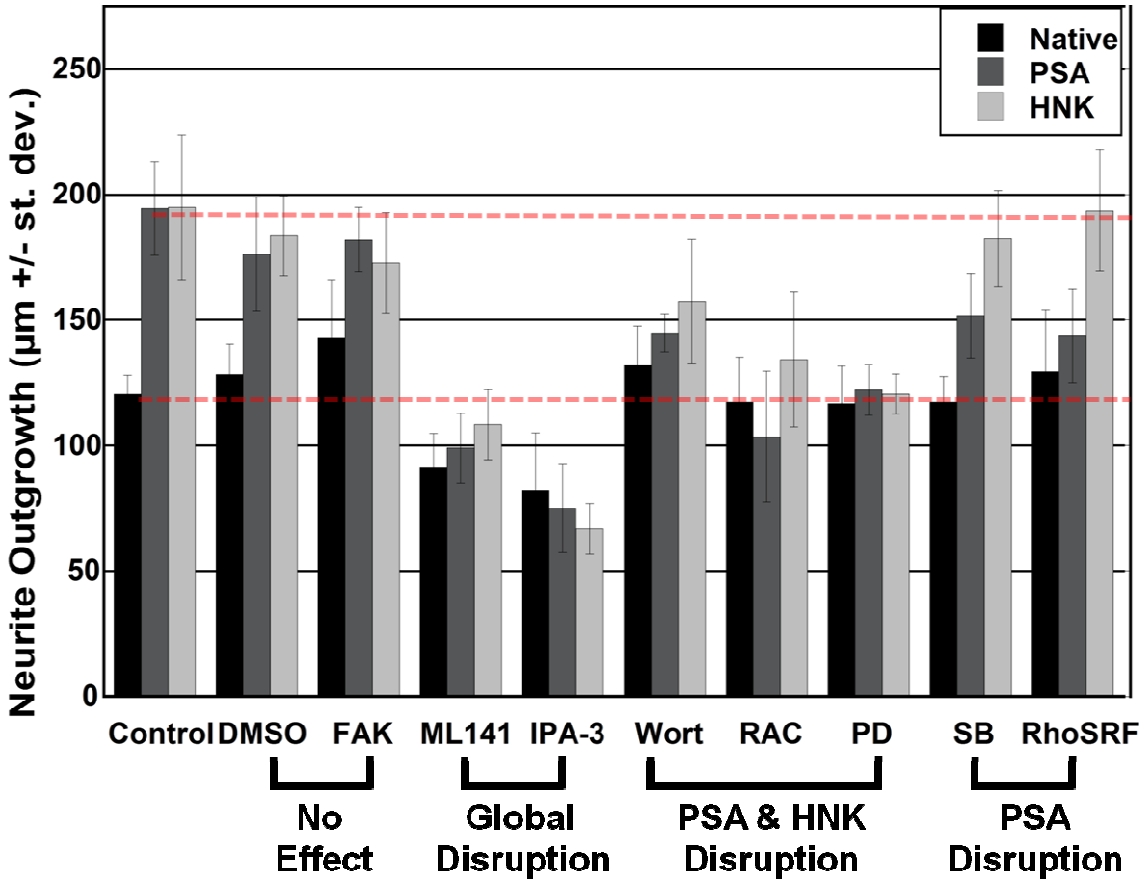

Figure 5.2 Summary of the dynamic response of kinase inhibitors on neurite outgrowth in dissociated spinal cord outgrowth. The red dashed lines indicate the baseline neurite outgrowth on native and glycomimetic functionalized hydrogels.

5.3.2 SC Explants

SC explants were cultured within a collagen hydrogel, allowing for three-dimensional outgrowth into the matrix. In all collagen conditions, we observed neurite extension and Schwann cell migration into the hydrogel (**Figure 5.3**). The Schwann cells migrated from the ventral root and generally neurites followed a similar trajectory. High magnification images of the explants demonstrated that Schwann cells and regenerating axons have significant interaction in these cultures.

The extent of neurite extension was quantified for control cultures (**Figure 5.4 A**). Spinal cord explants cultured on PSA- and HNK- functionalized collagen demonstrated significantly longer outgrowth than explants on native collagen ($p = 0.0222$ and $p < 0.0001$, respectively). However, neurite outgrowth between the glycomimetic-functionalized hydrogels was not significantly different. When Schwann cell migration was compared in these hydrogels (**Figure 5.4 B**), HNK-functionalized hydrogels caused Schwann cells to migrate significantly further than native hydrogels ($p = 0.0276$). However, there were no significant differences between glycomimetic-functionalized hydrogels or between PSA-functionalized and native hydrogels.

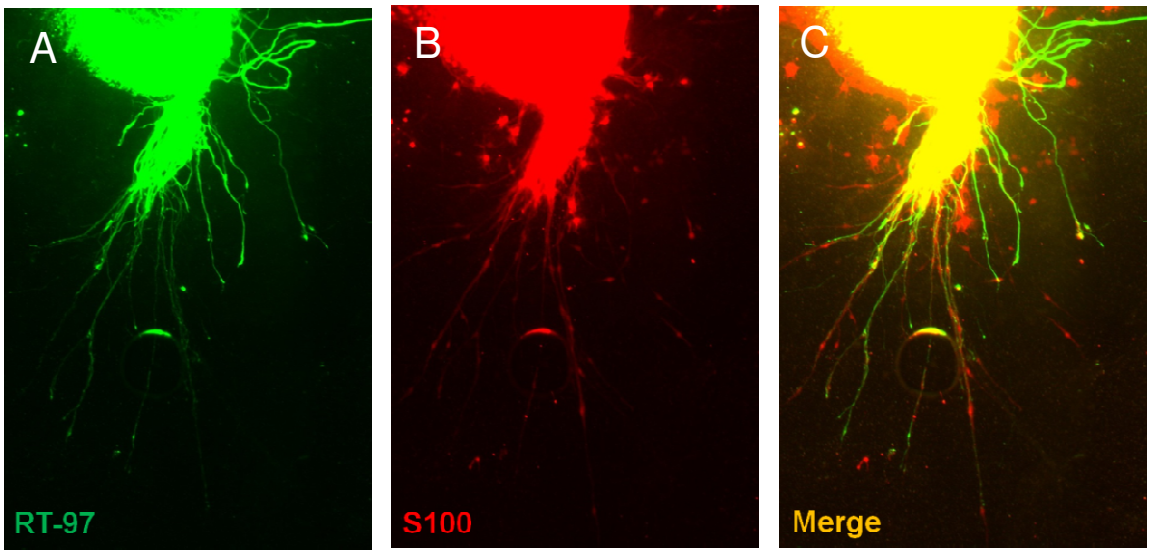

Figure 5.3 Representative image of regenerating motoneurons and migrating Schwann cells from a spinal cord explant culture after 5 DIV. Neurofilaments are labeled with RT-97 (A) and Schwann cells are labeled with anti-S100 (B), and a merged image (C) depicts the strong interaction between both cell types.

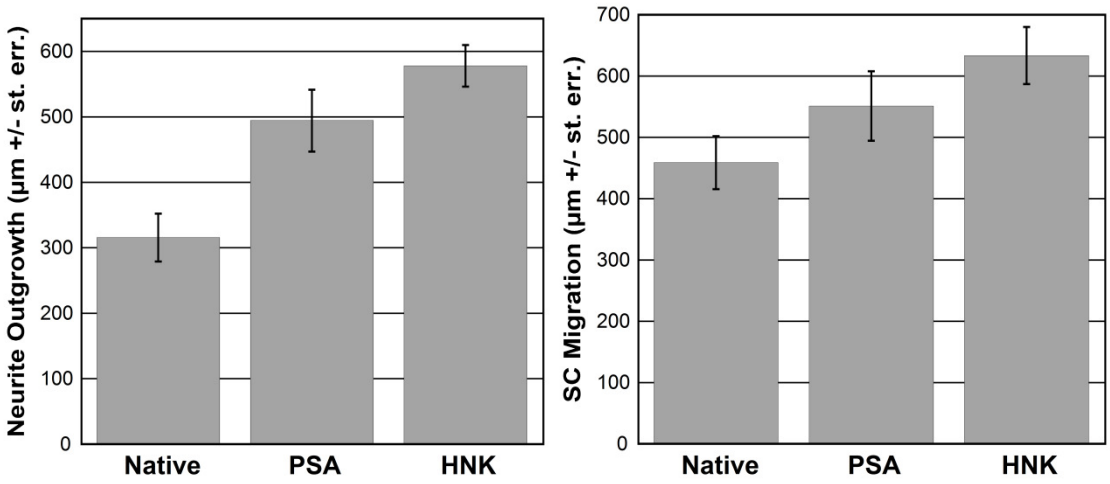

Figure 5.4 Phenotypic responses of spinal cord explants on native and glycomimetic-functionalized hydrogels. (A) Neurite extension on glycomimetic-functionalized hydrogels was significantly longer than native hydrogels. (B) Schwann cell migration on HNK-functionalized hydrogels was significantly longer than native hydrogels. Means are reported +/− standard error. Differences were considered significant at $p < 0.05$ using one-way analysis of variance.

In our preliminary experiments with the kinase inhibitors, the neurobasal media was supplemented with the inhibitors on DIV1. When S600125, PD98059, or U0126 were added, SC explants demonstrated motoneuron death and limited to no Schwann cell migration across all conditions. Given this induced toxicity, kinase inhibitors were added on DIV3 in all follow-up experiments.

With the addition of SB415286, a GSK inhibitor, there were no significant differences in neurite length between native and glycomimetic-functionalized conditions (**Figure 5.5 A**). When compared to control cultures, there were no significant differences in the native hydrogels, however PSA- and HNK-functionalized hydrogels yielded significantly shorter neurites with the addition of the kinase inhibitor ($p = 0.00258$ and $p = 0.001$). With respect to Schwann cell migration, there were no significant differences between hydrogel conditions with addition of SB415286 (**Figure 5.5 B**). However, when compared to control cultures, there was a significant drop in migration for both PSA- and HNK- functionalized hydrogels ($p = 0.00233$ and $p = 0.00343$). No significant differences were noted for native hydrogels.

With the addition of wortmannin, there was motoneuron cell death across all conditions, however Schwann cell migration was preserved. There were no significant differences noted between hydrogel conditions after wortmannin treatment. Also, no significant differences were noted between control and wortmannin-treated conditions (**Figure 5.5 B**).

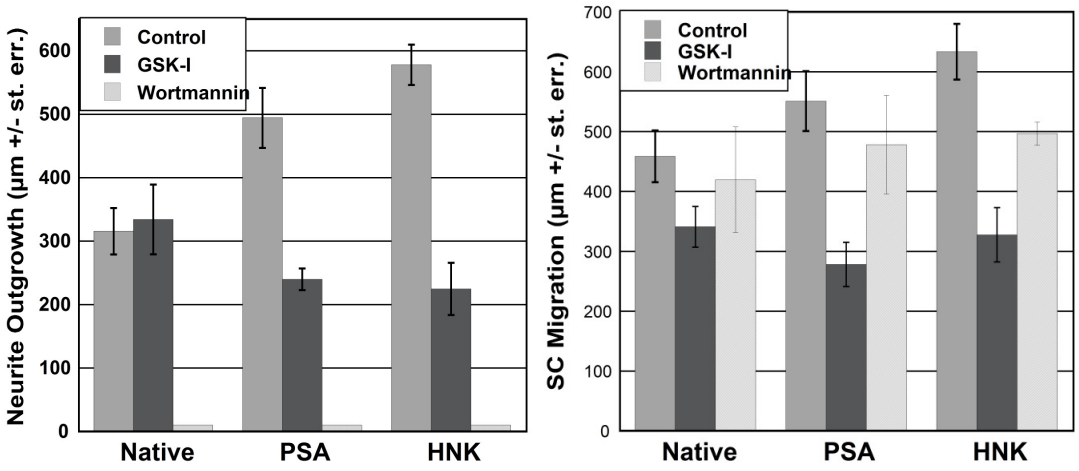

Figure 5.5 Phenotypic responses of spinal cord explants on native and glycomimetic-functionalized hydrogels with the addition of kinase inhibitors. (A) After addition of the GSK Inhibitor, neurite outgrowth was significantly reduced in glycomimetic-functionalized hydrogels, but was unaffected on native hydrogels. The addition of wortmannin resulted in death of motoneurons. (B) Addition of GSK Inhibitor, there was a significant decrease in Schwann migration within glycomimetic-functionalized hydrogels. Means are reported +/− standard error. Differences were considered significant at $p < 0.05$ using one-way analysis of variance.

5. 4. DISCUSSION

Developing a better understanding of cell/biomaterial interaction may increase the efficacy of its use. While the ideal method to address relevant questions related to this interaction will likely involve in vivo systems, this may not be a suitable approach when there are a large number of conditions or there is limited understanding of underlying pathways. Herein we have described the use of an in vitro platform to assess potential signaling pathways involved in the action of glycomimetic-functionalized collagen hydrogels. We use motoneuron cultures from two distinct sources, dissociated embryonic spinal cord neurons and spinal cord explants, and supplement these cultures with kinase inhibitors to begin to understand signaling pathways that may potentially be involved.

The responses that we observed with addition of kinase inhibitors to the dissociated SCN cultures can be categorized into the following: no effect, neurotoxic, inhibits glycomimetic-mediated activity, or inhibits PSA-mediated activity. We show that FAK Inhibitor had no effect on our cultures and addition of IPA-3 and ML141 was neurotoxic. The addition of PD98059, RAC1 Inhibitor, and wortmaninn resulted in a specific reduction of neurite outgrowth in glycomimetic-functionalized hydrogels. Finally, the addition of Rho/SRF inhibitor and SB202190 only affected PSA-functionalized hydrogels. Although these results do not provide causative evidence of individual pathway involvement, they do generate interesting hypotheses that can be used in follow-up studies.

Our initial work with the spinal cord explants provides proof of concept evidence that these cultures can be used to probe biomaterial function. These cultures generate viable motoneurons, outgrowth of neurites, and migration of Schwann cells. Our

characterization of the cultures also showed a significant interaction between regenerating neurites and Schwann cells. Numerous studies have shown that neuron/Schwann cell apposition is fundamentally important in the response following peripheral nerve injury. Therefore, these cultures can potentially be used to examine higher-order signaling mechanisms that may be important to the regenerative process.

Glycomimetic-functionalized collagen yielded significantly longer neurites than native hydrogels suggesting that cells in these cultures respond differentially to cues in their environment. This response also aligns well with previously reported in vitro and in vivo results. Interestingly, only HNK-functionalized hydrogels showed significantly greater Schwann cell migration compared to native hydrogels. In our initial in vitro work using the immortalized Schwann cell line RSC-96, only cells cultured on PSA-functionalized hydrogels showed an increase in proliferation and extension when compared to native hydrogels [2]. It is possible that Schwann cells in the SC explant cultures more adequately recapitulate features of this cell type in vivo. Recent work by Hoke et al. has described differences in Schwann cells as a function of their association with either motor or sensory axons [10]. However, it has also been demonstrated that maintenance of these specific features in vitro is not trivial as their profile of trophic factor release is quickly lost with traditional culture techniques [11]. It is possible that Schwann cells migrating from ventral roots represent a motor phenotype that may not have been represented by RSC-96 cultures. Future work will attempt to characterize the phenotype of Schwann cells within these cultures using immunohistochemical techniques and analysis of growth factor release.

Our preliminary work using kinase inhibitors with SC explants demonstrated some interesting results. The addition of a GSK Inhibitor resulted in a reduction of neurite outgrowth and Schwann cell migration, although the current work cannot be used to differentiate whether this relationship is causative or correlative. The addition of wortmannin resulted in motoneuron death, but did not affect Schwann cell migration. These results suggest that there are distinct pathways at work between the two measured phenotypic outcomes. Currently, we are investigating the effects of a larger library of kinase inhibitors in order to adequately compare the results observed with dissociated SCNs.

While we have focused on using specific phenotypic outcomes as our metric for the effects of these kinase inhibitors in SC explant cultures, including neurite outgrowth and Schwann cell migration, this platform is amenable to other analyses, including motoneuron survival, neurite arborization, Schwann cell morphology, and Schwann cell proliferation. More advanced immunohistochemical techniques can be used to probe for receptor expression, protein expression, and cytoskeletal protein arrangement. Finally, it may be possible to use these cultures for real-time analysis of cell/biomaterial interaction through the use of fluorescent probes suitable for live-cell imaging (i.e. CellTracker). The cultures may also be used with biochemical techniques including Western blot, ELISA, co-immunopreciptation, gene expression arrays, and PCR.

Of course, the critical feature to be studied is axonal targeting. It may be possible to interface these cultures within microfluidic devices with branches that mimic motor and sensory targets. Since P7-P10 explant cultures do not require end organs in order to extend neurites, it may be merited to use older animals that are sensitive to the presence

of these cues. Notably, explant cultures can also be generated from knockout mice [12] which would provide higher throughput than large scale in vivo studies.

In conclusion, dissociated SCNs and SC explant cultures can be used as complementary approaches for the rational analysis of cell/biomaterial interaction in the context of peripheral nerve regeneration. We suggest the use of dissociated SCNs as a primary screening tool, where potentially involved pathways can be 'cherry-picked' and studied further. Additionally, dissociated SCNs can be used to titer effective concentrations needed for kinase inhibitors. The SC explant cultures can then be utilized as a higher order system to assess the behavior of Schwann cell and motoneurons. As mentioned earlier, appropriate tools can be chosen to assess various behaviors, spanning from neurite outgrowth to gene expression analysis. It should also be noted that while we have focused on the use of kinase inhibitors in our studies, these techniques can also be used with neutralizing antibodies, growth factors, and siRNA.

5.5 REFERENCES

1. Masand SN, Chen J, Perron IJ, Hammerling BC, Loers G, Schachner M, et al. The effect of glycomimetic functionalized collagen on peripheral nerve repair. Biomaterials. 2012. Epub 2012/08/25.
2. Masand SN, Perron IJ, Schachner M, Shreiber DI. Neural cell type-specific responses to glycomimetic functionalized collagen. Biomaterials. 2012;33(3):790-7. Epub 2011/10/27.
3. Tucker BA, Mearow KM. Peripheral sensory axon growth: from receptor binding to cellular signaling. The Canadian journal of neurological sciences Le journal canadien des sciences neurologiques. 2008;35(5):551-66. Epub 2009/02/25.
4. Jessen KR, Mirsky R. Schwann cells and their precursors emerge as major regulators of nerve development. Trends in neurosciences. 1999;22(9):402-10. Epub 1999/08/11.
5. Delfs J, Friend J, Ishimoto S, Saroff D. Ventral and dorsal horn acetylcholinesterase neurons are maintained in organotypic cultures of postnatal rat spinal cord explants. Brain research. 1989;488(1-2):31-42. Epub 1989/05/29.

6. Bonnici B, Kapfhammer JP. Spontaneous regeneration of intrinsic spinal cord axons in a novel spinal cord slice culture model. The European journal of neuroscience. 2008;27(10):2483-92. Epub 2008/06/03.
7. Allodi I, Guzman-Lenis MS, Hernandez J, Navarro X, Udina E. In vitro comparison of motor and sensory neuron outgrowth in a 3D collagen matrix. J Neurosci Methods. 2011;198(1):53-61. Epub 2011/03/16.
8. Jiang XY, Fu SL, Nie BM, Li Y, Lin L, Yin L, et al. Methods for isolating highly-enriched embryonic spinal cord neurons: a comparison between enzymatic and mechanical dissociations. J Neurosci Methods. 2006;158(1):13-8. Epub 2006/06/22.
9. Shreiber DI, Barocas VH, Tranquillo RT. Temporal variations in cell migration and traction during fibroblast-mediated gel compaction. Biophysical journal. 2003;84(6):4102-14. Epub 2003/05/29.
10. Hoke A, Redett R, Hameed H, Jari R, Zhou C, Li ZB, et al. Schwann cells express motor and sensory phenotypes that regulate axon regeneration. J Neurosci. 2006;26(38):9646-55. Epub 2006/09/22.
11. Jesuraj NJ, Nguyen PK, Wood MD, Moore AM, Borschel GH, Mackinnon SE, et al. Differential gene expression in motor and sensory Schwann cells in the rat femoral nerve. Journal of neuroscience research. 2012;90(1):96-104. Epub 2011/09/21.
12. Krassioukov AV, Ackery A, Schwartz G, Adamchik Y, Liu Y, Fehlings MG. An in vitro model of neurotrauma in organotypic spinal cord cultures from adult mice. Brain research Brain research protocols. 2002;10(2):60-8. Epub 2002/11/15.

CHAPTER 6. CONCLUSIONS AND FUTURE WORK

6.1 SUMMARY

Although glycans have been shown to be important regulators of nervous system development, regeneration, and synaptic plasticity, their therapeutic use has been limited due to the difficulty in synthesizing and purifying carbohydrates. Recently however, the discovery of glycomimetics has expanded opportunities to study these molecules. In this thesis, we have described the development and characterization of a novel biomaterial strategy for repair following peripheral nerve injury. Specifically, we use peptide mimics of two glycans, polysialic acid (PSA) and an epitope first discovered on human natural killer cells (HNK-1), to functionalize type I collagen hydrogels providing well-controlled, sustained, physiologically relevant presentation of these cues. Previous studies have shown that these molecules, in their glycan and glycomimetic form, are associated with acceleration of neurite outgrowth, glial cell proliferation, and motoneuron targeting.

In Chapter 2, we demonstrated the retained functionality of the PSA and HNK-1 peptide glycomimetics after conjugation to a type I collagen backbone. While HNK-functionalized collagen increased motor neurite outgrowth, PSA-functionalized collagen encouraged motor and sensory neurite outgrowth and Schwann cell extension and proliferation. In Chapter 3, we introduced these glycomimetic-functionalized collagen hydrogels into a critical gap femoral nerve model. We show that while both of PSA and HNK-functionalized hydrogels yielded a significant increase in functional recovery when compared to saline, native and scramble-coupled hydrogels, there was an interesting divergence in the morphological results. PSA-functionalized hydrogels increased axon

count and HNK-1 functionalized hydrogels increased motoneuron targeting and myelination. We believed that these differences may be attributed to distinct mechanisms by which the glycomimetics impart their benefit. Interestingly, however, we found no synergistic gain in functional or morphological recovery with the use of our composite hydrogels which we speculated may be due to an inadequate dose of the individual glycomimetic. To address this possibility, in Chapter 4 we assessed the efficacy of using composite hydrogels with higher concentrations of each glycomimetic within the same critical gap femoral nerve model. We showed that increasing the amount of peptide functionalized to the collagen backbone in our composite hydrogels led to increases in axon count and area of regeneration, but did not affect the amount of functional recovery. We also showed in Chapter 4 that our glycomimetic-functionalized hydrogels can interface with degradable tubes without a loss of functional benefit. Finally, in Chapter 5 we aimed to address the potential mechanism by which our glycomimetics impart benefit. To this end, we developed a novel platform for studying neural cell/biomaterial interaction through the use of two types of motoneuron cultures, dissociated spinal cord neurons and organotypic spinal cord slices. We show promising evidence that this strategy can be used to probe signaling pathways which may be involved.

While we have demonstrated the in vitro and in vivo efficacy of glycomimetic-functionalized collagen hydrogels, future work may be necessary to further optimize and broaden its utilization. Several of these suggestions are discussed below.

6.2 STUDY LIMITATIONS

In Chapter 2, we aimed to develop and characterize glycomimetic-functionalized hydrogels using in vitro neural cell cultures. Follow-up studies are suggested to more adequately characterize the scaffolds. To begin, the initial concentration of peptides used was based off of previously published reports using the glycomimetics [1, 2]. More robust dosing studies may be merited in order to find optimal functionalization ratios. Also, while we did attempt to assess the response of glial cells on our material, we used an immortalized Schwann cell line (RSC-96). Unfortunately, these cells may not adequately recapitulate the in vivo glial cell population. For example, Hoke et al. showed that Schwann cells can be subdivided into motor and sensory subtypes based on the type of axon they are associated with [3]. Future studies may attempt to use primary Schwann cells from motor or sensory nerves. It should be noted, however, that maintenance of these phenotypes is not trivial. Jesuraj et al. have shown that during expansion of Schwann cells in vitro, the trophic factor release patterns of these subtypes are disrupted [4]. It is possible that more complex culturing technique will be required in order to effectively maintain the phenotypic-specific genes in these subpopulations, including supplementing with specific growth factors, co-culture with motor/sensory axons, or supplementing with conditioned media from motor/sensory axons. Additionally, it may be appropriate to assess whether the concentration of collagen used is ideal. In our model, we used collagen concentrations that our lab has historically used successfully for in vitro assays of neurite outgrowth. In vivo studies have suggested that small differences in collagen hydrogel concentrations can have profound changes on the outcome of regeneration.

In Chapters 3 and 4, we assessed the efficacy of these glycomimetic-functionalized biomaterials in repair following critical gap femoral nerve injury. We noticed an upper limit in the amount of functional recovery observed among all of the independent cohorts ran. While this may be a function of the treatment conditions, it may also represent an inherent limitation in the animal model. Therefore, several potential changes are recommended for future in vivo work, including: larger animal models (rat, rabbit), alternative nerve models (sciatic, tibial), and longer regeneration times. Also, in our studies we focused on return of motor function. Behavioral techniques do exist to assess return of sensation, termed algesimetry tests, and these may also be merited to include in future studies.

While we show that the glycomimetic-functionalized hydrogels yielded interesting differences in morphological recovery, more in vivo work may be useful in addressing potential sources for their dynamic responses. For example, it is unclear whether the PSA-functionalized hydrogels had significantly higher axon counts due to an increase in a specific sub-population of axons (motor vs. sensory) or are simply exhibiting an increase in arborization. Further, Franz et al. have demonstrated that there are intrinsic differences in motoneuron pools in their ability to express PSA-NCAM after injury, and that this expression is integral to their ability to selectively target the appropriate end organ [5]. To this end, it is reasonable to speculate that perhaps only a sub-population of axons will be affected by inclusion of PSA-functionalized hydrogels at the injury site. To address these concerns, in vivo studies can be conducted where the endogenous expression of PSA is disrupted using NCAM knockouts or by enzymatic

removal using Endo-N. Regenerated nerve samples can also be immunohistochemically stained to assess the number of motor verse sensory axons.

Also, HNK-functionalized hydrogels showed an increase in motoneuron targeting. There are several possible explanations for this outcome: 1) HNK-functionalized hydrogels increase the number of motoneurons, which may increase the raw number of motoneurons that reach the muscle, 2) HNK-functionalized hydrogels prime motoneurons for interaction with downstream pathway choices, and/or 3) the pruning response is enhanced in HNK-functionalized hydrogels. Several potential studies are suggested to assess the validity of these explanations, including the use of earlier time points to assess the number of motoneurons, immunohistochemical staining for choline acetyltransferase (ChAT) to quantify the number of motor verse sensory axons, and histomorphometric analysis of nerve samples distal to the point of bifurcation.

Finally, several relatively simple control experiments may be merited to address more fundamental questions. For one, assessing the effect of the glycomimetic-functionalized hydrogels when transplanted into pure motor or sensory nerves may be useful. Also, it may be useful to look at shorter time points of regeneration to assess the behavior of infiltrating Schwann cells. Finally, assessing the effects of glycomimetic-functionalized collagen on the level of endogenous PSA and HNK-1 expression may provide further insight.

6.3 ANISOTROPY

6.3.1 Chemical Anisotropy

During regeneration and development in the nervous system, there are precisely orchestrated cues that direct axonal growth. While the response of growth cones to

gradients of soluble substances has been well-studied, only in the in the last decade has the response to substrate-bound cues been investigated [6, 7]. Recent work has shown that growth cones are responsive to gradients of a multitude of conjugated cues including laminin and NGF, and that these anisotropic cues can often accelerate the rate of regeneration in vitro and in vivo [8-10]. In a similar vein, anisotropic presentation of these glycomimetic cues may potentially increase the rate of regeneration.

Within our lab, we have developed several methodologies to generate highly controlled environments for cellular studies within microfluidic devices [11]. Microfluidics is a type of Biological Micro Electromechanical System (*BioMEMS*), where features can be manipulated in a cost-effective and timely manner. The small channel size in the devices is utilized to create regions of laminar, well-controlled flow. As such, it becomes reasonable to create a complex, controlled substrate for cellular growth, including control of adhesive properties of the substrate. In one particular model, we can create linear concentration gradients of the peptide-functionalized hydrogel by using a source-sink 'H' model. The two legs of the H can have different collagen solutions, with diffusive mixing in the cross channel creating the gradient. Previous work in our lab has used these techniques to assess the effects of anisotropic presentation of IKVAV- and YIGSR- functionalized collagen and found that the slope of the gradient effected the rate of outgrowth [12]. Notably, cells are cultured in 3D in this configuration providing important insight into the 3D behavior of cells versus 2D culture systems.

While this is a useful approach to measure the growth bias of DRGs, sensory populations are not affected by HNK-1. Unfortunately, other cell types have limited viability when sealed with PDMS or glass. We speculate that this due to limited transport

of oxygen, nutrients, and waste product in and out of the devices. Thus, a complementary approach is required for other cell populations. Recently, we have developed a method to seal microfluidic devices with a microdialysis membrane. We have validated this approach with fibroblasts and have shown that this technique is amenable to long-term culture and IHC (Appendix A, ref: [13]). Ongoing studies are evaluating the efficacy of microdialysis membrane-sealed on neural cell cultures.

Additionally, microfluidic devices can also be used to learn about the potential mechanism by which the glycomimetics impart benefit. For example, glycomimetic-functionalized hydrogels can be run in opposition to one another (i.e. through different legs of the device) within the H-model. The results from these studies may provide insight into which cue is more potent when there is a choice between both. Additional configurations can also be used to answer more fundamental questions. For example, a Y-channel may be used to develop a model of axonal targeting where one branch represents a sensory target and another a motor target. Intrinsic to the success of such a model will be the discovery of appropriate trophic cues to mimic motor and sensory end targets. Potential choices may include motor/sensory Schwann cells, muscle lysate, or skin lysate.

6.3.2 Structural Anisotropy

Following injury to the PNS, a fibrin cable forms between the two stumps and within this cable are longitudinally aligned channels called Bands of Bunger providing structural orientation to regenerating axons. Similarly, several studies have shown that a two-dimensional interface for growth within a three-dimensional scaffolds elicits

enhanced and directed outgrowth of neurites. Thus, several biomaterial strategies for PNR have included structurally aligned fibers to provide growth bias [14-16]. Although the use of hydrogels is certainly merited, the random fiber arrangement does not motivate this preference in outgrowth.

Several known methods exist to align collagen fibers, including magnetic alignment, electrospinning, and flow-based alignment in small channels [17-20]. Unfortunately, magnetic alignment is resource prohibitive, electrospinning may denature protein, and flow-based alignment results in very small, brittle fibers. Currently, we are investigating a relatively simple approach to create longitudinally aligned collagen fibers that in amenable to functionalized scaffolds. Collagen hydrogels are made in cylindrical tubes, and following self-assembly are frozen. The aqueous phase of the hydrogel forms oriented ice crystals which can then be removed with sublimation by lyophilization. This methodology is a modification of a recently published technique to align chitosan/collagen composite materials [21]. The potential also exists that the combination of structural and chemical anistropy will lead to a synergistic enhancement in neural cell behavior. Gradients of glycomimetics can potentially be made within the aligned fibers.

6.4 PREFERENTIAL SENSORY REINNERVATION/ELECTRICAL STIMULATION

While this thesis has focused on encouraging motoneuron targeting, there is increasing evidence to suggest that similar phenomena may exist for sensory reinnervation. Hoke et al. demonstated that Schwann cells express phenotypic differences as a function of their association with either motor or sensory axons. In

particular, he found that nerve growth factor (NGF) has increased expression in cutaneous nerves as compared to ventral roots [3], and has been shown to play an integral role in the growth and guidance of sensory axons [22, 23]. In recent work by the Smith group, a recombinant adenovirus encoding NGF was delivered to cutaneous branch of the femoral branch near the point of bifurcation to encourage sensory axon targeting. They show that inclusion of NGF increased the number of appropriate sensory reconnection without enhancing overall axon counts [24].

Another particularly interesting strategy that has been explored to increase the accuracy of both motor and sensory reinnervation is the use of electrical stimulation. Al-Majed et al. showed that 1 hour of electrical stimulation of the femoral nerve proximal to the transection increases motoneuron regeneration and also enhances the PMR response 3 fold [25]. In this study they show that in the absence of electrical stimulation axonal regeneration commences 10 weeks after the initial transection (staggered regeneration), however with electrical stimulation this time drops dramatically to 3 weeks. This stimulation has also been associated with increases in the regeneration-associated genes GAP-43 and Tα1 tubulin, BDNF secretion, and TrkB expression [26]. In follow up studies, it was shown that similar results can be seen in sensory axon populations where the introduction of electrical stimulation leads to an increase in the efficiency of sensory target reinnervation [27]. Similar increases in GAP-43 and BDNF expression were also seen in sensory axon populations following treatment [28]. Given these findings, it would interesting to assess the effect of electrical stimulation and glycomimetic treatment in combination. It is reasonable to hypothesize that such a multi-modal approach may lead

to acceleration of regeneration and increases in the accuracy motor and sensory target reinnervation.

6.5 LEARNING FROM DEVELOPMENT

There is substantial redundancy in the cues expressed during neural development and following nervous system injury, likely due to the shared requirement for development of neural tissue. While research into this recapitulation of developmental guidance has been primarily restricted to spinal cord injury [29], there may be lessons to be learned in the context of peripheral nerve injury.

One particularly interesting family of molecules are the Ephrin/Ephs, which are tyrosine kinase receptors that communicate positional information to cells [30]. During development, these molecules are integral to tissue formation through their regulation of cell migration and tissue patterning. Communication between ephrin and Eph receptors can trigger complex cellular behaviors including cell adhesion and repulsion via actin [31]. For example, Gallarda et al show that Ephrin-A/EphA interaction is integral to segregation of motor and sensory axonal pathways, and genetic ablation of this signaling results in severe miswiring [32]. Notably, recent work has shown that EphB signaling is important in directing Schwann cell behavior following peripheral nerve injury [33]. Collectively, these studies provide exciting evidence that this class of molecules may represent an interesting target to further encourage the efficiency of synaptic reconnection following PNS injury. It should be noted that this particular class of molecules is amenable to use within our functionalized collagen platform as several peptide mimics have been discovered [34, 35].

Sophisticated methods have been developed to assess axonal targeting during development and several of these techniques can potentially be utilized for the study of axonal targeting following regeneration. For example, motor column explants have been selectively dissected using fluorescence-guided microdissection from Hb9::eGFP mouse embryos and co-cultured with dorsal root ganglia to understand motor-sensory axon interaction [32].

6.6 OTHER USES FOR GLYCOMIMETIC-FUNCTIONALIZED COLLAGEN

6.6.1 Stem Cells

Human embryonic stem cells (hESCs) are pluripotent cells that have the ability to differentiate into cell lineages from all three germ layers. The broad use of hESCs in regenerative medicine lies in its enormous potential to replace lost or damaged tissue. This seemingly limitless cell source is particularly useful in cases of nervous system disease of trauma as neurons are post-mitotic and cannot be endogenously replaced [36]. Therefore, hESCs stand to provide therapeutic options for conditions that are currently treated with primarily palliative care.

The progenitor class within hESCs from which all neurons and glial cells are derived is the neural stem cells (NSCs). This population of cells is definied by its high proliferative potential and self-renewal ability. When derived from hESCs in vitro, NSCs implanted into the adult rodent brain differentiate into neurons, astrocytes, and oligodendrocytes. Notably, NSCs implanted into various nervous system injury models have been shown to survive, migrate to the site of injury, and differentiate into relevant cell types. In some cases the implantation of these cells has also led to functional

improvement. Additionally, these cells have been shown to have a remarkable capacity to home to sites of injury, disease, or inflammation and also provide trophic support to native tissue post-trauma [37].

Despite these promising results, the therapeutic potential and clinical translation of NSCs relies on the ability to control lineage commitment. However, this goal has yet to be adequately achieved as the resulting populations from ex vivo culture methods are often heterogenous. In vivo, NSCs reside in a specialized, regulated environment composed of growth factors, extracellular matrix ligands, and controlled cell-cell interactions, dubbed the stem cell 'niche'. There is increasing evidence to suggest that control of stem cell self-renewal and differentiation can be achieved through a combinatorial approach of using optimal mechanical, soluble, and adhesive cues to recapitulate this microniche.

As NSCs are particularly sensitive to the chemical and physical state of their surroundings, engineered matrices can be generated that can facilitate spatiotemporal control of differentiation. Little et al described these in vitro culture methods as the combination of two components: soluble and solid phases. The soluble phase consists of the media constituents which may include several growth factors. The solid phase is the physical matrix to which cells will adhere and may be composed of natural, synthetic, of hybrid materials. These materials can be modified to optimize topography, stiffness, and ligand presentation [38].

Glycoconjugates, including HNK-1 and PSA, have been largely implicated in the fine-tuning of stem cell interaction with its local environment. This spatiotemporal

control is integral for neural development and plasticity [39, 40]. Interestingly, the mechanism by which each of these glycoconjuates imparts their function is unique. PSA is a post-translational modification of NCAM and its expression has been shown to be developmentally regulated, with high expression patterns during embryonic and neonatal stages and limited expression in the adult nervous system. Loss of function studies with PSA shows detrimentally impacted survival and migration of NPCs, hindered neuronal guidance, and compromised synapse formation in these animals [41, 42]. Conversely, gain of function studies using virally induced PSA expression promotes ESC migration and homing capacity in injury models [43]. HNK-1 is present on ECM proteins, glycoproteins (L1, P0, NCAM), and glycolipids. Several receptors for HNK-1 have been identified which are particularly important during neural development, including amphoterin and laminin[39]. Additionally, the expression of HNK-1 is generally associated with neural crest cells. A recent paper by Yagi et al. shows that HNK-1 regulates the proliferative capacity of mouse embryonic neural stem cells through its interaction with Tenasin-C [44]. However, the role of HNK-1 in neural stem cell differentiation and lineage commitment remains to be elucidated.

Robust studies investigating the roles of PSA and HNK-1 in stem cell differentation have been limited due to the difficulty in synthesizing carbohydrates. However, the discovery of their glycomimetics offers opportunity to discover potential mechanism of action and, by extension, a method to exploit it. Previous research in our lab (Monteiro, unpublished results) has found promising evidence that glycomimetic functionalized scaffolds can direct neural differentiation in a mouse embryonic stem cell population. However, these cells were not neurally induced and may not have been

'prepared' for interaction with these particular cell-instructive cues. Thus, the results may be enhanced with cells that express the correct receptors for interaction these bioactive ligands, such as neural stem cells.

6.6.2 Central nervous system (CNS) injury

CNS trauma results in axonal discontinuity, loss of communication, and function. Unfortunately, the damage is primarily irreparable due to the incapability of neurons to reconnect with their synaptic targets. In the adult mammalian brain and spinal cord, axonal growth is limited after axotomy due to conditions in the microenvironment peripheral to injury. More specifically, this microenvironment is thought to include chemical and mechanical cues which limit the growth potential of neurons. Currently, SCI research has three primary goals in reaching a potential therapy- to promote neurite growth, to direct neurites to correctly reconnect and communicate with their targets, and to restore original 'wiring'.

Recent evidence has suggested that the use of PSA may represent an interesting target to increase the permissiveness of the injury microenvironment. The molecule's ability to reduce contact-dependent cell interactions has been correlated with an increase in the ability for tissue to repair by allowing for architectural remodeling. For example, Dusart et al. show that astrocytes within a glial scar that express PSA-NCAM allow for sprouting of regenering neurites [45]. Interestingly, when astrocytes in the glial scar are transfected with a viral vector which leads to increased expression of PSA following spinal cord injury, a substantial number of injured corticospinal tract axons grow through the injury site [46]. Similarly, overexpression of PSA on Schwann cells grafted into a

spinal cord injury site promoted functional recovery [47]. However, these techniques are not easily translated to a clinical setting. Recent evidence has suggested that acute administration of the glycomimetics in an spinal cord injury microenviroment improves functional and morphological outcome. However, this delivery mechanism resulted in clearance from the injury site by 48 hours, likely not long enough to elicit maximal benefit [48]. Mehanna et al. performed similar studies with the added improvement of delivery via an osmotic pump. While the results were improved, the likelihood of this delivery mechanism into a clinical setting is limited [49]. To this end, PSA-functionalized collagen hydrogels may serve as a useful biomaterial strategy for repair following central nervous system injury.

6.7 CONCLUSION

Despite the innate regenerative potential of the peripheral nervous system, functional recovery is often limited. This has been attributed to a number of sources, including the inability of axons to cross large gap sizes and the malrouted reinnervation of regenerated axons. The goal of this dissertation was to develop clinically relevant biomaterial strategy to (1) encourage the regrowth of axons and (2) direct them down their appropriate motor tracts. To this end, we have developed glycomimetic-functionalized collagen hydrogels for peripheral nerve regeneration.

Two naturally occurring glycans, polysialic acid (PSA) and an epitope first discovered on human natural killer cells (HNK-1), have been shown to be integrally involved in preferential motor reinnervation, neuron survival, and acceleration of regrowth. Type I collagen scaffolds have been functionalized with peptide mimics of these molecules, thereby providing well-controlled, sustained, physiologically relevant

presentation of these cues. We show that inclusion of these instructive cues within our biomaterial improves functional and morphological recovery, and that these materials can be successfully interfaced with a degradable outer conduit.

While these results presented have provided promising evidence that PSA and HNK-1 mimicking peptides represent an interesting approach to encourage the efficiency of synaptic reconnection, clinical translation of these materials will require more thorough characterization. Further, it is likely that an ideal approach to the treatment of PNS injury will be multi-modal.

6.8. REFERENCES:

1. Mehanna A, Mishra B, Kurschat N, Schulze C, Bian S, Loers G, et al. Polysialic acid glycomimetics promote myelination and functional recovery after peripheral nerve injury in mice. Brain : a journal of neurology. 2009;132(Pt 6):1449-62. Epub 2009/05/21.
2. Simova O, Irintchev A, Mehanna A, Liu J, Dihne M, Bachle D, et al. Carbohydrate mimics promote functional recovery after peripheral nerve repair. Annals of neurology. 2006;60(4):430-7. Epub 2006/09/08.
3. Hoke A, Redett R, Hameed H, Jari R, Zhou C, Li ZB, et al. Schwann cells express motor and sensory phenotypes that regulate axon regeneration. J Neurosci. 2006;26(38):9646-55. Epub 2006/09/22.
4. Jesuraj NJ, Nguyen PK, Wood MD, Moore AM, Borschel GH, Mackinnon SE, et al. Differential gene expression in motor and sensory Schwann cells in the rat femoral nerve. Journal of neuroscience research. 2012;90(1):96-104. Epub 2011/09/21.
5. Franz CK, Rutishauser U, Rafuse VF. Intrinsic neuronal properties control selective targeting of regenerating motoneurons. Brain : a journal of neurology. 2008;131(Pt 6):1492-505. Epub 2008/03/13.
6. Dertinger SK, Jiang X, Li Z, Murthy VN, Whitesides GM. Gradients of substrate-bound laminin orient axonal specification of neurons. Proc Natl Acad Sci U S A. 2002;99(20):12542-7. Epub 2002/09/19.
7. Kapur TA, Shoichet MS. Immobilized concentration gradients of nerve growth factor guide neurite outgrowth. J Biomed Mater Res A. 2004;68(2):235-43. Epub 2004/01/06.
8. Dodla MC, Bellamkonda RV. Differences between the effect of anisotropic and isotropic laminin and nerve growth factor presenting scaffolds on nerve regeneration across long peripheral nerve gaps. Biomaterials. 2008;29(1):33-46. Epub 2007/10/13.
9. Cao X, Shoichet MS. Defining the concentration gradient of nerve growth factor for guided neurite outgrowth. Neuroscience. 2001;103(3):831-40. Epub 2001/03/29.

10. Moore K, MacSween M, Shoichet M. Immobilized concentration gradients of neurotrophic factors guide neurite outgrowth of primary neurons in macroporous scaffolds. Tissue Eng. 2006;12(2):267-78. Epub 2006/03/22.
11. Sundararaghavan HG, Monteiro GA, Firestein BL, Shreiber DI. Neurite growth in 3D collagen gels with gradients of mechanical properties. Biotechnol Bioeng. 2009;102(2):632-43. Epub 2008/09/04.
12. Sundararaghavan HG, Masand SN, Shreiber DI. Microfluidic generation of haptotactic gradients through 3D collagen gels for enhanced neurite growth. Journal of neurotrauma. 2011;28(11):2377-87. Epub 2011/04/09.
13. Masand SN, Mignone L, Zahn JD, Shreiber DI. Nanoporous membrane-sealed microfluidic devices for improved cell viability. Biomed Microdevices. 2011;13(6):955-61.
14. Yang F, Murugan R, Wang S, Ramakrishna S. Electrospinning of nano/micro scale poly(L-lactic acid) aligned fibers and their potential in neural tissue engineering. Biomaterials. 2005;26(15):2603-10. Epub 2004/12/09.
15. Kim YT, Haftel VK, Kumar S, Bellamkonda RV. The role of aligned polymer fiber-based constructs in the bridging of long peripheral nerve gaps. Biomaterials. 2008;29(21):3117-27. Epub 2008/05/02.
16. Bellamkonda RV. Peripheral nerve regeneration: an opinion on channels, scaffolds and anisotropy. Biomaterials. 2006;27(19):3515-8. Epub 2006/03/15.
17. Ceballos D, Navarro X, Dubey N, Wendelschafer-Crabb G, Kennedy WR, Tranquillo RT. Magnetically aligned collagen gel filling a collagen nerve guide improves peripheral nerve regeneration. Exp Neurol. 1999;158(2):290-300. Epub 1999/07/23.
18. Verdu E, Labrador RO, Rodriguez FJ, Ceballos D, Fores J, Navarro X. Alignment of collagen and laminin-containing gels improve nerve regeneration within silicone tubes. Restor Neurol Neurosci. 2002;20(5):169-79. Epub 2003/01/08.
19. Lee P, Lin R, Moon J, Lee LP. Microfluidic alignment of collagen fibers for in vitro cell culture. Biomed Microdevices. 2006;8(1):35-41. Epub 2006/02/24.
20. Matthews JA, Wnek GE, Simpson DG, Bowlin GL. Electrospinning of collagen nanofibers. Biomacromolecules. 2002;3(2):232-8. Epub 2002/03/13.
21. Hu X, Huang J, Ye Z, Xia L, Li M, Lv B, et al. A novel scaffold with longitudinally oriented microchannels promotes peripheral nerve regeneration. Tissue Eng Part A. 2009;15(11):3297-308. Epub 2009/04/23.
22. Heron PM, Sutton BM, Curinga GM, Smith GM, Snow DM. Localized gene expression of axon guidance molecules in neuronal co-cultures. Journal of neuroscience methods. 2007;159(2):203-14. Epub 2006/08/29.
23. Zhou FQ, Walzer M, Wu YH, Zhou J, Dedhar S, Snider WD. Neurotrophins support regenerative axon assembly over CSPGs by an ECM-integrin-independent mechanism. Journal of cell science. 2006;119(Pt 13):2787-96. Epub 2006/06/15.
24. Hu X, Cai J, Yang J, Smith GM. Sensory axon targeting is increased by NGF gene therapy within the lesioned adult femoral nerve. Experimental neurology. 2010;223(1):153-65. Epub 2009/09/08.
25. Al-Majed AA, Brushart TM, Gordon T. Electrical stimulation accelerates and increases expression of BDNF and trkB mRNA in regenerating rat femoral motoneurons. The European journal of neuroscience. 2000;12(12):4381-90. Epub 2000/12/21.
26. Al-Majed AA, Tam SL, Gordon T. Electrical stimulation accelerates and enhances expression of regeneration-associated genes in regenerating rat femoral motoneurons. Cellular and molecular neurobiology. 2004;24(3):379-402. Epub 2004/06/23.

27. Brushart TM, Jari R, Verge V, Rohde C, Gordon T. Electrical stimulation restores the specificity of sensory axon regeneration. Experimental neurology. 2005;194(1):221-9. Epub 2005/05/19.
28. Geremia NM, Gordon T, Brushart TM, Al-Majed AA, Verge VM. Electrical stimulation promotes sensory neuron regeneration and growth-associated gene expression. Experimental neurology. 2007;205(2):347-59. Epub 2007/04/13.
29. Harel NY, Strittmatter SM. Can regenerating axons recapitulate developmental guidance during recovery from spinal cord injury? Nature reviews Neuroscience. 2006;7(8):603-16. Epub 2006/07/22.
30. Pasquale EB. Eph-ephrin bidirectional signaling in physiology and disease. Cell. 2008;133(1):38-52. Epub 2008/04/09.
31. Arvanitis D, Davy A. Eph/ephrin signaling: networks. Genes & development. 2008;22(4):416-29. Epub 2008/02/19.
32. Gallarda BW, Bonanomi D, Muller D, Brown A, Alaynick WA, Andrews SE, et al. Segregation of axial motor and sensory pathways via heterotypic trans-axonal signaling. Science. 2008;320(5873):233-6. Epub 2008/04/12.
33. Parrinello S, Napoli I, Ribeiro S, Digby PW, Fedorova M, Parkinson DB, et al. EphB signaling directs peripheral nerve regeneration through Sox2-dependent Schwann cell sorting. Cell. 2010;143(1):145-55. Epub 2010/09/28.
34. Koolpe M, Burgess R, Dail M, Pasquale EB. EphB receptor-binding peptides identified by phage display enable design of an antagonist with ephrin-like affinity. The Journal of biological chemistry. 2005;280(17):17301-11. Epub 2005/02/22.
35. Koolpe M, Dail M, Pasquale EB. An ephrin mimetic peptide that selectively targets the EphA2 receptor. The Journal of biological chemistry. 2002;277(49):46974-9. Epub 2002/09/28.
36. Singec I, Jandial R, Crain A, Nikkhah G, Snyder EY. The leading edge of stem cell therapeutics. Annu Rev Med. 2007;58:313-28. Epub 2006/11/15.
37. Teixeira AI, Duckworth JK, Hermanson O. Getting the right stuff: controlling neural stem cell state and fate in vivo and in vitro with biomaterials. Cell Res. 2007;17(1):56-61. Epub 2007/01/11.
38. Little L, Healy KE, Schaffer D. Engineering biomaterials for synthetic neural stem cell microenvironments. Chem Rev. 2008;108(5):1787-96. Epub 2008/05/15.
39. Kleene R, Schachner M. Glycans and neural cell interactions. Nat Rev Neurosci. 2004;5(3):195-208. Epub 2004/02/21.
40. Yu RK, Yanagisawa M. Glycosignaling in neural stem cells: involvement of glycoconjugates in signal transduction modulating the neural stem cell fate. J Neurochem. 2007;103 Suppl 1:39-46. Epub 2007/12/06.
41. Angata K, Huckaby V, Ranscht B, Terskikh A, Marth JD, Fukuda M. Polysialic acid-directed migration and differentiation of neural precursors are essential for mouse brain development. Mol Cell Biol. 2007;27(19):6659-68. Epub 2007/08/08.
42. Weinhold B, Seidenfaden R, Rockle I, Muhlenhoff M, Schertzinger F, Conzelmann S, et al. Genetic ablation of polysialic acid causes severe neurodevelopmental defects rescued by deletion of the neural cell adhesion molecule. J Biol Chem. 2005;280(52):42971-7. Epub 2005/11/04.
43. Glaser T, Brose C, Franceschini I, Hamann K, Smorodchenko A, Zipp F, et al. Neural cell adhesion molecule polysialylation enhances the sensitivity of embryonic stem cell-derived neural precursors to migration guidance cues. Stem Cells. 2007;25(12):3016-25. Epub 2007/09/08.

44. Yagi H, Yanagisawa M, Suzuki Y, Nakatani Y, Ariga T, Kato K, et al. HNK-1 epitope-carrying tenascin-C spliced variant regulates the proliferation of mouse embryonic neural stem cells. J Biol Chem.285(48):37293-301. Epub 2010/09/22.
45. Dusart I, Morel MP, Wehrle R, Sotelo C. Late axonal sprouting of injured Purkinje cells and its temporal correlation with permissive changes in the glial scar. The Journal of comparative neurology. 1999;408(3):399-418. Epub 1999/05/26.
46. El Maarouf A, Petridis AK, Rutishauser U. Use of polysialic acid in repair of the central nervous system. Proceedings of the National Academy of Sciences of the United States of America. 2006;103(45):16989-94. Epub 2006/11/01.
47. Papastefanaki F, Chen J, Lavdas AA, Thomaidou D, Schachner M, Matsas R. Grafts of Schwann cells engineered to express PSA-NCAM promote functional recovery after spinal cord injury. Brain : a journal of neurology. 2007;130(Pt 8):2159-74. Epub 2007/07/13.
48. Marino P, Norreel JC, Schachner M, Rougon G, Amoureux MC. A polysialic acid mimetic peptide promotes functional recovery in a mouse model of spinal cord injury. Experimental neurology. 2009;219(1):163-74. Epub 2009/05/19.
49. Mehanna A, Jakovcevski I, Acar A, Xiao M, Loers G, Rougon G, et al. Polysialic acid glycomimetic promotes functional recovery and plasticity after spinal cord injury in mice. Molecular therapy : the journal of the American Society of Gene Therapy. 2010;18(1):34-43. Epub 2009/10/15.

APPENDIX A: NANOPOROUS MEMBRANE-SEALED MICROFLUIDIC DEVICES FOR IMPROVED CELL VIABILITY

Note: This appendix is reproduced from the following publication:

Masand SN, Mignone L, Zahn JD, Shreiber DI. Nanoporous membrane-sealed microfluidic devices for improved cell viability. Biomedical Microdevices. 2011;13(6):955-61.

A.1 INTRODUCTION

Microfluidic based cell culture devices allow for well controlled manipulation of the local environment within microchannels, and thereby potentially enables recapitulation of the complexity of cellular microniches [1]. While a broad range of biomedical applications including, drug discovery and tissue engineering could benefit from cell-laden devices, limited cell viability has narrowed its utility. Thus, the design of reliable and approachable methods to improve culture conditions within microdevices will be integral to its broadened use.

The limited viability of cells within microfluidic devices, especially in long term cultures, has been attributed to poor transport of nutrients and gases to cells, especially in long microchannels. Compared to standard culture techniques, microscale culture systems have increased surface area-to-volume ratios, which greatly decreases the average amount of media available per cell [2]. As these systems are generally sealed with polydimethylsiloxane (PDMS), glass, or other surface with limited or no permeability, gas delivery and removal is further compromised [3]. Perfusion-based systems have been used to overcome these diffusive limitations by allowing for constant replenishment of

soluble factors. However, active perfusion typically requires complex pumps and increases the likelihood for media contamination and the introduction of destructive bubbles. Active perfusion also introduces shear stress with flow which can induce a wide range of phenotypic effects in shear sensitive cells [4, 5]. Several approaches have been developed to limit the amount of shear introduced to cells, including periodic 'flow-stop' perfusion [2], microgrooved glass substrates [6], and orthogonal networks [7]. However, the need for specialized control equipment, more complicated fabrication approaches, and supplies with these methods limits its practical value to most laboratories. The issue of cell viability becomes even more challenging within three-dimensional (3D) cultures where cells are grown not on the walls of a microchannel but within a suspending matrix. While 3D cultures provide increased physiological relevance, increased transport limitations often lead to cell necrosis [8]. Perfusion within these cell-encapsulated scaffolds is difficult because flow can disrupt the integrity of the material and bubbles can completely destroy the architecture. While systems have been designed to overcome some of these drawbacks, most techniques fail in the long-term.

In addition to shear effects, the convective delivery of nutrients has other drawbacks. With traditional static culture, diffusion is the primary modality for transport. Thus, locally secreted factors are available in the microenvironment in a manner similar to in vivo conditions. However, in both two-dimensional and three-dimensional perfusion based systems, convective flow removes these secreted factors which may be of importance to cell function and signaling. For example, Korin et al. noted significant differences in cell proliferation of human foreskin fibroblasts when comparing traditional culture techniques with perfusion and pulsed flow methods [2].

Aside from issues with cell viability, a significant hurdle to overcome in cell-laden microfluidic devices is developing methods for efficient analysis. Sealed devices often limit the practicality of real-time analysis and complicate labeling of cells within the devices. While devices are attached to perfusion systems, the ability to image within the experimental duration is sacrificed or at best compromised. Further, histological stains can only reach cells within devices using the same perfusion modality, with associated resource limitations and burdensome time requirements, and can often yield inconsistent results.

In the present study, we have developed a simple technique to preserve cell viability and simplify labeling within microfluidic networks. Instead of bonding a PDMS microchannel network to an impermeable substrate, the network is bonded to a semi-permeable nanoporous membrane, which allows for free exchange of gases, proteins, nutrients, buffers, and labeling reagents between the microfluidic channels and culture media in static culture plates. While this system is amenable to perfusion for desired experimental needs (i.e. pulsed delivery of soluble factors), the porous membrane removes its constant requirement. We have validated the device for 2D and 3D cell culture under static and perfused conditions. We also demonstrate the ability to stain these cell-laden devices without the need for laborious perfusion. Finally, we show the ability to maintain pattern fidelity for 3D cultures within membrane-sealed devices. Collectively, the technique promises to introduce significant time and cost savings without compromising the hallmarks of microculture systems.

A.2 METHODS

A.2.1 Device Fabrication

Microfluidic networks were formed using standard soft lithography techniques [9]. Briefly, a PDMS solution was poured over a silicon wafer with the SU-8 relief of the network, and left to polymerize at 70°C overnight. The network comprised a single, straight channel 6mm long, 500 µm wide and 100 µm deep. Inlet and outlet holes were punched through the PDMS with a 19-gauge blunt syringe. The microchannel-side of the devices was inked with a thin layer of a cell-tolerated silicone sealant (Dow Corning). The silicone coated devices were immediately sealed to either a polycarbonate membrane with a 0.4 µm pore size (Whatman, Piscataway, NJ) or a clean glass microslide. We note that, the membrane was bonded to the PDMS with a silicone sealant, but any approach that reliably bonds the membrane to the substrate is feasible. In static culture and at low perfusion rates, the stress on the membrane-substrate interface is minimal, but in cases where perfusion pressures are elevated, an approach where an irreversible bond is formed may be warranted [10]. Devices were allowed to cure for 24 hours, after which Tygon tubing with a Luer hub adapter was inserted into the inlet holes. Open devices, placed channel-side up and which were not sealed with membrane or glass, were used as controls. Immediately before inoculation, devices were sterilized using ultraviolet light for 15 minutes followed by O_2 plasma treatment.

A.2.2 Cell Culture

Primary rat dermal fibroblasts (RDFs) were isolated from transgenic rats engineered to express green fluorescent protein (GFP) via an actin promoter. When metabolically

active, the cells emit fluorescence at 509 nm when excited at 395 nm, and lose their fluorescence rapidly upon dying. Cultures were maintained in a 37°C humidified environment with 5% CO_2. Media consisted of Dulbecco's Modified Eagle's Medium (DMEM) supplemented with 10% fetal bovine serum (FBS), 1% L-glutamine (L-glut), and 1% Penicillin/Streptomyocin (P/S). Cells were harvested using 1× trypsin/EDTA.

A.2.3 Device Inoculation

In separate Petri dishes, glass and membrane-sealed devices were positioned microchannel-side up on a PDMS block which provided clearance for inlet tubing. For two-dimensional cultures, RDFs were resuspended at $5x10^5$ cells/ml in culture media and transferred to a 3 ml syringe. The suspension was flowed into the device and cells were allowed to attach for 1 hour. Following this initial attachment time, inlet tubing was removed and devices were covered with culture medium. In separate Petri dishes, open device controls were filled with the RDF suspension using a micropipette. Devices were incubated for 1 hour to allow for cell attachment and then covered with culture medium.

For three-dimensional cultures, RDFs were encapsulated within a type I collagen hydrogel using previously described methods [11]. Briefly, lyophilized collagen was reconstituted to 3mg/ml in 0.02 N acetic acid. The reconstituted solution was neutralized with the following materials: 20 µl 1M Hepes (Fluka), 140 µl 0.1 N NaOH, 100 µl 10× Minimum Essential Medium (Sigma), 1 µl P/S, 10 µl L-glut, 677 µl type I collagen (Elastin Products), and 52 µl of RDFs resuspended to $1x10^6$ cells/ml in M199. This solution was transferred to a 3 ml syringe and flowed into the microchannel. Open device controls were filled using a micropipette tip. All three device configurations were incubated at 37°C for 1 hour to allow for self assembly of the collagen network.

Following this initial incubation, tubing was removed and devices were transferred into individual Petri dishes and covered with culture medium.

A.2.4 Perfusion

Inlet tubing used for perfusion studies were connected to three-way values. Equivalent inoculation methods were used as described above. Following cell attachment and fibrillogenesis under static culture conditions, inlet valves were connected to 1 ml syringes driven by a syringe pump (Harvard Apparatus). Both 2D and 3D cultures were perfused at 0.05 µl/min, a suitable flow rate based off of published results (Kim, 2006). Both 2D and 3D device configurations were submerged in excess media for the duration of perfusion.

A.2.5 Cell Viability

Microchannels were inspected at various time points with epifluorescent microscopy using an Olympus IX81 inverted microscope. Images were acquired using a 10× objective and analyzed using ImageJ (NIH). Devices were visualized one hour post-seeding to ensure uniformity of cell number and distribution. At 12 and 24 hours, the number of GFP-expressing cells in 2D and 3D configurations was quantified for static conditions. For perfusion studies, cell viability was assessed quantitatively 12 hours after initiation of flow. Long term cultures were monitored for up to 7 days and qualitatively assessed for cell proliferation and survival.

A.2.6 Cell Labeling

2-D cultures were fixed by replacing the culture media with 4% paraformaldehyde for 1 hour at room temperature followed by several rinses with an immunobuffer solution

consisting of phosphate buffered saline (PBS) supplemented with 0.5% Triton-X and 1% bovine serum albumin (BSA). Devices were then prepared for either histological or immunohistochemical labeling of cytoskeletal elements. For histological staining, cells were incubated with 1 μM TRITC-conjugated phalloidin and counterstained with 300 nM DAPI for 1 hour at room temperature. For immunohistochemical labeling, devices were blocked with goat serum, incubated with mouse anti-tubulin (1:100) overnight at 4ºC, fluorescently tagged using goat-anti mouse AlexaFluor 568 conjugated secondary antibody, and also counterstained with DAPI.

A.2.7 Maintenance of Predicted Flow

A Y-shaped device, intended to produce two parallel stripes of solution, was designed with two inlet channels, each 500 μm in width, using standard soft lithography techniques. The device was sealed using a semi-permeable membrane as described above. One inlet was connected to a FITC-tagged collagen solution and the other to a native collagen solution; solutions were flowed into the device manually. Immediately following filling, devices were carefully moved into the incubator to allow for fibrillogenesis. Devices were then imaged using bright field and epifluorescent microscopy to assess stripe formation.

A.3 RESULTS AND DISCUSSION

A.3.1 Cell Viability in Static Culture

Three device configurations, as shown in **Figure 1**, were assessed for their effects on cell viability in both 2D and 3D static cultures. An equal number of primary fibroblasts were seeded in glass-sealed, membrane-sealed, and open microchannels. Cell viability in the

three device configurations was quantified at 12 and 24 hours. Results show that viability was compromised significantly in traditionally sealed microfluidic channels exposed statically to culture medium only through inlet and outlet holes. However, viability when sealed with a semi-permeable membrane was statistically equivalent to fully open cultures (**Figure 2**). Consistent with cell proliferation, there was a significant increase in total cell number in the membrane-bonded devices (ANOVA, followed by post hoc comparisons with Tukey's test, $P = 0.007$) from 12 to 24 hours. The number of cells in these devices was significantly greater than the number of cells in the glass-bonded devices at both 12 and 24 hours ($P = 0.003$ and $P < 0.001$, respectively). Cell number in the membrane-bonded devices was not significantly different from that in the open devices at 12 and 24 hours ($P = 0.867$ and $P = 0.821$, respectively).

RDFs demonstrated typical fibroblast morphology and spreading kinetics in the 2D (**Figure 3A-C**) and 3D (**Figure 3 D-F**) microculture experiments. Interestingly, at 24 hours cells were markedly aligned in the 3D cultures, but not the 2D cultures, which may reflect the alignment of the collagen fibers induced by the channel geometry [12]. In longer term cultures, cells in membrane-sealed devices continued to proliferate and reached confluence by 7 days (**Figure 4**). By 3 days, however, no cells remained in the glass-bonded devices.

Different cells are variably sensitive to culture conditions, including nutrient and oxygen availability. Even in perfused systems, cell viability is often dependent on distance from the source of media replenishment. For example, Ling et al. noted a significant decrease in cell viability as the distance from the perfusion channel increased within their cell-embedded agarose channels at 3 days post-seeding (2007). Additionally, oxygen

gradients can form in the direction of flow as a result of consumption by cells, and this phenomenon can be particularly strong in the case of cells with high oxygen requirements, like hepatocytes [3, 13]. In membrane-sealed devices, the pore size of the membrane was sufficiently small to preclude escape of cells and ECM components but large enough to allow the transport of crucial proteins, nutrients, and gases into the channel along its entire length. Additionally, the growth to confluence of the cultures in suggests no protein fouling of the membrane.

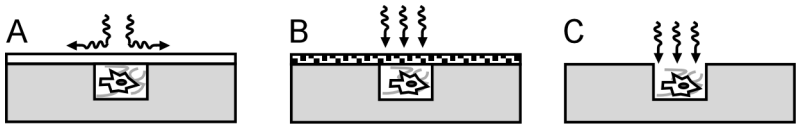

Figure 1. Schematic of approach to improve cell viability by sealing channels with a semi-permeable membrane. (A) Culture sealed with a glass microslide or coverslip. Medium enters the culture through inlet and outlet ports (not shown in schematic). (B) Sealing the culture with a semi-permeable microdialysis membrane allows transport into the culture similar to an open channel (C).

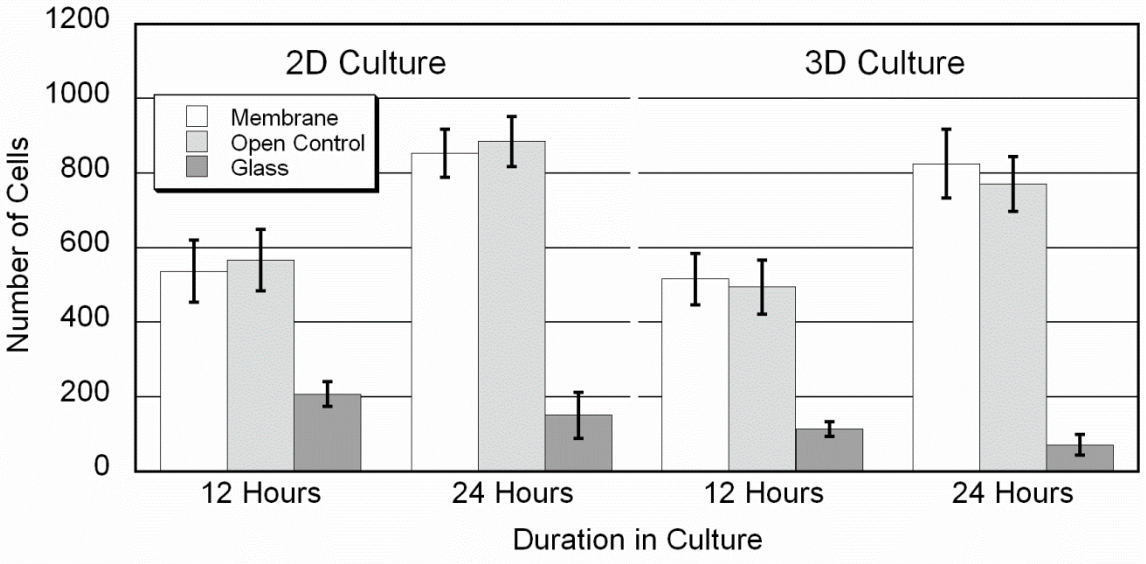

Figure 2. Cell viability in static cultures (average +/- standard error of the mean). Equal numbers of fibroblasts were seeded in glass-sealed, membrane-sealed, and open microfluidic channels. At 12 hours and 24 hours, cell number was significantly greater in the membrane-sealed and open networks than those sealed with glass. Cell number significantly increased from 12 to 24 hours in membrane-and glass sealed networks, but decreased in glass-sealed ones.

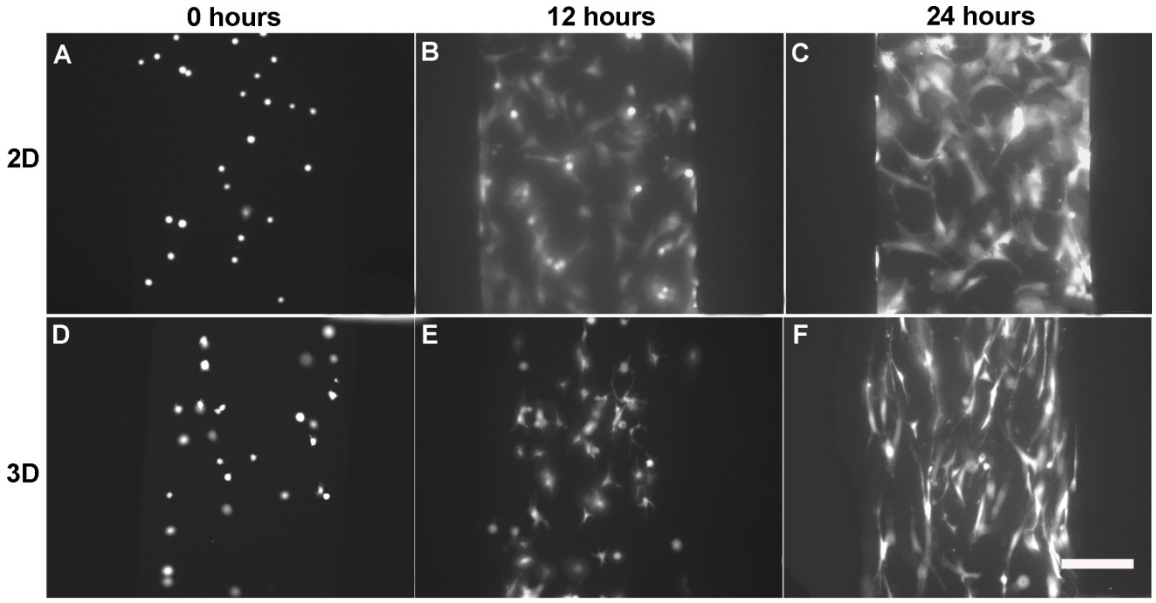

Figure 3. Cell morphology in representative 2D (A-C) and 3D (D-F) microscale cultures in membrane-sealed networks. Initially rounded cells (A, D) began spreading by 12 hours (B, E) and continued to spread and multiply by 24 hours (C, F). Cells in the 3D culture displayed noticeable alignment at 24 hours (F). Scale bar = 200 μm.

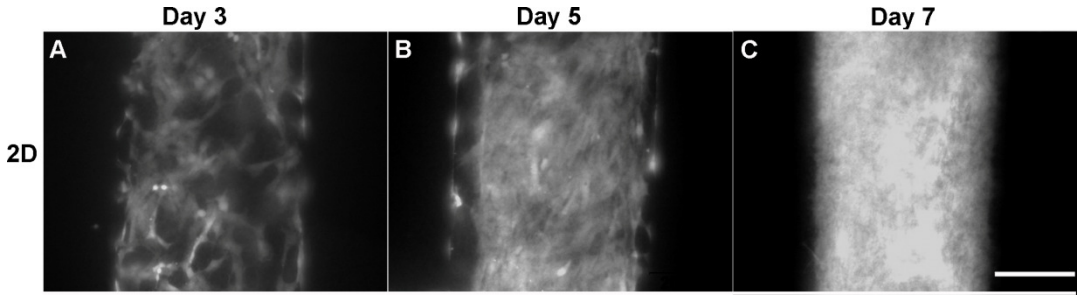

Figure 4. Cell morphology in representative 2D microscale long-term cultures in membrane sealed networks. Fibroblasts continue to proliferate and spread from 3 days (G) to 5 days (H) and reach full confluence by 7 days in culture (I). Scale bar = 200 µm

A.3.2 Cell Viability in Perfused Culture

Glass and membrane sealed devices were subjected to pump-driven perfusion for both 2D and 3D microcultures to assess whether media replenishment could recover viability. Following an initial attachment period, cells were perfused at 0.05 µl/min for 12 hours and cell viability was quantified. As shown in **Figure 5A**, even with perfusion, membrane sealed devices retained viability better than glass sealed devices in both 2D ($P = 0.0006$) and 3D cultures ($P = 0.015$).

In glass-sealed 2D cultures, cell viability was highest at the inlet, decreased throughout the length of the microchannel, and recovered as a function of the distance from the outlet (**Figure 5B**), whereas the viability of fibroblasts was uniform in membrane-sealed devices. As mentioned above, oxygen gradients can form within devices which may account for these results. Further, while membrane sealed devices outperformed glass-sealed devices, the morphology of fibroblasts subjected to perfusion in 3D was rounded compared to the hallmark cellular extensions seen in static culture (Data not shown). These qualitative findings highlight the impact of flow-based systems on cellular phenotype, an important consideration in experimental design.

Generally, perfusion based systems require rigorous optimization in order to identify appropriate flow rates to minimize shear while maximizing cell viability. Further, these flow rates are dependent on a number of variables specific to the experimental setup, including cell type, seeding density, and device design. In our studies, we utilized a flow rate based on previously published reports and show that this was adequate for cell survival in membrane-sealed devices. Thus, membrane-sealed devices can be easily

modified to include perfusion without sacrificing viability as this is not the sole modality by which cells receive their nutrients and oxygen.

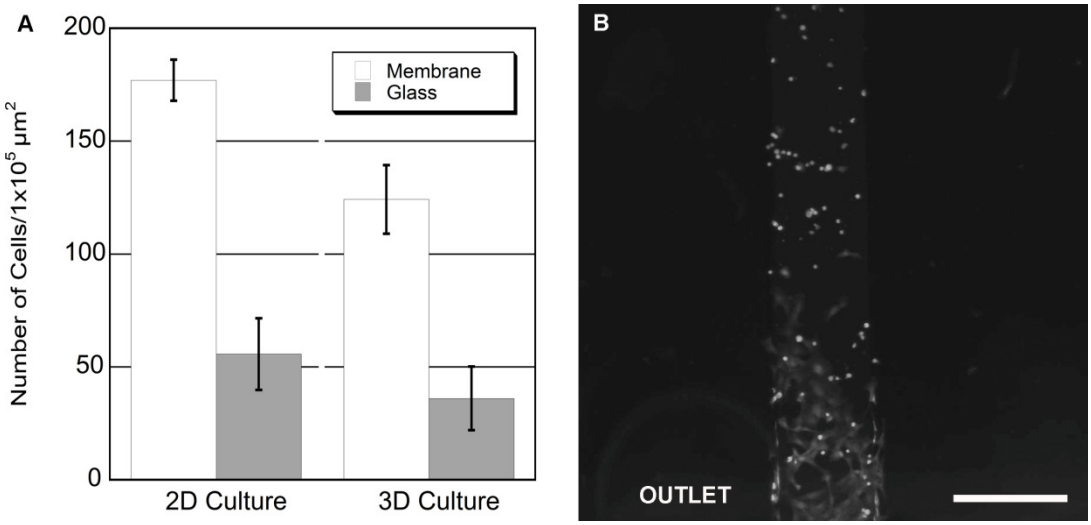

Figure 5: Cell viability in membrane and glass-sealed perfused cultures. (A) Cell viability in 2D and 3D perfused cultures (average +/- standard error of the mean). Equal numbers of fibroblasts were seeded in glass-sealed and membrane-sealed microfluidic channels. After 12 hours of pump-driven perfusion, cell number was significantly greater in the membrane-sealed networks than those sealed with glass for both 2D and 3D cultures. (B) Cell morphology in representative 2D glass-sealed perfused microchannel. There is a noticeable decrease in cell number and a more rounded morphology as the distances from the outlet increases. Scale bar = 500 µm.

A.3.4 Staining in Devices

Devices that are sealed using an impermeable surface require perfusion for histological processing, which uses larger volumes of expensive labeling agents, can often be a long, laborious process with inconsistent results. In addition to improving cell viability, the enhanced mass transport using membrane-sealed devices simplifies labeling of cells within the microculture. At discrete time points, separate membrane-bonded cultures were fixed and labeled with a DAPI, a nuclear probe, and TRITC-conjugated phalloidin, a cytoskeletal probe. As shown in **Figure 6A**, the semi-permeable membrane allowed simplified and uniform fluorescent labeling in an hour.

While with DAPI and phalloidin are useful histological markers, immunohistochemical analysis is often used to label for specific ligands. However, IgG antibodies generally have a molecular weight in the range of $1.5x10^5$ Da, which is two orders of magnitude larger than TRITC labeled phalloidin. As shown in **Figure 6B**, we successfully stained fibroblasts with an antibody against tubulin, a cytoskeletal protein, followed by a fluorescently tagged secondary antibody. Additionally, there was no significant background due to the presence of the membrane. Thus, these larger molecules diffuse through the membrane without significant obstruction. From our own experience, perfusion techniques used for labeling within cell-laden microfluidic devices can take several days, where the membrane-sealed devices can be stained in several hours. Further, the number of syringe pumps required creates a resource limitation on devices that can be histologically processed at one time. Conversely, multiple membrane-sealed devices can be treated as separate slides or submerged simultaneously in a bath

containing the appropriate probes providing additional time savings with batch processing.

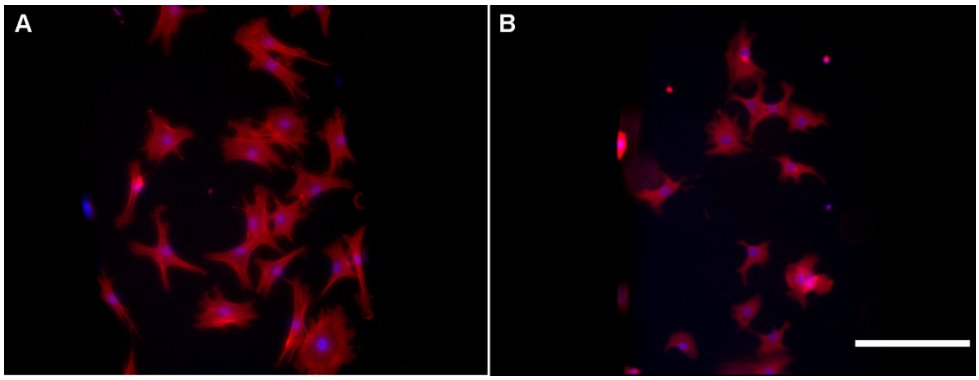

Figure 6: Cell labeling within membrane-sealed networks. (A) DAPI-labeled nuclei and TRITC-phalloidin labeled F-actin at 24 hours post seeding. (B) DAPI-labeled nuclei and immunohistologically labeled tubulin at 12 hours post seeding. Scale bar = 200 µm.

A.3.5 Maintenance of Predicted Flow Pattern

Spatiotemporally regulated signals are important to a diverse range of physiological processes, including embryogenesis, wound healing, and nerve regeneration. However, it is difficult to mimic these cues using standard tissue culture technique. Microfluidic systems allow for precise control of the presentation of stimuli and may aid in our understanding and manipulation of various biological phenomena [14]. While many microfluidic device designs have focused on the use of surface-immobilized or soluble gradients, tissue engineering and biomaterial applications could benefit from the use of 3D microcultures. One methodology used to generate spatially reproducible gradients is patterning scaffolds with immobilized biomolecules, a technique used successfully with collagen [15] and agarose [16].

A representative 3D configuration was used to ensure bonding of a semi-permeable membrane does not interfere with the ability to pattern within microchannels. A "Y"-shaped, stripe generating device was used as a representative model [17]. By using fluorescently tagged type I collagen in one inlet and native collagen in the other, we were able to maintain predicted flow patterns and form a linear stripe with flow (**Figure 7**). We speculate that this is expandable to other liquid-swelled polymers, including synthetic (PEG) and natural (alginate, chitosan) oligomers, as well as with 2D cultures exposed to laminar flow patterns.

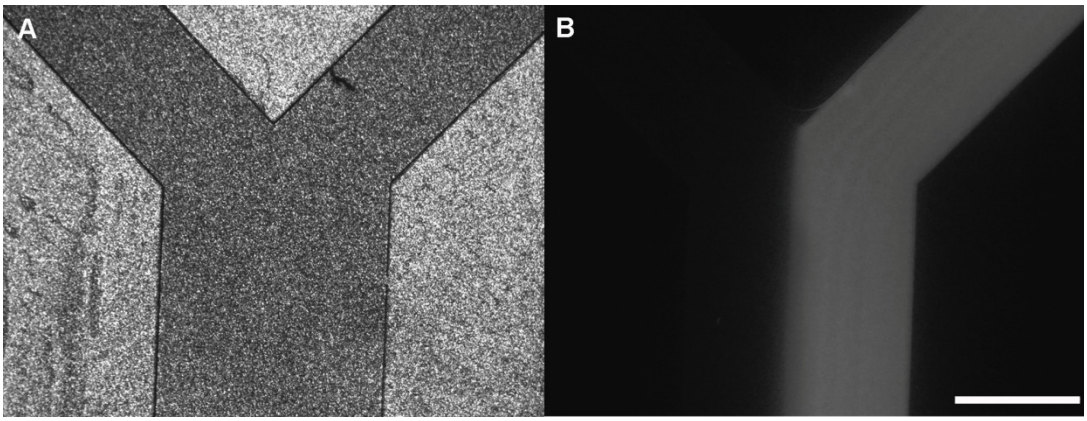

Figure 7: Pattern fidelity in three-dimensional microcultures. A Y-shaped, stripe-generating microfluidic device was sealed with a nanoporous membrane (A). Two solutions, native and fluorescently tagged type I collagen, were pumped through individual inlets. The predicted flow was not significantly affected by sealing with the nanoporous membrane as shown by the boundary of fluorescence (B). Scale bar = 500 μm.

A.4 CONCLUSION

Microfluidic systems offer great potential as customized microenvironments for cell culture for assays of genotypic and phenotypic behavior as well as regenerative medicine [1]. However, extended culture in these systems has been difficult because of diffusive limitations for static culture and the complexity and unwanted, inconsistent, and perhaps destructive effects of active perfusion systems. Herein, we have presented a simple yet effective means of dramatically improving cell viability by sealing the microfluidic network with a semi-permeable membrane. The improved transport extends the period of time for cell culture, which broadly increases the potential for micro-scale assays of cell behavior as well as micro-tissue engineering. The simplicity allows for more cultures to be maintained at once. The approach also simplifies methods associated with evaluating cellular responses via soluble probes, and eases handling and use of disposable supplies, and is also cost-effective, as membranes can be purchased for less than 10 cents apiece. As such, the technique promises to introduce significant time and cost savings.

A.5 REFERENCES

1. El-Ali J, Sorger PK, Jensen KF. Cells on chips. Nature. 2006;442(7101):403-11. Epub 2006/07/28.
2. Korin N, Bransky A, Dinnar U, Levenberg S. Periodic "flow-stop" perfusion microchannel bioreactors for mammalian and human embryonic stem cell long-term culture. Biomed Microdevices. 2009;11(1):87-94. Epub 2008/09/20.
3. Mehta G, Mehta K, Sud D, Song JW, Bersano-Begey T, Futai N, et al. Quantitative measurement and control of oxygen levels in microfluidic poly(dimethylsiloxane) bioreactors during cell culture. Biomed Microdevices. 2007;9(2):123-34. Epub 2006/12/13.
4. Walker GM, Zeringue HC, Beebe DJ. Microenvironment design considerations for cellular scale studies. Lab Chip. 2004;4(2):91-7. Epub 2004/03/31.
5. Walker GM, Sai J, Richmond A, Stremler M, Chung CY, Wikswo JP. Effects of flow and diffusion on chemotaxis studies in a microfabricated gradient generator. Lab Chip. 2005;5(6):611-8. Epub 2005/05/26.

6. Park J, Berthiaume F, Toner M, Yarmush ML, Tilles AW. Microfabricated grooved substrates as platforms for bioartificial liver reactors. Biotechnol Bioeng. 2005;90(5):632-44. Epub 2005/04/19.
7. Tourovskaia A, Figueroa-Masot X, Folch A. Differentiation-on-a-chip: a microfluidic platform for long-term cell culture studies. Lab Chip. 2005;5(1):14-9. Epub 2004/12/24.
8. Ling Y, Rubin J, Deng Y, Huang C, Demirci U, Karp JM, et al. A cell-laden microfluidic hydrogel. Lab Chip. 2007;7(6):756-62. Epub 2007/06/01.
9. Whitesides GM, Ostuni E, Takayama S, Jiang X, Ingber DE. Soft lithography in biology and biochemistry. Annu Rev Biomed Eng. 2001;3:335-73. Epub 2001/07/12.
10. Aran K, Sasso LA, Kamdar N, Zahn JD. Irreversible, direct bonding of nanoporous polymer membranes to PDMS or glass microdevices. Lab Chip. 2010;10(5):548-52. Epub 2010/02/18.
11. Shreiber DI, Enever PA, Tranquillo RT. Effects of pdgf-bb on rat dermal fibroblast behavior in mechanically stressed and unstressed collagen and fibrin gels. Exp Cell Res. 2001;266(1):155-66. Epub 2001/05/08.
12. Lee P, Lin R, Moon J, Lee LP. Microfluidic alignment of collagen fibers for in vitro cell culture. Biomed Microdevices. 2006;8(1):35-41. Epub 2006/02/24.
13. Korin N, Bransky A, Khoury M, Dinnar U, Levenberg S. Design of well and groove microchannel bioreactors for cell culture. Biotechnol Bioeng. 2009;102(4):1222-30. Epub 2008/11/01.
14. Khademhosseini A, Langer R, Borenstein J, Vacanti JP. Microscale technologies for tissue engineering and biology. Proc Natl Acad Sci U S A. 2006;103(8):2480-7. Epub 2006/02/16.
15. Sundararaghavan HG, Masand SN, Shreiber DI. Microfluidic generation of haptotactic gradients through 3D collagen gels for enhanced neurite growth. J Neurotrauma. 2011. Epub 2011/04/09.
16. Luo Y, Shoichet MS. A photolabile hydrogel for guided three-dimensional cell growth and migration. Nat Mater. 2004;3(4):249-53. Epub 2004/03/23.
17. Takayama S, McDonald JC, Ostuni E, Liang MN, Kenis PJ, Ismagilov RF, et al. Patterning cells and their environments using multiple laminar fluid flows in capillary networks. Proc Natl Acad Sci U S A. 1999;96(10):5545-8. Epub 1999/05/13.

SHIRLEY N. MASAND

CURRENT POSITION

Fellow, NSF IGERT on Integrated Science and Engineering of Stem Cells
Fellow, Rutgers Pre-doctoral Leadership Development Institute

EDUCATION

Ph.D in Biomedical Engineering **Jan 2013**
Rutgers University, New Brunswick, New Jersey

B.S. in Biochemistry **May 2005**
Lehigh University, Bethlehem, Pennsylvania
Honors Thesis: *"The effects of estrus on activity and anxiety in female mice."*

WORK EXPERIENCE

Research Scientist I **Mar. 2005 – Jan. 2006**
Wyeth-Ayerst Research, Pearl River, New York

Research Associate **Aug. 2004 – Mar. 2005**
Lundbeck Research USA, Paramus, New Jersey

RESEARCH ACTIVITIES

Publications:

1.) **Masand SN,** Chen J, Schachner M, Shreiber DI. "Glycomimetic Functionalized Collagen Hydrogels For Peripheral Nerve Regeneration." Biomaterials 2012 (IF: 7.404)
2.) **Masand SN**, Perron IJ, Schachner M, Shreiber DI."Neural cell type-specific responses to glycomimetic functionalized collagen." Biomaterials 2011(IF: 7.404)
3.) **Masand SN**, Mignone L, Zahn J, Shreiber DI. "Nanoporous membrane sealed microfluidic devices for improved cell viability." Biomedical Microdevices 2011 (IF: 3.032)
4.) Sundararaghavan HG, **Masand SN**, Shreiber DI. "Microfluidic generation of haptotactic gradients through 3D collagen gels for enhanced neurite growth." J Neurotrauma 2011 (IF: 3.654)
5.) **Masand SN**, Blazier AB, Bradley C, Shreiber DI. "Tryptophan as an Intrinsic Fluororeporter for Functionalized Peptide." (In preparation)
6.) Lee YS, Griffin J, **Masand SN**, Shreiber DI, Uhrich KE. "Fabrication and evaluation of a salicylic acid-based poly(anhydride-ester) blend nerve guidance conduits" (In preparation)